NONLINEAR AUTOREGRESSIVE MOVING AVERAGE BASED MODELING OF AUTONOMIC CONTROL OF HEART RATE

PIYAWAN MASSA-ARD

A THESIS SUBMITTED IN PARTIAL FULFILLMENT
OF THE REQUIREMENTS FOR
THE DEGREE OF MASTER OF ENGINEERING
(BIOMEDICAL ENGINEERING)
FACULTY OF GRADUATE STUDIES
MAHIDOL UNIVERSITY
2006

ISBN 974-04-7650-3

Thesis
Entitled

NONLINEAR AUTOREGRESSIVE MOVING AVERAGE BASED MODELING OF AUTONOMIC CONTROL OF HEART RATE

Piyawan Massa-ard
.....
Miss Piyawan Massa-ard
Candidate

.....
Assist.Prof. Warakorn Charoensuk,
Ph.D. (Electrical Engineering)
Major-Advisor

.....
Assist.Prof. Wattana B. Wattanapa,
M.D, Ph.D. (Physiology)
Co-Advisor

.....
Prof. M.R. Jisnuson Svasti, Ph.D.
Dean
Faculty of Graduate Studies

Theeraporn Rubcumintara
.....
Assist.Prof. Theeraporn Rubcumintara,
Ph.D. (Materials Engineering & Science)
Chair
Master of Engineering Programme in
Biomedical Engineering
Faculty of Engineering

Thesis
Entitled

NONLINEAR AUTOREGRESSIVE MOVING AVERAGE BASED MODELING OF AUTONOMIC CONTROL OF HEART RATE

was submitted to the Faculty of Graduate Studies, Mahidol University
for the degree of Master of Engineering (Biomedical Engineering)
on
1 September 2006

Piyawan Massa-ard
.....
Miss Piyawan Massa-ard
Candidate

.....
Assist.Prof. Warakorn Charoensuk,
Ph.D. (Electrical Engineering)
Chair

.....
Assist.Prof. Wattana B. Wattanapa,
M.D, Ph.D. (Physiology)
Member

.....
Mr. Panuthat Boonpramuk,
Ph.D. (Engineering)
Member

.....
Assist.Prof. Udom Tipayamontri,
Ph.D. (Physiology)
Member

.....
Prof. M.R. Jisnuson Svasti, Ph.D.
Dean
Faculty of Graduate Studies
Mahidol University

.....
Assist.Prof. Piya Rattanasuwan,
M.Eng.
Dean
Faculty of Engineering
Mahidol University

ACKNOWLEDGEMENT

I would like to express my appreciation and gratitude to my thesis advisor, Asst.Prof. Warakorn Charoensuk, for his valuable advice and constructive suggestions provided through this study. Also I would like to give my special thanks to Assist.Prof. Dr. Wattana Watanapa, for many valuable suggestions, comments and advises. I am grateful to thank Dr. Fernando B. Costa for valuable data collection.

Moreover, I would like to give thanks to all my teachers in the Biomedical Engineering Programme for giving me their knowledge during the studying time in master degree.

I also would like to thank all my friends at Biomedical Engineering Programme for their friendship, love, and support. Special thanks for all my friends, who are too numerous to name here but everyone is in my mind for everything they have done for me.

Last but not least, I would like to thank my parents and my family for their love, support and continuing faith in me that enable me to get to this point in my life. The usefulness of this thesis, I dedicate to my father, my mother and all the teachers who have taught me since my childhood.

Piyawan Massa-ard

NONLINEAR AUTOREGRESSIVE MOVING AVERAGE BASED MODELING OF AUTONOMIC CONTROL OF HEART RATE

PIYAWAN MASSA-ARD 4536774 EGBE/M

M.Eng.(BIOMEDICAL ENGINEERING)

THESIS ADVISORS : WARAKORN CHAROENSUK, Ph.D.(ELECTRICAL ENGINEERING), WATTANA B.WATANAPA, M.D.,Ph.D. (Physiology)

ABSTRACT

A mathematical model of the relationship between respiration and RR interval is important for understanding physiological mechanisms and in clinical practices. Linear approaches are not sufficient to characterize the interactions because these interactions are complex and nonlinear. In this study, heart rate variability was studied during handgrip exercise. As result, the sympatho-vagal balance (LF/HF ratio) was found to have increased during dynamic handgrip exercise. Moreover, the nonlinear model that assesses the dynamic changes in cardiovascular regulation was investigated by using Nonlinear AutoRegressive Moving Average (NARMA) method. Arterial blood pressure, respiration and electrocardiography (ECG) were recorded from healthy subjects in supine position. These signals were separated into training sets and test sets. Parameters of the NARMA model were estimated by applying the training set in an artificial neural network. Normalize Mean Square Error (NMSE) and Mean Absolute Percentage Error (MAPE) were computed to indicate the performance of the model. NMSE and MAPE were very low when compared with previous methods (nonparametric method, ARX model and Volterra-Weiner model). These findings indicated that the NARMA model may be useful to complete the cardiovascular regulation mechanism.

KEY WORDS : AUTONOMIC NERVOUS SYSTEM/ ARTERIAL BLOOD PRESSURE/ RESPIRATION/ RR INTETVAL/ NONLINEAR MODEL/ NARMA MODEL

99 P. ISBN 974-04-7650-3

การจำลองการควบคุมอัตราหัวใจเต้นโดยประสาทอัตโนมัติ ด้วยวิธีเฉลี่ยเคลื่อนที่แบบถดถอยในตัวเองโดยใช้สมการไม่เชิงเส้น
(NONLINEAR AUTOREGRESSIVE MOVING AVERAGE BASED MODELING OF AUTONOMIC CONTROL OF HEART RATE)

ปิยะวรรณ มาสสะอาด 4536774 EGBE/M

วศ.ม. (วิศวกรรมชีวการแพทย์)

คณะกรรมการควบคุมวิทยานิพนธ์ : วรากร เจริญสุข, Ph.D. (Electical Engineering),
วัฒนา วัฒนาภา, M.D., Ph.D. (Physiology)

บทคัดย่อ

แบบจำลองทางคณิตศาสตร์ของความสัมพันธ์ระหว่างระบบการหายใจและอัตราหัวใจเต้นมีความสำคัญต่อกลไกการทำงานและการประยุกต์ใช้ทางคลินิก ความสัมพันธ์เชิงเส้นไม่เพียงพอที่จะอธิบายคุณลักษณะของความสัมพันธ์นี้ เนื่องจากเป็นความสัมพันธ์ที่ซับซ้อนและไม่เชิงเส้น ในการศึกษานี้ เราได้ศึกษาถึงความแปรผันของอัตราหัวใจเต้นในระหว่างการออกกำลังบีบมือ จากผลที่ได้ เราพบว่า sympatho-vagal balance (LF/HF ratio) เพิ่มขึ้นระหว่างการออกกำลังกาย นอกเหนือจากนั้น เราได้ค้นคว้าแบบจำลองไม่เชิงเส้นที่ใช้ในการวิเคราะห์การเปลี่ยนแปลงที่เกิดขึ้นในการปรับสมดุลของระบบหัวใจและหลอดเลือดโดยใช้ วิธีการวิธีเคลื่อนที่แบบถดถอยในตัวเองโดยใช้สมการไม่เชิงเส้น ความดันเลือดในหลอดเลือดแดง อัตราหัวใจเต้น และ การหายใจ ถูกบันทึกจากอาสาสมัครที่มีสุขภาพดีในท่านอน สัญญาณเหล่านี้ได้ถูกแบ่งออกเป็นชุดข้อมูลที่ใช้ในการฝึกและชุดข้อมูลที่ใช้ในการทดสอบ ค่าสัมประสิทธิ์ของแบบจำลองวิธีเคลื่อนที่แบบถดถอยในตัวเองโดยใช้สมการไม่เชิงเส้นถูกประมาณค่าโดยการป้อนชุดข้อมูลที่ใช้ในการฝึกให้แก่เครือข่ายจำลองระบบประสาท Normalized Mean Square Error (NMSE) และ Mean Absolute Percentage Error (MAPE) ถูกคำนวณเพื่อประเมินประสิทธิภาพของแบบจำลอง NMSE และ MAPE นั้นมีค่าต่ำมากเมื่อถูกเปรียบเทียบกับวิธีการก่อนหน้า (Nonparametric method, ARX model and Volterra-Weiner model) การค้นพบนี้เป็นการระบุว่า แบบจำลอง NARMA อาจมีประโยชน์ในการเติมเต็มกลไกการปรับสมดุลของระบบหัวใจและหลอดเลือด

99 หน้า ISBN 974-04-7650-3

CONTENTS

CONTENTS (Continued)

CONTENTS (Continued)

LIST OF ABBREVIATIONS

ABP	Arterial blood pressure
Ach	Acetylcholine
ADH	Antidiuretic hormone
ANP	Atrial natriuretic peptide
ANS	Autonomic nervous system
AR	Autoregressive process
ARX	Autoregressive with exogeneos input
AV node	Atrioventicular node
CNS	Central nervous system
DBP	Diastolic blood pressures
E	Epinephrine
ECG	Electrocardiography
EPO	Erythropoietin
HF	High frequency
HRV	Heart rate variability
ILV	Instantaneous lung volume
LBNP	Lower body negative pressure
LF	Low frequency
NE	Norepinephrine
NMSE	Normalized mean squared error
NARMA	Nonlinear autoregressive moving average
MAPE	Absolute percentage error
MDL	Minimum Descriptive Length Criterion
MSNA	Muscle sympathetic nerve activity
MVA	Malignant ventricular arrhythmia

LIST OF ABBREVIATIONS (Continued)

OSA	Obstructive sleep apnea
RESP	Respiration
RAP	Right atrial pressure
RSA	Respiratory sinus arrhythmia
SA node	Sinoatrial node
SBP	Systolic blood pressure
SV	Stroke volume
TPR	Total peripheral resistance
VHF	Very low frequency

LIST OF SYMBOLS

a_i and b_i	Parameters of AR, ARX, NARMA model
d	Desired response
DTFT	Discrete time Fourier transform operator
IDTFT	Inverse discrete time Fourier transform operator
E	Expectation operator
$e(n)$	Unobserved white noise disturbance
G	Matrix of Green's functions
h_0, h_1, $h_2(n_1, n_2)$	Volterra kernels
$H(\omega)$	Transfer function
p and q	Order of AR, ARX, NARMA model
$\hat{r}_{xx}(k)$	Autocorrelation
$\hat{r}_{xy}(k)$	Cross correlation
s_p^2	Variance of the error sequence
$S(f)$.	Power spectrum
$\hat{S}_{xy}(\omega)$	Cross spectrum
$\hat{S}_{xx}(\omega)$	Autospectrum
$x(n)$	Input signal
X^*	Conjugation operator
$y(n)$	Output signal
$y_0(n)$	Zero order response residual
$y_L(n)$	Linear response
$y_Q(n)$	Quadratic response
w	Weights
$\| \|$	Euclidean norm

LIST OF FIGURES

LIST OF FIGURES (Continued)

LIST OF FIGURES (Continued)

LIST OF FIGURES (Continued)

LIST OF FIGURES (Continued)

LIST OF TABLES

CHAPTER I
INTRODUCTION

1.1 Background

Autonomic nervous system (ANS) is a division of central nervous system (CNS) which is unconsciously controlled [1]. The smooth and cardiac muscles, glands and fat cells are controlled by ANS. The important function of ANS is maintenance of homeostasis of organs and physiological functions. ANS can be divided into sympathetic and parasympathetic divisions. Both sympathetic and parasympathetic divisions affect various organs such as eyes, skin, skeleton muscle, tear glands, adrenal glands, digestive system, urinary system, respiratory system and cardiovascular system.

Especially in cardiovascular system, ANS adjusts blood vessel and heart to keep adequate blood flow. The sympathetic division controls the vasoconstriction and vasodilation in blood vessel. Sympathetic division also increases the heart rate, forces of contraction and blood pressure in heart, but parasympathetic division decreases these activities [1]. ANS has a cardiovascular center, which consists of cardiac and vasomotor centers to monitor the alteration in blood pressure, pH, and dissolved gas concentrations [1]. The cardiac centers control cardiac output and they consist of cardioacceleratory and cardioinhibition centers. The cardioacceleratory centers enhance cardiac output via sympathetic innervation while the cardioinhibition centers decrease, the cardiac output via parasympathetic nervous system. The vasomotor centers function is to adjust the peripheral resistance and it can be classified into vasodilation, vasoconstriction and venoconstriction [1]. Vasodilation occur when the vasomotor center is inhibited, thus decreases the peripheral resistance by increasing the diameter of arterioles. Both vasoconstriction and venoconstriction increase peripheral resistance when the vasomotor center is stimulated, by compressing the peripheral arterioles and veins, respectively.

In the cardiovascular system there are autonomic reflexes that response to the change in blood pressure and chemical compositions. The autonomic reflex are baroreflex and chemoreceptor reflex. Baroreflex responds to fluctuations in blood pressure and returns sensory information to the medulla oblongata. If the blood pressure is increased, the cardioacceleratory and vasomotor centers are inhibited; cardioinhibitory center is stimulated to reduce blood pressure. On the other hand, when blood pressure is below the normal range, baroreflex inhibits the cardioinhibitory centers and stimulate cardioacceleratory centers and vasomotor center in order to restore blood pressure. Chemoreceptor reflex is other type of autonomic reflex and it is sensitive to the change in carbondioxide level, oxygen level or pH in blood and cerebrospinal fluid. The chemoreceptor reflex is stimulated when there is a decrease in oxygen level or pH, increase in carbondioxide level in blood or cerebrospinal fluid. Then the chemoreceptor reflex stimulates the cardioinhibitory center and vasomotor center. Moreover, the chemoreceptor reflex also stimulates the respiratory centers in medulla oblongata to increase the respiratory rate. The effect of this stimulation cause increased oxygen and pH levels and decreased carbondioxide level in blood. Finally, homeostasis is restored in normal level.

Since these mechanisms of ANS and cardiovascular system have reciprocal interactions and are not independent, a change in any single parameter can influence entire structure with the complex mechanism through the neural system. The evaluations of ANS support the integration function of cardiovascular regulatory mechanisms in both health improvement and disease progression [2]. Thus, many research works tried to study the relationship between ANS and cardiovascular system, for example, heart rate variability (HRV), the relationship between RR interval and systolic blood pressure (the mechanical path), the reversal causal path (the baroreflex path), etc.

HRV is a beat to beat alteration in heart rate [3]. ANS affects HRV through the sinus node, the natural pacemaker of heart. Measurement of heart rate can be widely used for evaluating cardiovascular autonomic function in various physiological conditions [4-9]. HRV analysis during exercise enhances our understanding of central autonomic control. The power spectral analyses of heart rate are applied to demonstrate the cardiac function depending on the autonomic nervous

system and physiological control. Power spectral method provides the basic information on the distribution of power as a frequency function of HR. The spectral band of HR can be divided into a very low frequency (VLF) (0-0.04 Hz), a low frequency (LF) (0.04-0.15 Hz) and a high frequency (HF) (0.15-0.4 Hz) components. The LF band is hypothesized to relate with the sympathetic activation but the HF band is suspected to relate with vagal activation [10]. Hence, the LF/HF ratio is an important index for studying the sympatho-vagal balance. For example, during and immediately after exercise, the risk of sudden death was increased [11-12]. Other studies [13-15] demonstrated that diminished parasympathetic nervous system activity at rest was associated with an increased mortality and sudden cardiac death.

Both the mechanical path and baroreflex path are also important factors that influence the ANS. The relationship between systolic blood pressure (SBP) and RR interval is a closed loop [16]. Thus, the alteration in SBP affects RR interval (the baroreflex path) as well as the change in RR interval also causes the modulation in SBP through a change in cardiac output (the mechanical path) [16]. The studies of the complicated behaviors enhance cardiovascular regulatory mechanisms in heath and disease. Furthermore, they provide new clinical tools that may be improve the care and management of patients with a variety of cardiovascular and neurologic disorders [2]. The power spectrum of RR interval and arterial blood pressure variability is a noninvasive method for assessing the autonomic nerve activity through frequency components of fluctuations [17]. The transfer function of SBP and RR interval explained the clinical baroreceptor function [16-18].

Muscle sympathetic nervous activity (MSNA) is a recording of multiunit sympathetic impulses and it can be recorded in skeletal muscles [19-20]. MSNA increase vasoconstrictor tone in skeletal muscles to adjust arterial blood pressure [19-20]. MSNA has been used to assess sympathetic nerve activity in patients with various pathophysiological conditions, such as hypertension [21,22], diabetes mellitus [23], myocardial infarction, and congestive heart failure [24].

Respiration influences the cardiovascular regulation in short term recording. The phenomena that affects cardiovascular regulation through heart rate, is known as respiratory sinus arrhythmia (RSA). RSA is the heart rate variability in synchrony with respiration, as seen through the RR interval on electrocardiography (ECG),

which is reduced during inspiration and extended during expiration [25]. This phenomenon is associated with the tidal volume and the breathing rate. The RSA can be found at a HF (0.20-0.25 Hz) of the fluctuation of the RR interval [26]. It is related with several parasympathetic controls including the vagal tone and its modulation. The vagal phase variation is related to respiration, and the parasympathetic baroreflex response [27]. HRV was applied for assessing autonomic function and also in neurologic disorders such as obstructive sleep apnea [28-30] and diabetes [31].

These evaluations of autonomic heart rate control provided better insight in both autonomic controls and clinical illnesses.

1.2 Problem Statement

To study the relationship of between ANS and cardiovascular system, the system identification method was applied. This method consists of two types of mathematical representations, linear and nonlinear. Linear approaches are more widely used than nonlinear approaches because there are simple and easy to understand. However, linear approaches have some drawbacks. Linear methods entirely estimate the system behavior around a given operating point. Nonetheless, the whole system should not be determined by operating point. Due to the linear consideration, linear system identification approaches can not analyze the nonlinear coupling in the system. The nonlinear interactions between respiration and heart rate have been proposed [32-33]. Saul et al [32] illustrated the nonlinear interactions between respiration and heart rate. During modulation of heart rate, nonlinear linear dynamics not only influence arterial blood pressure but also affect the instantaneous lung volume (ILV) [33]. Thus, to conduct the autonomic function studies, nonlinear system identification methods can be used to analyze the interactions between respiration and heart rate effectively.

1.3 Challenges

The nonlinear interaction in autonomic control is an integrated trouble to analysis the autonomic heart rate control. Thus, the nonlinear modelings were applied to clear this problem. For previous researches, the applications of nonlinear method are very scarce due to their complexity. There are many hindrances in theoretical foundations and also practical applications. However, the usefulness of nonlinear approaches in cardiovascular evaluation requires the comprehensive and further studies. These reasons inspire us to propose the better nonlinear method for studying the autonomic function.

1.4 Goals of the Thesis

The main objectives of this research study as follows.

1. To study the responses of HRV during handgrip exercise for examine autonomic control by using the power spectral analysis.
2. To evaluate the relationships between the RR interval and arterial blood pressure by using NARMA model.
3. To study the interaction between muscle sympathetic nerve activity and RR interval by using NARMA model.
4. To analyze the effect of autonomic heart rate control and broadband respiration by using NARMA model.
5. To examine the effect of various lower body negative pressure on autonomic control of heart rate.

1.5 Research Outcomes

First of all, the responses of HRV during handgrip exercise can be determined for assessing autonomic control. Next, this research proposed a novel method for assessing the autonomic heart rate control. It provides several advantages. For example, it evaluates the relationships between the RR interval-arterial blood pressure (ABP) and muscle sympathetic nerve activity-RR interval. It determines the interaction between respiration and RR interval. This model provides a suitable result

to predict the RR interval by using broadband respiration. Moreover, RR interval can be evaluated during the various lower body negative pressures.

1.6 Thesis Organization

This thesis is organized as follows:

- Chapter I: *Introduction* consists of the background, problem statement, challenges, goals of this thesis and research outcomes.
- Chapter II: *Literature Review* briefs on physiology of ANS, cardiovascular system. The system identification method and related work are also discussed in this chapter.
- Chapter III: *Materials and Methods* propose the schematic of the experimental design. It consists of data collection, preprocessing, model analysis, model validation.
- Chapter IV: *Experimental Results* provide the consequence of model validation and model prediction.
- Chapter V: *Discussion* affords comments and suggestions for revision or improvement model.
- Chapter VI: *Conclusion* gives a summarization of this research.

CHAPTER II
LITERTURE REVIEW

This chapter consists of 3 parts. The first part explains brief reviews of physiology of ANS cardiovascular system. The next part describes a frequent system identification method for assessing relationship between cardiovascular control and autonomic nervous system. The related works are shown in the last part of this chapter. The advantages and disadvantages of each model are also discussed in this part.

2.1 Anatomy and physiology

In the first part can be classified into 3 sections. Each section explains short reviews of anatomy and physiology of autonomic nervous system, cardiovascular system and respiratory system, respectively.

2.1.1 Autonomic nervous system (ANS)

Autonomic nervous system (ANS) is the subdivision of the nervous system. It provides involuntary regulation of smooth muscle, cardiac muscle and glandular activity or secretion [1]. Figure 2.1 shows the anatomy of the ANS, there is a synapse between central nervous system (CNS) and peripheral effector. The preganglionic motor neuron in the CNS, transmit an efferent nerve to autonomic ganglia outside the CNS through their axons, known as preganglionic fibers. In these ganglia, there are synapses between preganglionic fiber and ganglionic neurons. The axons of ganglionic neurons, called the postganglionic fiber stimulate the cardiac muscle, gland and fat cells.

The ANS can be divided into 2 subsystems: the sympathetic and parasympathetic nervous systems based on anatomical and functional differences. Figure 2.2 summarizes major differences of two subsystems.

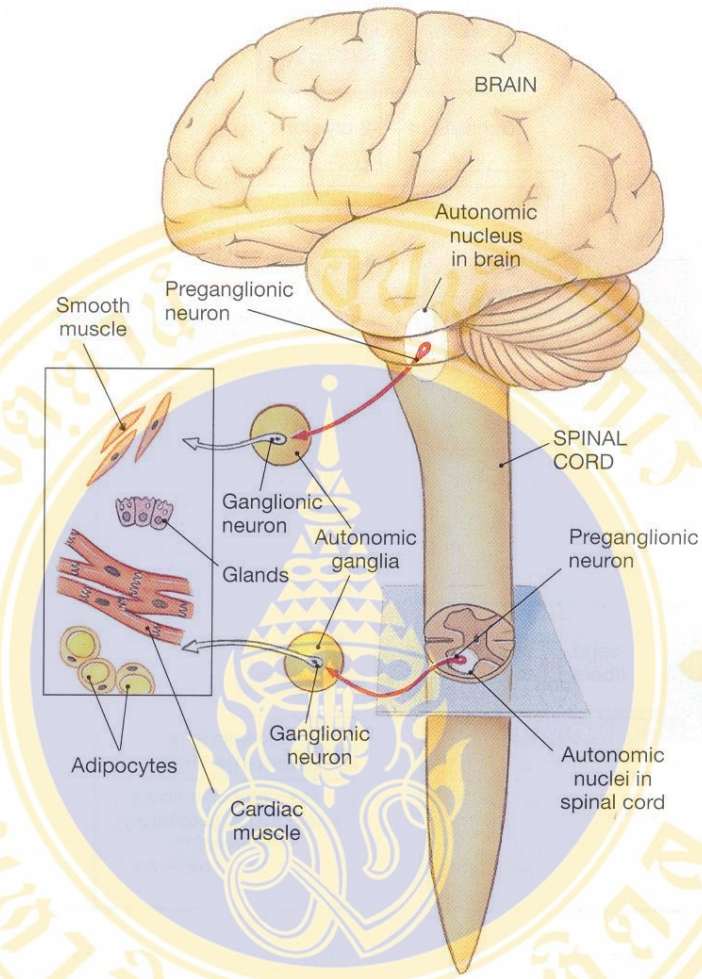

Figure 2.1 Autonomic nervous system.
(adapted from [1])

The sympathetic nervous system is known as “fight or flight” system because it stimulates organs and physiological systems to deal with emergencies. The sympathetic division includes the preganglionic neurons, ganglionic neurons, and specialize neurons inside the adrenal gland. The preganglionic neurons of sympathetic division lies between the vertebrae segments T_1 and L_2. The ganglionic neurons are near the spinal cord. The preganglionic neurons connect to ganglia via the preganglionic fiber. At the preganglionic synapse, acetylcholine (Ach) is released to stimulate ganglia neuron. After stimulation at ganglia, the norepinephrine (NE) and

epinephrine (E) are released at postganglionic synapse. Then, the signal is transmitted to the next nerve or organ.

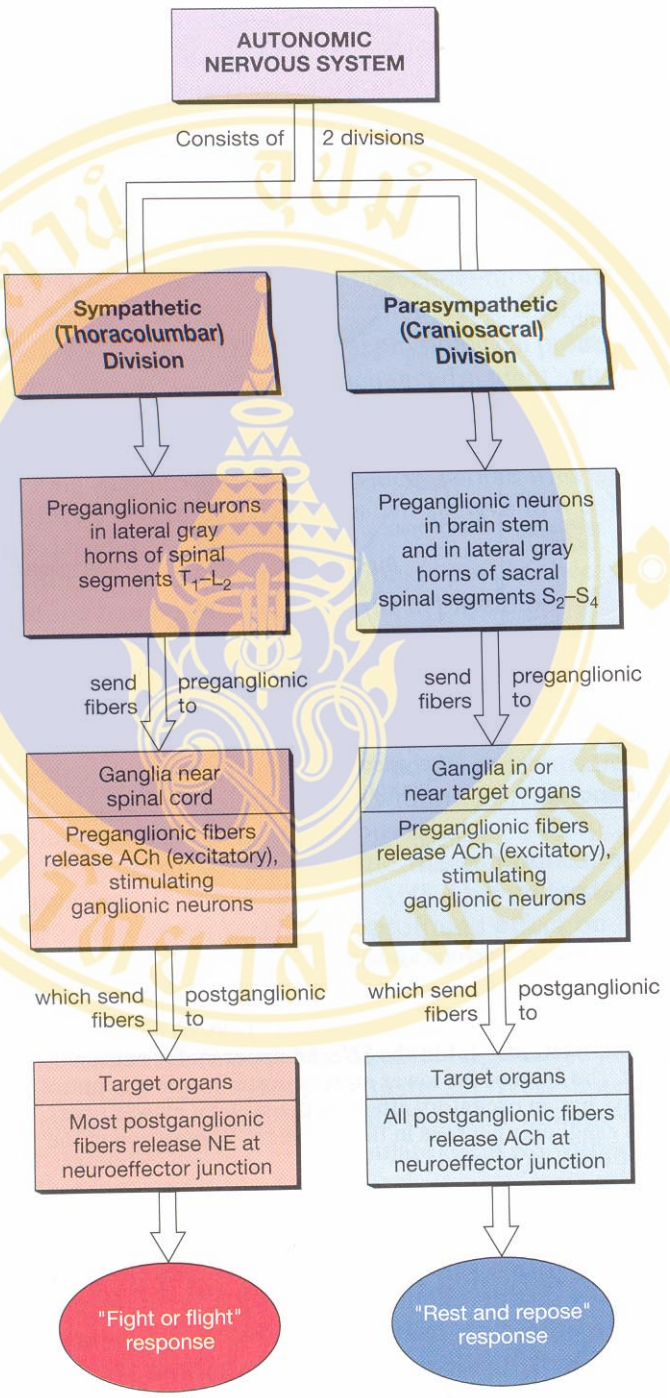

Figure 2.2 Division of the autonomic nervous system.
(adapted from [1])

On the other hand, the parasympathetic is frequently referred as the “rest and repose” system because it slows and relaxes roles of organs and body systems. The parasympathetic division also consists of the preganglionic neurons and ganglionic neurons. The preganglionic neurons of parasympathetic division lie between brain stem and sacral segments of the spinal cord. The ganglionic neurons locate within or next to target organ. The preganglionic neurons connect to ganglia via the preganglionic fiber. The neurotransmitter, Ach, is released to stimulate ganglia neuron at preganglionic synapse. After stimulation at ganglia, the Ach are released at postganglionic synapse and the signal is carried to the next nerve or organ. The responses of various organs to sympathetic and parasympathetic nervous system are summarized in Table 2.1.

Table 2.1 The effects of sympathetic and parasympathetic nervous system on various organs. (adapted from [1])

Structure	Sympathetic innervation effect	Parasympathetic innervation effect
EYE	Dilation of pupil Focusing for the distance vision	Constriction of pupil Focusing for near vision
SKIN Sweat glands Arrector pili muscles	 Increase secretion Contraction, erection of hairs	 None (not innervated) None (not innervated)
TEAR GLANDS	None (not innervated)	Secretion
CARDIOVASCULAR SYSTEM Blood vessels Heart	 Vasoconstriction and vasodilation Increases heart rate, force of contraction, and blood pressure	 None (not innervated) Decreases heart rate, force of contraction, and blood pressure

Table 2.1 The effects of sympathetic and parasympathetic nervous system on various organs. (Cont.) (adapted from [1])

Structure	Sympathetic innervation effect	Parasympathetic innervation effect
ADRENAL GLANDS	Secretion of epinephrine and norepinephrine by adrenal medullae	None (not innervated)
RESPIRATORY SYSTEM Airways Respiratory rate	 Increases diameter Increases rate	 Decreases diameter Decreases rate
DIGESTIVE SYSTEM General level of activity Liver	 Decreases activity Glycogen break down, glucose synthesis and release	 Increases activity Glycogen synthesis
SKELETAL MUSCLES	Increase force of contraction, glycogen break down	None (not innervated)
URINARY SYSTEM Kidneys Bladder	 Decreases urine production Constricts sphincter, relaxes urinary bladder	 Increases urine production Tenses urinary bladder, relaxes sphincter to eliminate urine

2.1.2 Cardiovascular system

The function of the cardiovascular system is mainly transports of substances such as food, hormones, metabolic wastes, and gases (oxygen, carbon dioxide) to and from cells. Moreover, it has an important role to maintain body temperature and pH (part of homeostasis). The basic components of the cardiovascular system are

circulating fluid (blood), conducting pipes (blood vessels such as arteries, veins, and capillaries) and a pump (the heart) [1]. The cardiovascular system consists of a pulmonary circuit and a systemic circuit. The pulmonary circuit transports blood to and from lungs whereas blood from the rest of body is carried by the systemic circuit. Both of these circuits start and stop at the heart. An overview of the cardiovascular system is shown in figure 2.3.

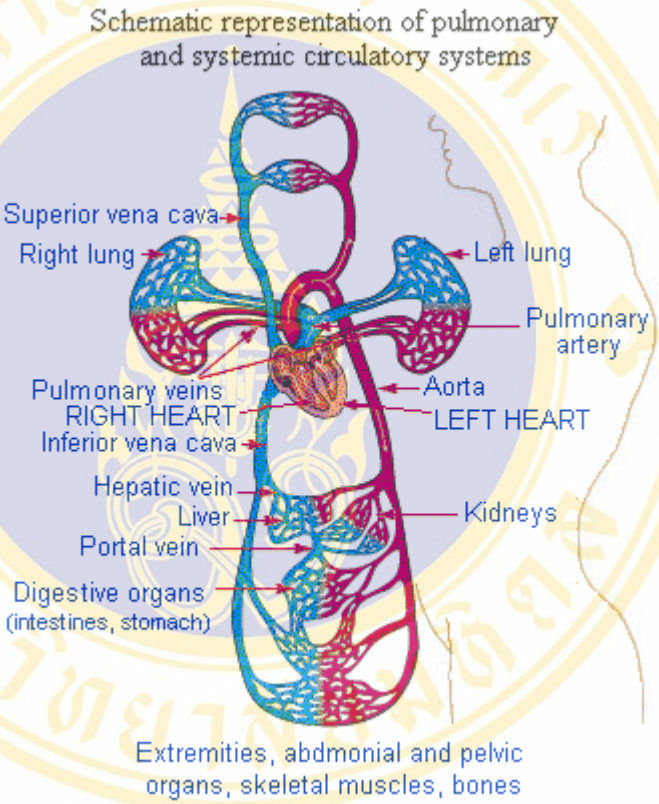

Figure 2.3 An overview of the cardiovascular system.
(adapted from http://webschoolsolutions.com/patts/systems/heart.htm)

In pulmonary circuit, beginning of the right atrium obtains deoxygenated blood from the systemic circuit via the inferior and superior vena cavae. The blood are passed to the right ventricle through the tricuspid valve, which has three flaps (or cusps) of tissue. In right ventricle, blood is pumped to pulmonary veins via the pulmonary or semilunar valve, which consists of three half-moon-shaped flaps. The blood is passed through pulmonary arteries to the lungs. The main function of lungs is to exchange carbon dioxide and oxygen. The lungs transmit oxygenated blood to the

left atrium via pulmonary vein, ending the pulmonary circuit. The systemic circuit begins at the left ventricle. The oxygenated blood is transported to the left atrium to left ventricle via mitral valve, which has two flaps (or cusps) of tissue. Then blood is pumped into the aorta through the aortic valve, which has a semilunar shape. The aorta consists of a lot of branches; blood is passed to the rest of body via these branches. Finally, the deoxygenated blood returns to the right atrium via inferior and superior vena cavae, finishing the systemic circuit.

The main function of the cardiovascular system mostly relates with the heart. Each heart contraction pumps blood to the whole body. To ensure that the blood is pumped in the right time and the right places, the heart has to have a special muscle, known as cardiac muscle. The cardiac muscle can be divided into: contractile cells and specialized cardiac muscles and called conducting system. Firstly, the contractile cells have an important function to contract for moving the blood. The other is conducting system; the function of this system is to control the contractile cells. The conducting system consists of the sinoatrial node (SA node), atrioventicular node (AV node), AV bundle, the bundle branches and the Purkinje fibers. The component of the conducting system of heart is summarized in figure 2.4.

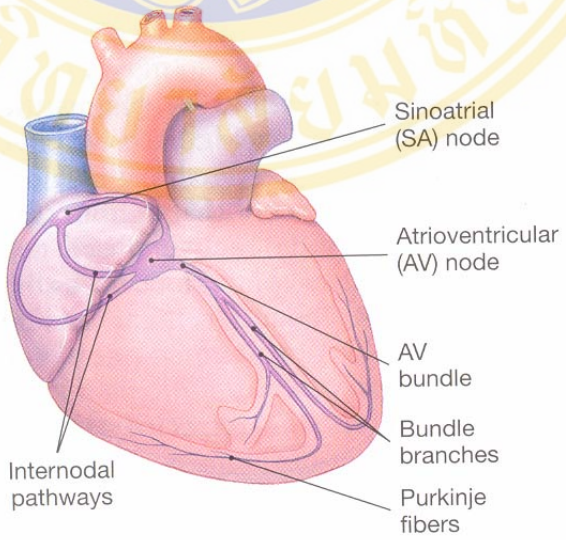

Figure 2.4 The conducting system of the heart.
(adapted from [28])

The impulse conduction through the heart consists of 5 steps. This process is summarized in figure 2.5. Firstly, beginning with the activation of the pacemaker, which is in the SA node, produces 60-100 action potentials per minute. Secondly, the action potentials from SA node are sent to the AV node through three different paths of conducting cell in atrial wall. The elapsed time in this process is 50 msec. For the next step, the impulse spreads over the cardiac muscle of the left and right atria causing atrial contraction. At the AV node, the impulse is delayed for about 100 ms. As a consequence of this time delay, the simultaneous contraction of atrium and ventricle is presented. The elapsed time is now150 ms. Next in the order, the impulse is sent through the interventricular septum via AV bundle. At this point, it is divided to left and right bundle branches, which are located in the inner surface of the left and right ventricles, respectively. The signal reaches to the Purkinje cell and the elapsed time become 175 ms. Finally, it is sent to the contractile cells of ventricular myocardium and the elapsed time is 225 ms. Ventricular contraction occur 75 ms, after the atrium contraction is ended,. The amount blood driven by a single ventricular contraction is known as the stroke volume (SV).

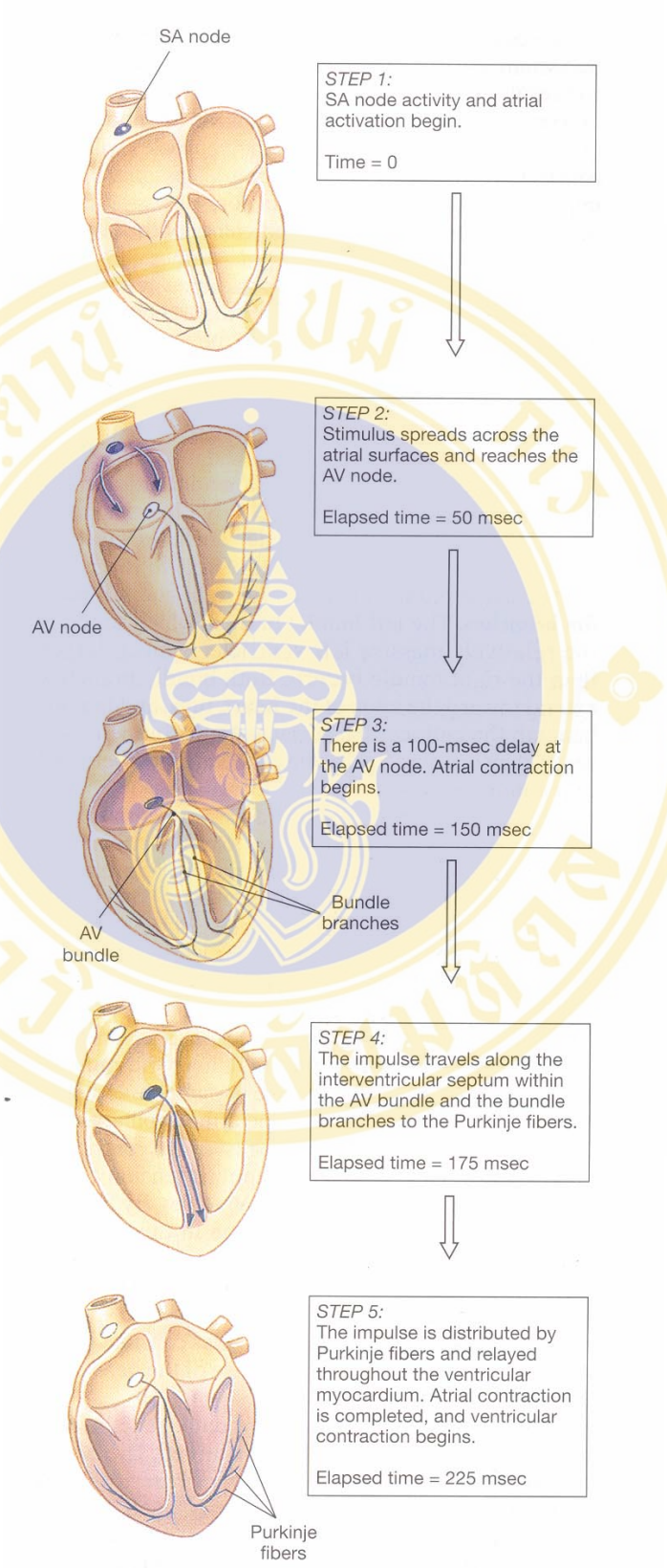

Figure 2.5 The impulse conduction through the heart.

(adapted from [1])

Electrical activity in the heart can be detected on the body surface and the recording of these signals is called the electrocardiogram (ECG and EKG) [1]. The ECG of a normal heart beat consists of: a P wave, a QRS complex and a T wave, as shown in figure 2.6.

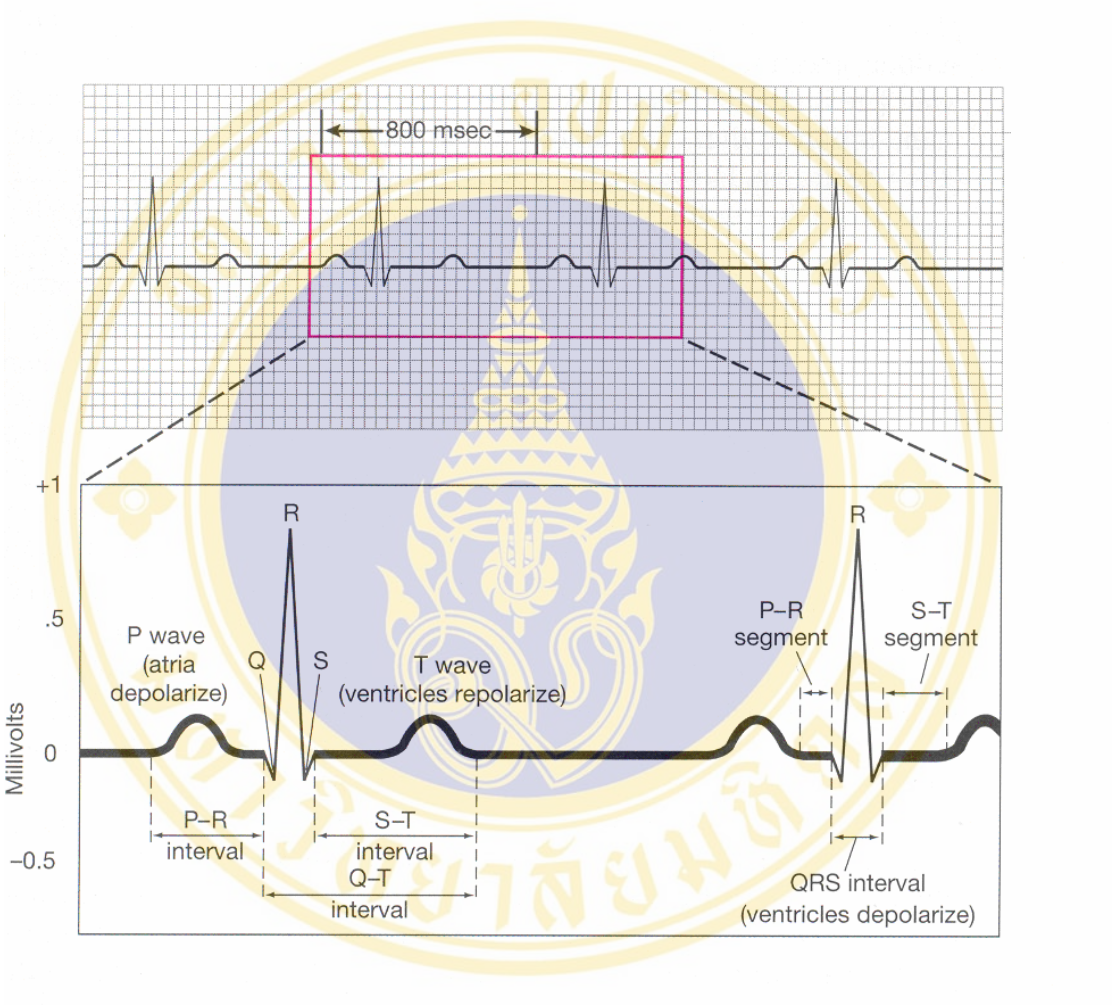

Figure 2.6 The Eletrocardiogram.
(adapted from [1])

The P wave represents the depolarization of the atria. The QRS complex signifies the ventricular depolarization. The T wave displays the ventricular repolarization. The ECG analysis is used for assessing abnormal cardiac activity, for example, myocardial (cardiac muscle) defects, enlargement of the heart, congenital defects, heart valve disease, arrhythmias (abnormal rhythms), tachycardia (heart rate too fast) or bradycardia (too slow), ectopic heartbeat, coronary artery disease, inflammation of the

heart (myocarditis), changes in the amount of electrolytes (chemicals in the blood), present or impending heart attack.

The principal function of the cardiovascular system is to maintain that the blood flows at the right time and to the right area. The factors that control this system can be classified into primary and secondary factors. The primary factors are blood volume reflex, autonomic innervations, and hormones. The secondary factors are the concentration of ions in the extracellular fluid and body temperature. These factors are summarized in figure 2.7.

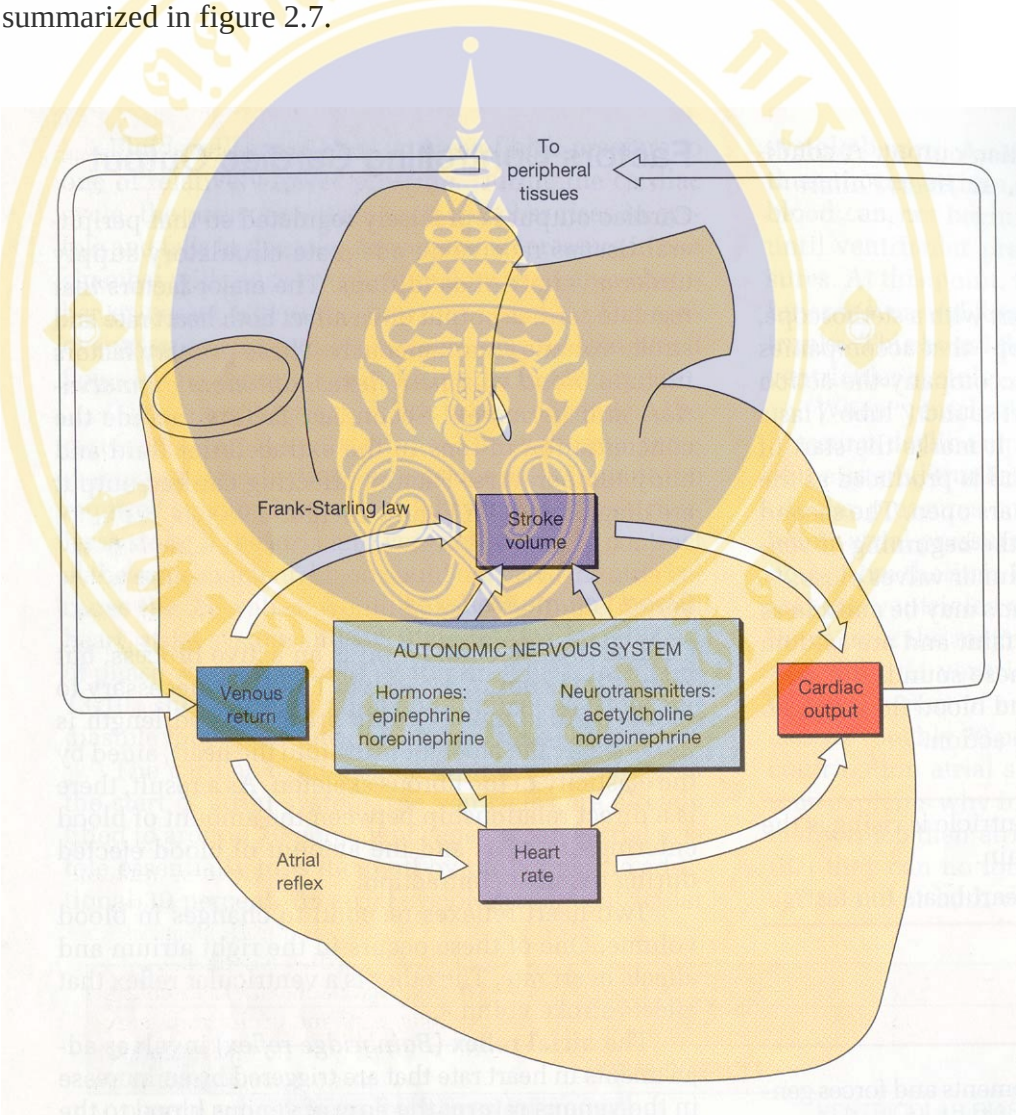

Figure 2.7 Factors affecting cardiac output.
(adapted from [1])

The first primary factor is blood volume reflex. Blood volume reflex consists of atrial reflex and ventricular reflex, which reacts the alteration in blood volume. The arterial reflex affects to cardiac output by increasing heart rate after an increasing venous return (the flow of venous blood to the heart); due to mechanical and neural factors. The ventricular reflex affects to stoke volume, when the venous return increase, the force of ventricular also increase, known as Frank-Starling law.

The second of primary factors is autonomic innervation and hormones. Both sympathetic and parasympathetic division of ANS influences the activity of the heart as shown in figure 2.8.

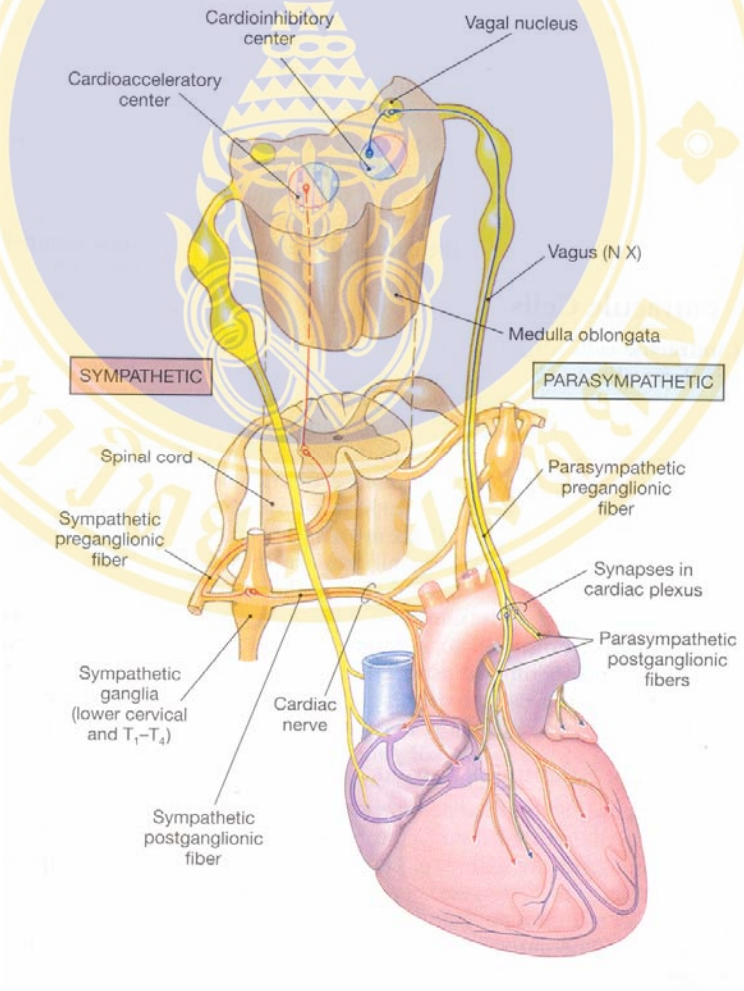

Figure 2.8 Autonomic innervations of the heart.
(adapted from [1])

For sympathetic division, the postganglionic sympathetic neurons locate in the cervical and upper thoracic ganglia. The vagus nerve conducts the parasympathetic preganglionic fibers to ganglia in the cardiac plexus. Both sympathetic and parasympathetic stimulate both the SA node, AV node, the atrial and ventricular cardiac muscle cells. The autonomic innervation affects to both heart rate and stroke volume to adjust cardiovascular function. These sympathetic neurons release the norepinephrine (NE) to increase heart rate and stroke volume. The parasympathetic neurons release the acetylcholine (ACh) to decrease heart rate and stroke volume. The epinephrine (E) and norepinephrine (NE) are hormones that are released by adrenal medullae to increase heart rate and stroke volume during sympathetic activation.

2.1.3 Cardiovascular regulation

The main function of the cardiovascular system is to maintain blood flow at the right time and area. There are 3 factors that affect cardiovascular regulation, as shown in figure 2.9: local factor (autoregulation of blood flow), neural mechanism and endocrine factors.

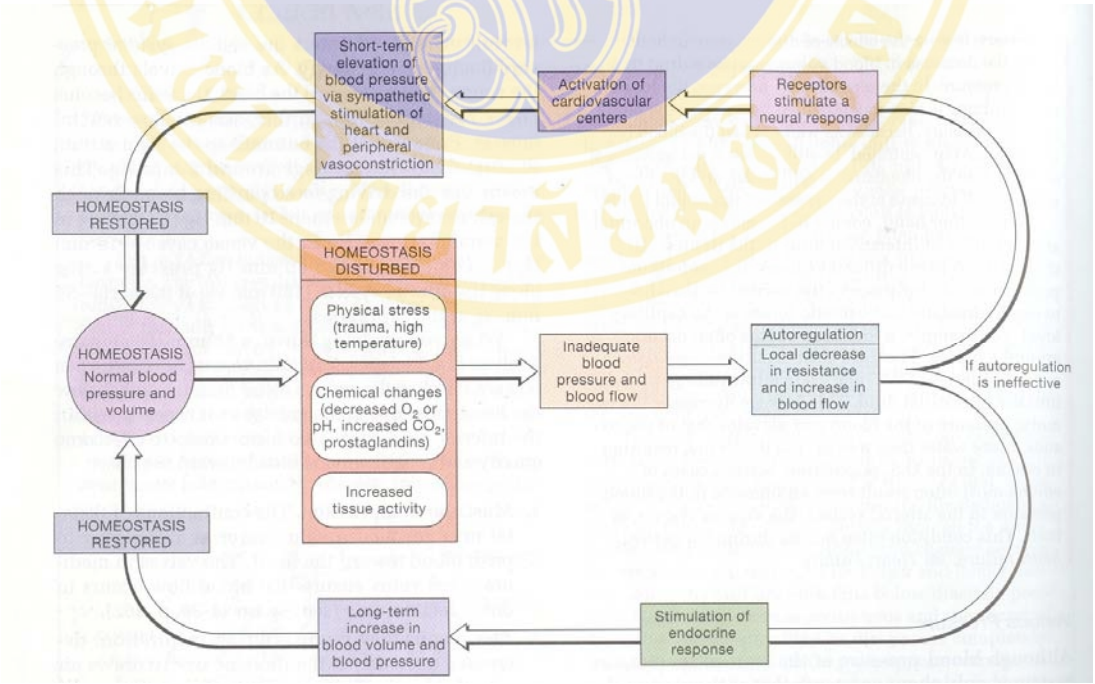

Figure 2.9 Local, neural and endocrine adjustments that maintain blood pressure and blood flow. (adapted from [1])

Local factor (autoregulation of blood flow) involves chemical changes in the interstitial fluid. In the resting condition, cardiac output still unchanged but peripheral resistance of each tissue is changed to maintain blood flow. A precapillary sphincter is the important factor to control blood flow. If it contracts, blood flow decreases; if it relaxes, blood flow increases. The local environment also influences the precapillary sphincter. For example, when oxygen levels increase, smooth muscle cells in the precapillary sphincter constrict and reduce the flow of blood. On the other hand, when oxygen levels falls, carbon dioxide levels increases, and the pH decreases, smooth muscle cells in the precapillary sphincter are induced relax and increasing blood flow. Other specific chemicals in the intestinal fluids affect to contraction of the precapillary sphincter. For example in the inflammation response, vasodilation occurs at an injury site because histamine, bacterial toxins, and prostaglandins also induce a relaxation of the precapillary sphincter. The factors that influence relaxation of precapillary sphincter are called vasodilators. The factors affect to contraction of precapillary sphincters are known as vasoconstrictors.

The other factor that affects cardiovascular regulation is neural mechanism. The nervous system maintains blood flow by adjusting the cardiac output and peripheral resistance. These factors are controlled by cardiovascular centers such as a cardiac centers and vasomotor centers of the medulla oblongata. The cardiac centers such cab de divided into cardioacceleratory and cardioinhibitory center. The cardioacceleratory centers enhance cardiac output via sympathetic innervation but the cardioinhibition centers decrease the cardiac output via parasympathetic nervous system. The vasomotor centers function is to adjust the peripheral resistance and it can be classified into vasodilation, vasoconstriction and venoconstriction. Vasodilation occur when the vasomotor centers are inhibited, they decrease peripheral resistance by increasing diameter of arterioles. Not only vasoconstriction but also venoconstriction increase peripheral resistance when the vasomotor centers are stimulated, by compressing the peripheral arterioles and veins, respectively.

In cardiovascular system, there are autonomic reflex that react to the alteration in blood pressure and chemical composition. These autonomic reflex are baroreflex and chemoreceptor .

The baroreceptor functions are to maintain arterial pressure by adjusting the cardiac output and peripheral resistance. Baroreceptors measure the change in the wall of distensible organ. They can be divided into aortic baroreceptors, carotid sinus baroreceptors and atiral baroreceptors.

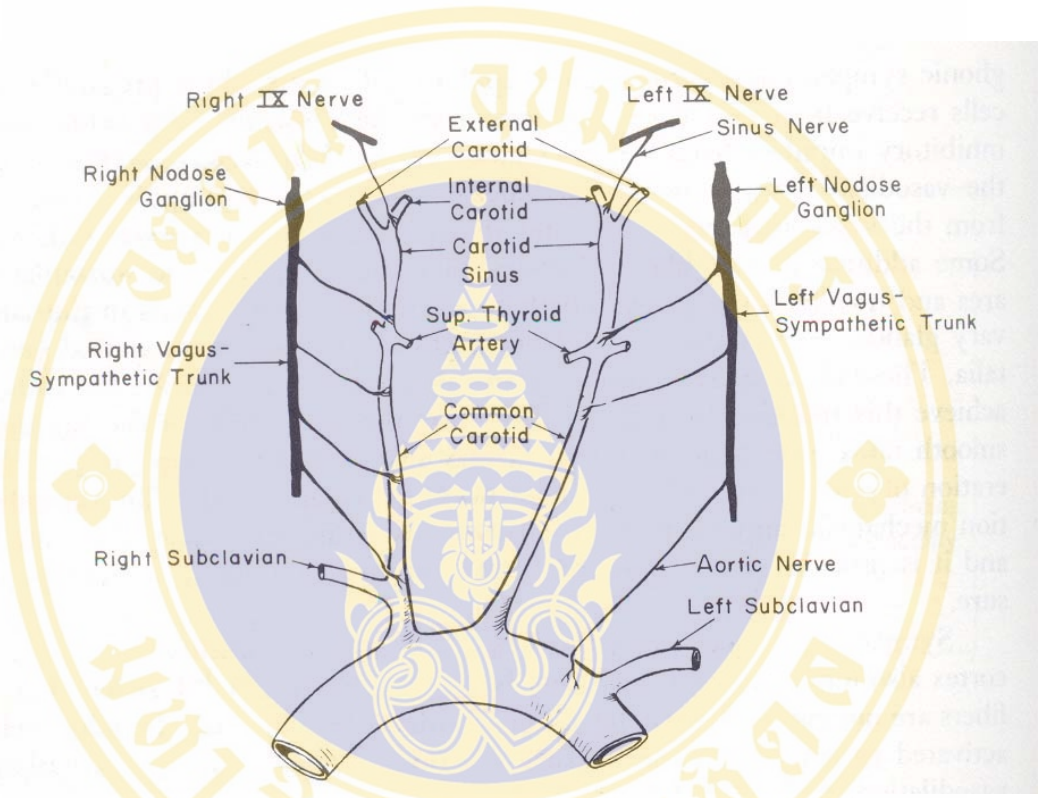

Figure 2.10 Diagrammatic representation of major arterial baroreceptors. (adapted from [34)

Aortic baroreceptors discover the location within the aortic sinuses; they measure the pressure change in aorta. Carotid sinus baroreceptors are located in the walls of the carotid sinuses and they are very sensitive because they measure the pressure change in brain. Both aortic and carotid sinus baroreceptors are undifferentiated terminal nerve fiber [34]. Their diameter is or less than 5 μ and their branch extent in the adventitial and medial of the wall. Fibers from carotid sinus baroreceptors connect to the sinus and glossopharyngeal nerves but the fiber from the aortic baroreceptors attach to the vagus nerve [34]. The end of fiber from both aortic and carotid sinus is in vasomotor area in medulla oblongata.

The last one is the atrial baraoreceptors. They are located in the wall of the right atrium. These receptors differ from the aortic and carotid sinus because they deal with blood pressure in atrium. When the pressure in atrium rises, the cardioaccelertor center is stimulated by atrial baroreceptors until the atrial pressure return to normal.

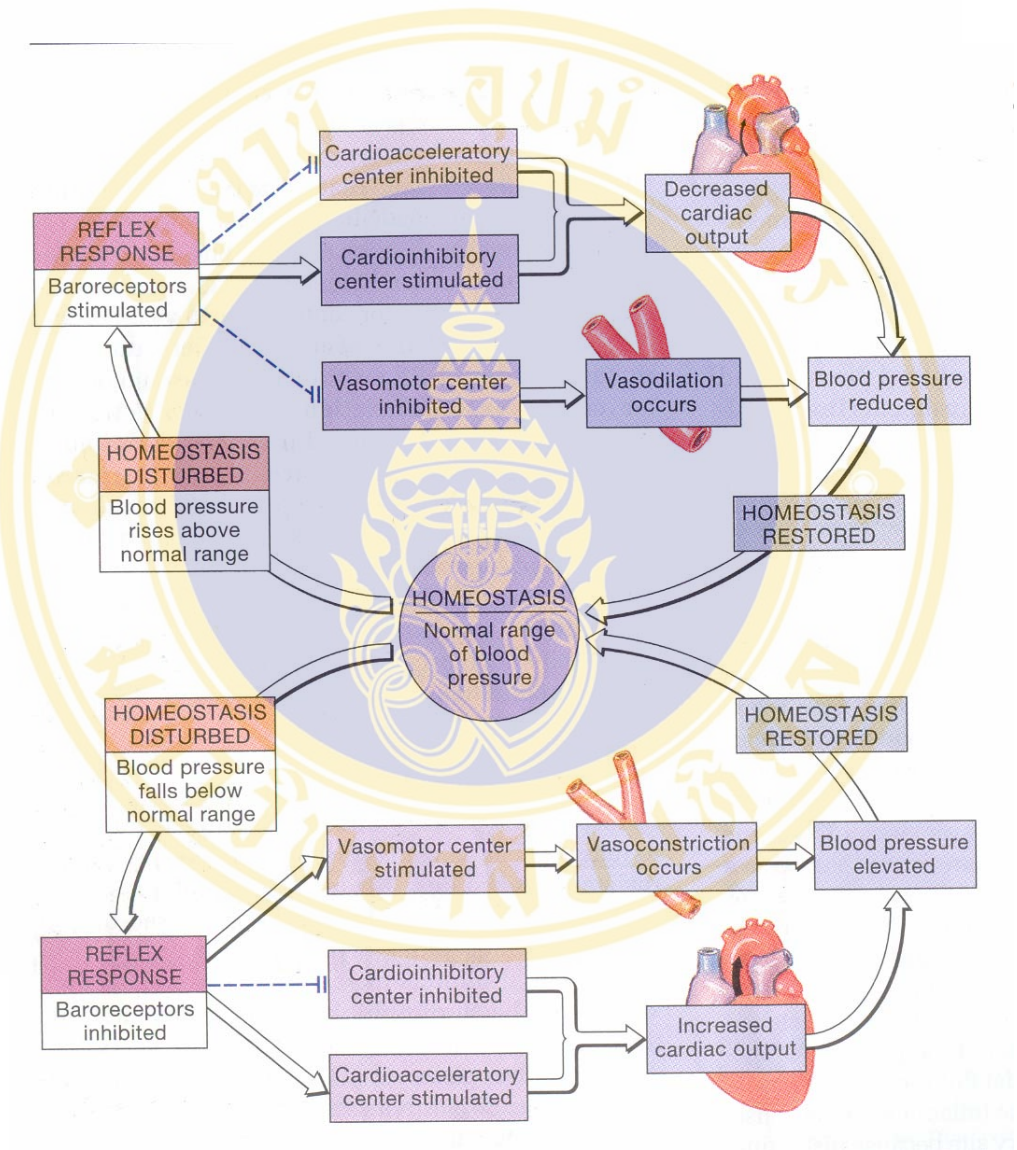

Figure 2.11 The carotid and aortic sinus baroreceptor reflex.
(adapted from [1])

The baroreceptors are stimulated when there is alteration in blood pressure. When blood pressure increases above normal range, baroreceptors are excited. They

send this information to the medulla oblongata. The medulla oblongata inhibits the cardioacceleratory center, stimulates the cardioinhibitory center to decrease the cardiac out put. They also inhibits vasomotor to reduce peripheral resistance. Finally, blood pressure is reduced into normal range as shown in figure 2.11. On the other hand, when blood pressure falls below normal range, baroreceptors are inhibited. The medulla oblongata stimulates the cardioacceleratory center, inhibits the cardioinhibitory center to increase cardiac output. The vasomotor centers are stimulated to increase peripheral resistance. In the final manner, blood pressure is restored to the normal range.

The chemoreceptor affects the alteration in the carbon dioxide levels, oxygen levels, or pH in the blood and cerebrospinal fluid. The chemoreceptor monitors the arterial blood pressure and they can be divided into carotid bodies and aortic bodies. They are located in close proximity in the carotid sinus and aortic arc [34]. Sensory nerves of these receptors connect to both the respiratory and cardiovascular centers in medulla oblongata [34]. Thus chemoreceptors affect to both pulmonary ventilation and peripheral resistance [34]. The other type of chemoreceptor is found on the ventrolateral surfaces of medulla oblongata. Their function is to measure the composition of cerebrospinal fluid. The mechanism of chemoreceptor starts when a decreased O_2, pH or increased CO_2 levels. The reflex response activates the cardioacceleratory center and inhibits the cardioinhibitory centers to increase cardiac output. The vasomotor centers are stimulated to increase the peripheral resistance. The respiratory centers are also stimulated to increase respiratory rate. As a result, the accelerating tissue blood flow increase O_2 and pH until the homeostasis is restored as shown in figure 2.12.

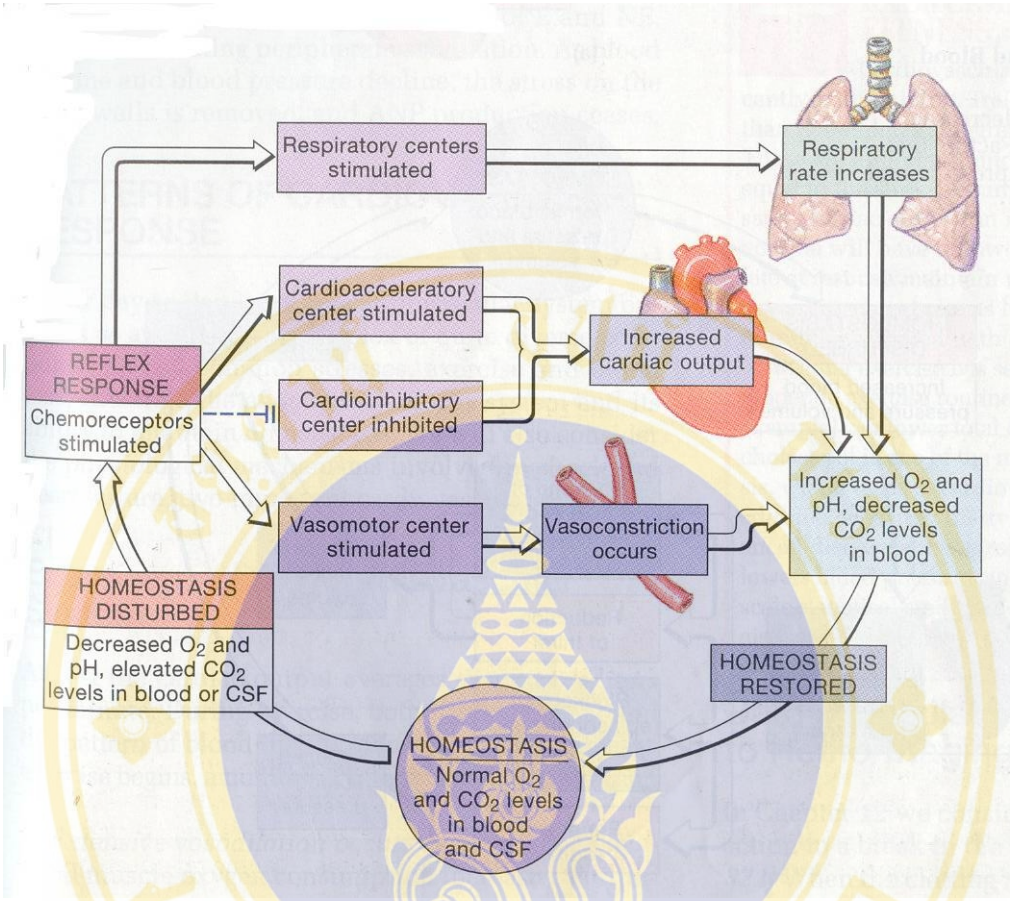

Figure 2.12 The chemoreceptor reflex.
(adapted from [1])

The last factor that influences cardiovascular regulation is hormones. Hormones affect the cardiovascular fluctuation in both short term and long term regulation. Hormones, influencing the short term regulation, are epinephrine (E) and norepinephrine (NE). Both epinephrine (E) and norepinephrine (NE) relate with cardiac output and peripheral resistance as discussed above. Hormones that affect the long term regulation, are antidiuretic hormone (ADH), angiotensin II, erythropoietin (EPO), and atrial natriuretic peptide (ANP). These hormones are associated with long term regulation of blood pressure and volume.

2.1.4 Respiratory system

The respiration system consists of the upper and the lower respiratory system. The upper respiratory system consists of the nose, nasal cavity, and sinuses. The

lower respiratory system involves the pharynx (throat); the larynx (voice box); the trachea (windpipe), the bronchi and bronchioles (conducting passageways) and the alveoli (exchange surface of the lungs) as shown in figure 2.13. The main functions of respiration are giving an area for gas exchange between air and circulating blood, moving air to and from the exchange surface of lung, saving respiration surfaces from environmental variations and protecting the respiratory system and other tissues from invasion by pathogen, allowing vocal communication and giving olfactory sensation in CNS [1].

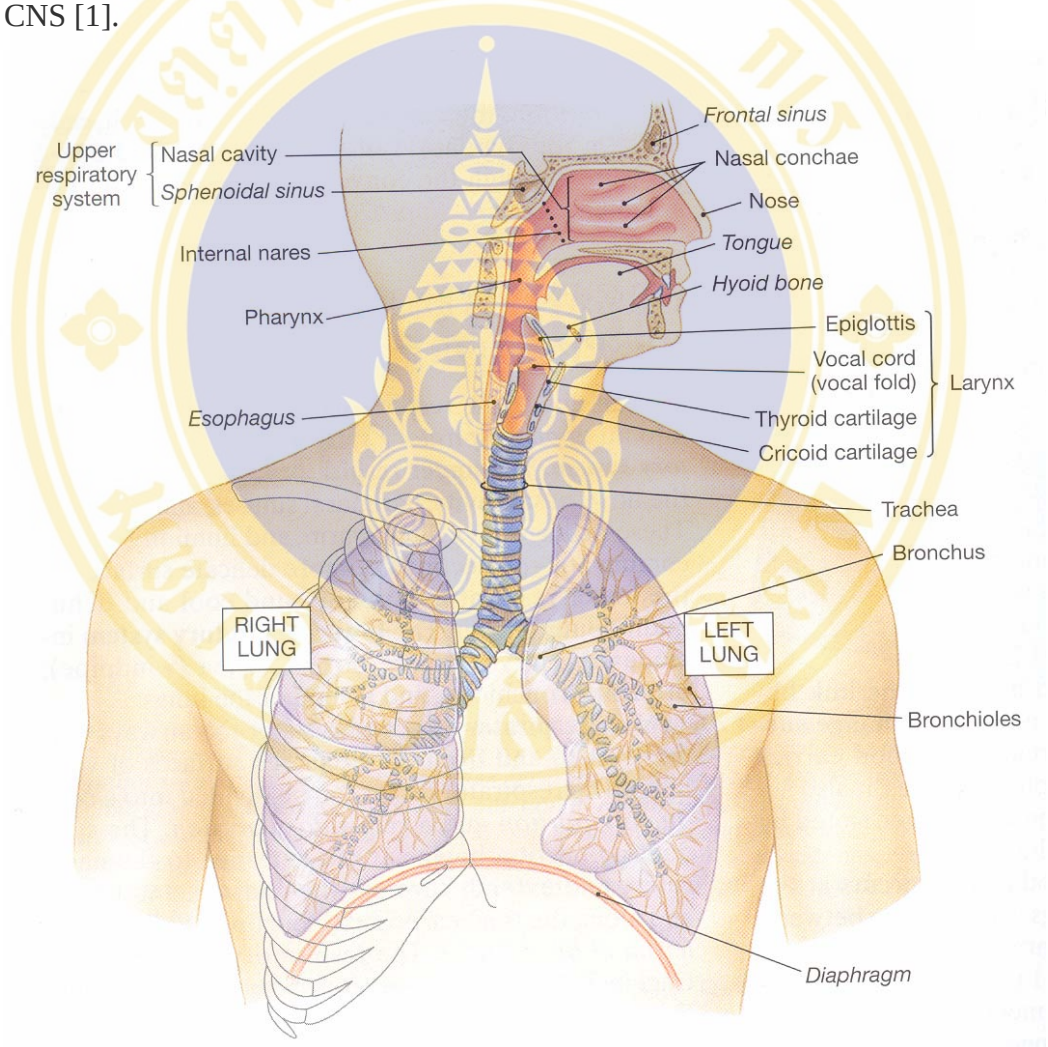

Figure 2.13 The components of the respiratory system.
(adapted from [1])

The routine of the respiration consists of four phases [1]. The first phase is pulmonary ventilation or breathing, which is the physical movement of air into and

out of lungs. The second phase is gas diffusion across the respiration membrane, which isolates the alveolar air from the blood within the alveolar capillaries. The third phase is the storage and transport of oxygen and carbondioxide between the alveolar capillary and capillary beds in the other tissues. The last phase is the exchange of dissolved gases between the interstitial fluids and blood.

The activity of respiration has important functions that describe above. The factors that affect control of the respiration are [1]

1. Local regulation compensates for small oscillations affecting individual tissues and organs; large scale or extended changes require the integration of cardiovascular and respiratory responses.

2. Local factors regulate blood flow (perfusion) and air flow (ventilation). Alveolar capillaries constrict under conditions of low oxygen, and bronchioles dilate under conditions of high carbon dioxide.

3. The respiratory centers include three pairs of nuclei in the reticular formation of the pons and medulla oblongata. The respiratory rhythmicity centers set the pace for respiration. The apneustic centers cause strong, sustained inspiratory movement and the pneumotaxic centers inhibit the apneustic centers and promote exhalation.

4. The inflation reflex prevents overexpansion of the lungs during force breathing. The deflation reflex stimulates inspiration when the lungs are collapsing. Chemoreceptor respond to changes in the P_{o2} and P_{co2} of the blood and cerebrospinal fluid.

5. Conscious and unconscious thought processes can affect respiration by affecting the respiratory centers.

In this section, the anatomy and physiology of ANS, cardiovascular system, cardiovascular regulation and respiratory system are discussed. These systems are not independent and very complex. Thus, the system identification approaches are considered to accessing this mechanism.

2.2 System identification

System identification approaches were applied in cardiovascular regulatory mechanisms for a longstanding tradition. These methods try to fit the parameters in

the used model by using the input-output data pairs. Recently, Ljung L. proposed the scheme of system identification as shown in figure 2.14 [35].

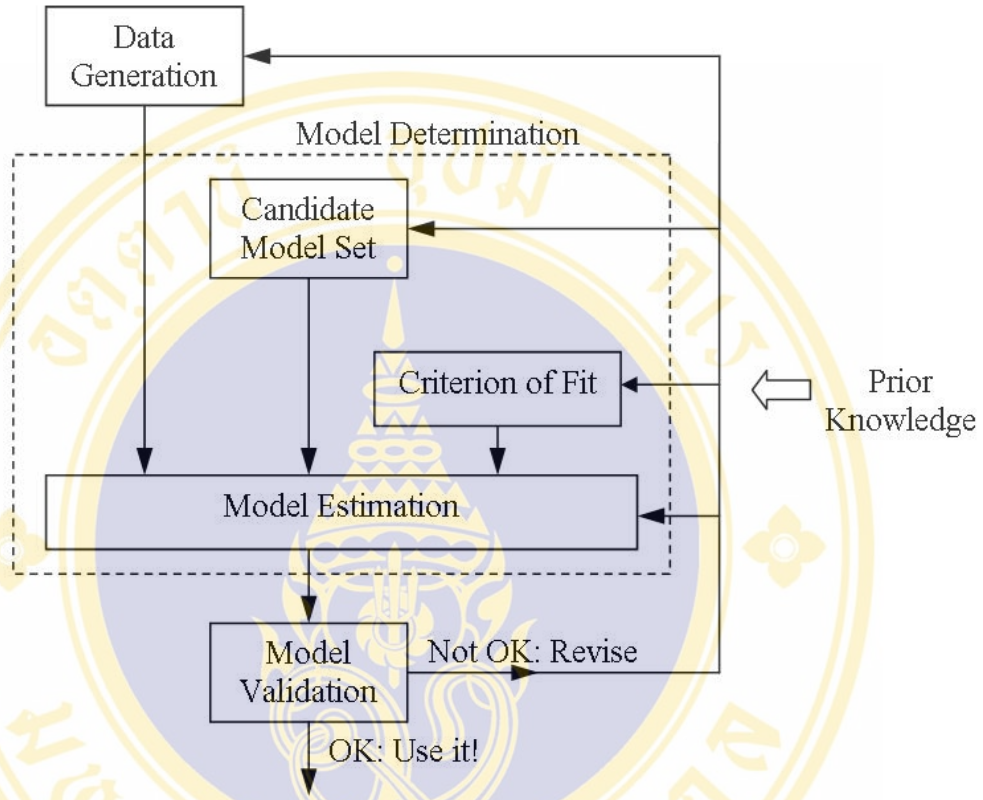

Figure 2.14 Scheme of system identification (adapted from [29])

There are three basic steps in system identification method; (1) data generation, (2) model determination, and (3) model validation. If the model is not validated, steps (1) and (2) will be repeated. The parameters in model will be adjusted until the satisfied model validation is obtained. A *priori* knowledge can be put in wherever appropriate in this process.

In this chapter, we will discuss advantages and disadvantages of linear and nonlinear system identification approaches. A number of interesting related works will be presented together with the open problems.

2.2.1 Linear Models

Linear system identification techniques are well-known methods for analyzing fluctuation in cardiovascular system due to their simple computing formulation and results interpretation. Linear system identification can be classified into nonparametric and parametric methods, as described below.

2.2.2 Nonparametric System Identification

Nonparametric system identification methods analyze data without assuming any underlying distribution. This method fits data into a mathematical equation without adjusting parameters. The noncausal Wiener filter is the most popular nonparametric system identification method for identifying fluctuation in the cardiovascular system [36-39]. Wiener filter is a ratio of cross spectrum over the autospectrum of the input and can be defined as

$$H(\omega) = \frac{\hat{S}_{xy}(\omega)}{\hat{S}_{xx}(\omega)} \tag{2.1}$$

where is the $\hat{S}_{xy}(\omega)$ is the cross spectrum between input ($x(n)$) and output ($y(n)$); $\hat{S}_{xx}(\omega)$ is the autospectrum of the input and $H(\omega)$ is called transfer function.

The cross spectrum is the Fourier transform of cross correlation ($\hat{r}_{xy}(k)$). The cross correlation is the mean of a cross product between input and output for a time difference and it defined as [40]:

$$\hat{r}_{xy}(k) = \frac{1}{N}\sum_{n=0}^{N-1} x(n)y(n+k), \qquad k = 0,1,2,...,N-1. \tag{2.2}$$

where k define as the number of time units that the signal y(n) is delayed or lagged, N is the length of signal.

Thus, the cross spectrum defines as [40]:

$$\hat{S}_{xy}(\omega) = \text{DTFT}\,[\,\hat{r}_{xy}(k)\,] \tag{2.3}$$

where DTFT defines as the discrete time Fourier transform.

The autospectrum is the Fourier transform of autocorrelation ($\hat{r}_{xx}(k)$). The cross correlation is the mean of a cross product of input for a time difference and it defined as [40]:

$$\hat{r}_{xx}(k) = \frac{1}{N}\sum_{n=0}^{N-1} x(n)x(n+k), \qquad k = 0,1,2,...,N-1. \tag{2.4}$$

Thus, the autospectrum is[40]:

$$\hat{S}_{xy}(\omega) = \text{DTFT}\,[\,\hat{r}_{xx}(k)\,] \tag{2.5}$$

The output of system can be calculated by using transfer function

$$y(n) = x(n) * \text{IDFT}\,[\,H(\omega)\,] \tag{2.6}$$

where * defines as the convolution operator, IDTFT is the inverse discrete time Fourier transform. Finally, we obtain the output of system by convolution between input and inverse Fourier transform of transfer function.

Generally, transfer function ($H(\omega)$) is a mathematical representation that describes to explain the behavior the input that influences the out put in linear time variant system.

2.2.3 Parametric System Identification

Parametric system identification methods are method that fit data by adjusting the parameters of the mathematical representation. The salient point is that when the system is causal, parametric system identification technique can be classified between the feedforward and feedback close loop system. Thus, this technique is meaningful for computing fluctuations in cardiovascular system. The parametric system identification approach consists of three steps: (1) choosing an appropriate parametric model (usually based on *a priori* knowledge about the process), (2) computing the model parameters, and (3) validating the model by using the obtained parameters [41]. In cardiovascular regulation, the popular parametric method is autoregressive with exogenous input (ARX). This will be presented shortly.

The autoregressive with an exogenous variable is more suitable for assessing cardiovascular regulation because cardiovascular regulation commonly consists of multiple inputs. The autoregressive with exogenous input (ARX) is defined as [41]:

$$y(n) = \sum_{i=1}^{p} a_i y(n-i) + \sum_{i=1}^{q} b_i x(n-i) + e(n). \tag{2.7}$$

where a_i and b_i are the autoregressive and moving average coefficients, respectively; *x(t)* is an exogenous input; *p* and *q* are order of the *y(n)* and *x(n)*, respectively. The

coefficients of the model can be obtained by the least squares minimization of residual error in conjunction with an ARX parameter reduction algorithm [41].

Rearrange the ARX in matrix notation, and it can be written as:

$$\mathbf{y} = \mathbf{H\theta} + \mathbf{e} \tag{2.8}$$

where $\mathbf{y} = [\ y(0)\quad y(1)\quad \ldots\quad y(N-1)]^T$

$\mathbf{e} = [\ e(0)\quad e(1)\quad \ldots\quad e(N-1)]^T$

$\boldsymbol{\theta} = [\ -a(1)\quad -a(2)\quad \ldots\quad -a(p)\quad b(1)\quad b(2)\quad \ldots\quad b(q)\ ]^T$

$$\mathbf{H} = \begin{bmatrix} y(-1) & y(-2) & \ldots & y(-p) & x(-1) & x(-2) & \ldots & x(-q) \\ y(0) & y(-1) & \ldots & y(-p+1) & x(0) & x(-1) & \ldots & x(-q+1) \\ \vdots & \vdots & \vdots & \vdots & \vdots & \vdots & \vdots & \vdots \\ y(N-2) & y(N-3) & \ldots & y(N-p-1) & x(N-2) & x(N-3) & \ldots & x(N-q-1) \end{bmatrix}$$

According to the least squares minimization, thus $\boldsymbol{\theta}$ can be estimated as [41]:

$$\boldsymbol{\theta} = (\mathbf{H}^T\mathbf{H})^{-1}\mathbf{H}^T\mathbf{y} \tag{2.9}$$

Then, we obtained the parameters ($\boldsymbol{\theta}$) of the model; we can rearrange general equations of ARX in Z-transformation as [42]:

$$A(z^{-1})Y(z) = B(z^{-1})X(z) + E(z). \tag{2.10}$$

where $A(z^{-1}) = 1 - a_1 z^{-1} - \ldots - a_p z^{-p}$ and $B(z^{-1}) = b_1 z^{-1} - \ldots - b_q z^{-q}$.

The transfer function of ARX model defines as [42]:

$$H(z) = \frac{B(z^{-1})}{A(z^{-1})} X(z) + \frac{1}{A(z^{-1})} E(z). \tag{2.11}$$

In the final manner, the output of the system can be obtained by convolution input and the inverse Z- transform.

2.2.4 Nonlinear Models

Volterra series is an important model for determining the general nonlinear input-output relationship. The Volterra series consist of an infinite sum of multidimensional convolutions of increasing order [43]. This series can be written as a generalization of linear convolution as the following [43]:

$$y(n) = h_0 + \sum_{i=0}^{N} h_1(i)x(n-i) + \sum_{i_1=0}^{N}\sum_{i_2=0}^{N} h_2(i_1,i_2)x(n-i_1)x(n-i_2) + \ldots . \tag{2.12}$$

where h_0, h_1, $h_2(n_1,n_2)$, … be the Volterra kernels. The zero-order constant kernel h_0 stands for the system response to zero input whereas the first-order kernel h_1 represents the linear convolution sum. The higher order kernels are defined as nonlinear interaction effects.

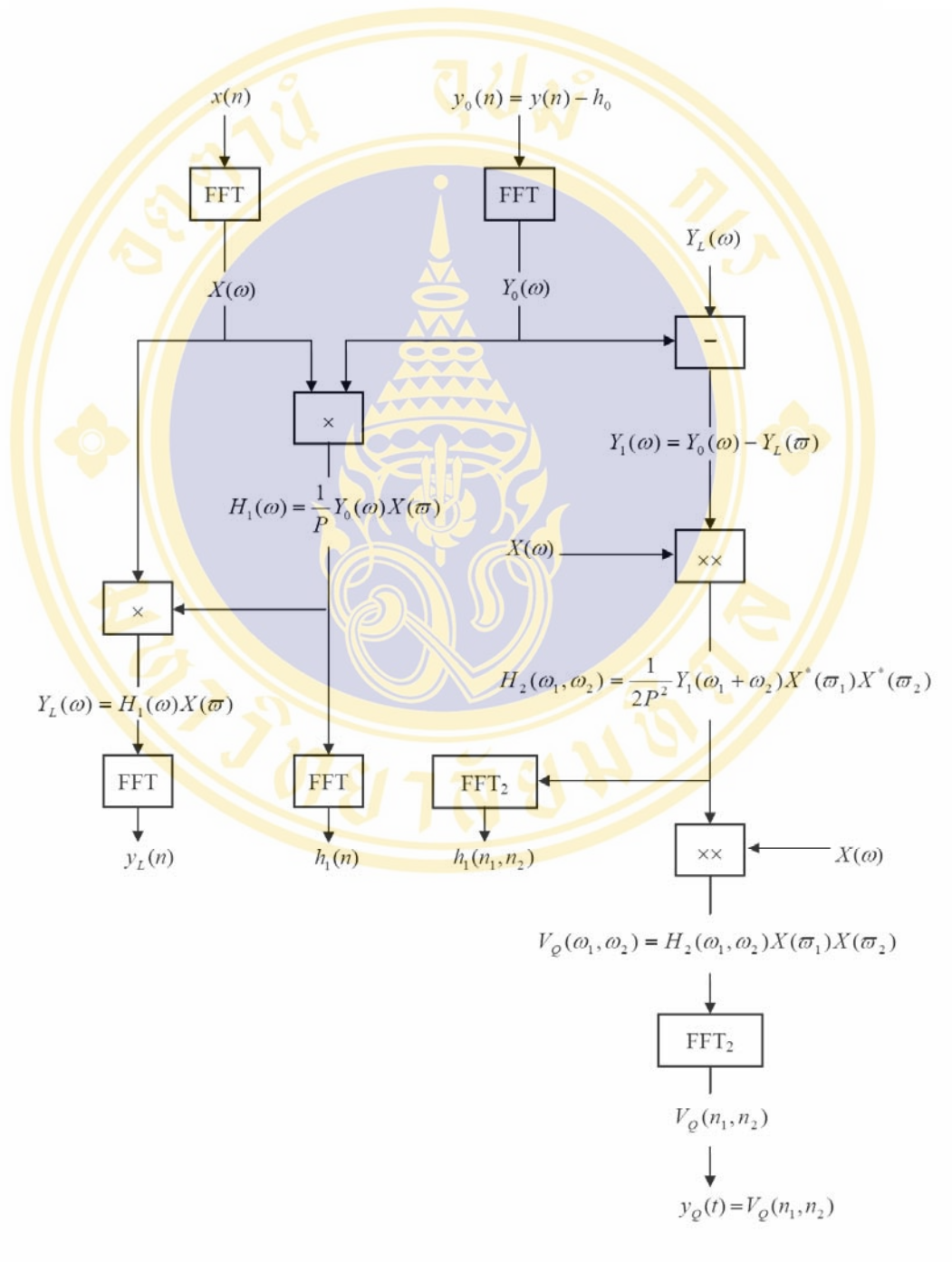

Figure 2.15 Scheme of Volterra Model
(adapted from [43])

For example, we consider the second order of Volterra series, Eq. (2.12) become [44]:

$$y(n) = h_0 + \sum_{i=0}^{N} h_1(i)x(n-i) + \sum_{i_1=0}^{N}\sum_{i_2=0}^{N} h_2(i_1,i_2)x(n-i_1)x(n-i_2) \quad (2.13)$$

To compute the second order kernel in Volterra model, Marmarelis et al [44] applied the frequency domain approach by using fast Fourier transform algorithm to estimate these kernels as shown in figure 2.15. The h_0 is the mean of $y(n)$. The h_1 can be computed by using Eq. (2.1) and linear response ($y_L(n)$) can be compute by convolution between $x(n)$ and h_1. The second order kernel (h_2) is quite complex and has several steps. First, the zero order response residual ($y_0(n)$) are computed by subtracting y(n) with h_0:

$$y_0(n) = y(n) - h_0 \quad (2.14)$$

Next, $y_0(n)$ and $x(n)$ are transformed into frequency domain by using fast Fourier transform and these paramets become $Y_0(\omega)$ and $X(\omega)$, respectively. Then, compute the first order response residual $Y_1(\omega)$ by subtracting zero order response residual ($Y_0(\omega)$) with the part of the response due to linear kernel ($Y_L(\omega)$). Then

$$Y_1(\omega) = Y_0(\omega) - Y_L(\omega) \quad (2.15)$$

The second order kernel can be estimated by using the second order cross correlation [44], then

$$h_2(n_1,n_2) = \frac{1}{2P^2} E[y(n)x(n-i_1)x(n-i_2)], \quad i_1, i_2 = 0, 1, ..., N \quad (2.16)$$

where $E[]$ is the expectation operator, and P is the power spectrum of $x(n)$.

Finally, apply Fourier transform in to Eq (2.16), it is changed into [44]:

$$H_2(\omega_1,\omega_2) = \frac{1}{2P^2} Y_1(\omega_1+\omega_2)X^*(\varpi_1)X^*(\varpi_2) \quad (2.17)$$

where $X^*(\omega)$ is conjugation operator. Let $V_Q(\omega_1,\omega_2)$ be the Fourier transform of input and cross kernel,

$$V_Q(\omega_1,\omega_2) = H_2(\omega_1,\omega_2)X(\varpi_1)X(\varpi_2) \quad (2.18)$$

Apply inverse Fourier transform in Eq (2.18), then $V_Q(\omega_1, \omega_2)$ become the convolution between input and cross kernel, know as quadratic response ($y_Q(n)$) [44]. Thus, output is

$$y(n) = h_0 + y_L(n) + y_Q(n) \tag{2.19}$$

Finally, the output of system can be obtained by summation mean, linear response and quadratic response.

2.3 Related Works

This part presents the previous work of autonomic nervous system. The applications in cardiovascular system of each model are considered. The advantages and disadvantages of each model are also discussed in this section.

2.3.1 Nonparametric method

Nonparametric method was applied to analyze the cardiovascular regulatory mechanisms [33,45-48]. Saul J. P, et. al. presented the sinoatrial node response as a low pass Wiener filter to fluctuations in either sympathetic or parasympathetic tone [46]. Their study resulted in sympathetic component appearing in low frequency component, whereas parasympathetic component appeared in both low and high frequency components [46]. Nonparametric approach also gave a sensitive measure of arterial baroreflex function in both experimental and clinical studies [46]. The neural arc of baroreflex system had a high pass filter characteristic in the frequency range of 0.1-1.0 Hz [47]. Generally, the respiration was used as the broadband exogenous noise source to identify the closed-loop magnitude and phase relation between heart rate and blood pressure [8,49]. The nonparametric method suggest that the complex transfer relations observed with a relatively simple analysis of respiration, HR and ABP can be understood in terms of a feedback loop between ABP and HR with respiration as an external noise source [50]. The transfer of respiration and HR had the low pass filter characteristics in both sympathetic and parasympathetic [50]. The gain of transfer function in parasympathetic activity expressed relatively broad-pass magnitude properties with near zero phase at all relevant frequencies, whereas the gain of sympathetic activity demonstrated a marked drop in magnitude with frequency

and a phase delay [50]. The phase of vagal activity near zero degrees at D.C. (0 Hz), while the phase of sympathetic activity near 180 degrees at D.C. At 0.15 Hz, the phase nears zero degrees for both systems [50]. To find the relationship between the heart rate and respiration, the transfer relation between respiration and HR, is that of a low-pass filter whose gain and phase characteristics change with the relative balance of the vagal and sympathetic contributions to HR control [8,49].

Nonparametric method is an interesting approach because it is a fast method and easy to compute. Nonetheless, this approach quantifies data without modifying parameters. The nonparametric identification can not classify the feedforward (HR fluctuation influences ABP fluctuation via heart and vasculature) and feedback mechanism (ABP fluctuation induce HR fluctuation through arterial baroreflex) of closed-loop system [2]. Therefore, nonparametric approach does not sufficient for analyzing the cardiovascular regulation mechanism because this regulation consist of both feedforward and feedback mechanisms.

2.3.2 ARX model

Parametric methods have also been used to estimate the affects of ANS to cardiovascular system. Berbieri et al found that RR interval decrease during inspiration [51]. The ARX method was applied to examine the arterial and cardiopulmonary baroreptors in dynamic closed-loop control of total peripheral resistance (TPR) [52,53]. In conscious sheep, dynamic closed loop affects of ABP and right atrial pressure (RAP) as predictors of TPR [52,53]. Additionally, this method is also applied to analyze the fluctuations in heart rate, ABP and ILV for estimating the cardiovascular control mechanisms [54]. The gain of transfer functions of ILV to RR interval generally increased with RAP from lower body negative pressure [54]. ARX method is an attractive method for identifying diabetic autonomic neuropathy and normal subject with alterations in cardiovascular control mechanisms. The peak amplitude of impulse response between ILV and heart rate decreased with increasing severity of the disease [55]. Mukkamala R., et. al. reported that ARX technique is more sensitive in detecting autonomic dysfunction than spectrum analysis [55]. The power spectrum of Autoregressive (AR) method is applied to implement sympatho-vagal balance in HRV [56,57]. Lang E., et. al. reported the power spectrum of AR

method was highly sensitive in different patients and increased risk of malignant ventricular arrhythmia (MVA) [56]. The power spectrum of HRV extracted a reliable measure to distinguish between periods of normal and sleep disordered breathing (SDB) in child patients [57]. The spectral power data and the damped oscillator of RSA showed that cardiac sympathetic outflow markedly reduces heart period oscillations at all frequencies [51]. It can be concluded that RSA is mediated simply by vagal-cardiac nerve activity [51]. The power spectrum analysis based on AR modeling of the RR interval and respiration was applied for specifying diabetic subjects [58,59].

Linear parametric models provide many useful close loop cardiovascular regulatory mechanisms as described above. However, there are some nonlinear interactions in the cardiovascular system such as between sympathetic and parasympathetic nervous system with respect to heart rate control [2].

2.3.3 Volterra-Weiner model

Volterra series was used to determine a nonlinear system analysis of the effect of fluctuations in instantaneous lung volume and arterial blood pressure on heart rate fluctuations [2,60,61]. The linear method provided the dominant role in hear rate fluctuation, but the second order nonlinear components also contribute significantly in describing the coupling of instantaneous lung volume and arterial blood pressure fluctuations to heart rate fluctuations [2]. The study based on second order Volterra-Weiner model revealed an important contribution of the second order kernels to description of the effect of lung volume and ABP on heart rate [60]. The first order and second order ILV to heart rate kernel amplitude reduced after autonomic double blockade [4]. The nonlinear dynamics played a quantitatively significant role in mediating the heart rate response to autonomic activation [61]. The second-order Volterra–Wiener model was applied to analysis the effect of respiration and arterial blood pressure on heart rate [62]. Jo et a l found that gain of RSA and arterial blood pressure in obstructive sleep apnea (OSA) was less than normal subjects. They found the increased sympathetic activity and decreased parasympathetic activity in OSA subjects [62].

To predict the system output from a given input, it is necessary to compute these kernels. There are different methods for computing the Volterra kernel [63,64]. However, the algorithm to obtain these parameters is very difficult [43]. Despite, Volterra model can deal with the nonlinear component in the system, Volterra series provided unsatisfactorily results in prediction of step depolarizations [65].

The previous studies indicated that nonlinear methods provided more insight into nonlinear components; however, model construction is quite hard and difficult. Thus, to assessing the cardiovascular autonomic regulation, we will propose a better and faster model in the next chapters.

CHAPTER III
MATERIALS AND METHODS

At this time, several mathematical approaches are applied to estimate mathematical model of autonomic heart rate control. These methods include linear and nonlinear methods. However, the previous models are not adequate, the interactions of autonomic heart rate control have not been clear. For this reason, we applied NARMA model for assessing the interaction in autonomic control of heart rate. We applied factors that may be influence to heart rate control in the mathematical model such as ABP, MSNA and respiration (RESP). Moreover, the physical activity (handgrip exercise) was also applied in this study.

In this chapter, method of this experiment can be separated into 2 parts: heart rate variability (HRV) during handgrip exercise and NARMA model of autonomic heart rate control.

3.1 An Overview

The overall of this thesis is summarized as shown in figure 3.1. The factors that effect to autonomic heart rate control can be classified into exercise, blood pressure, MSNA and respiration. All data were passed through preprocessing step to eliminate noise. These signals were implemented by mathematical model. The models were validated to find the optimal model. Finally, the optimal model were analyzed and implemented.

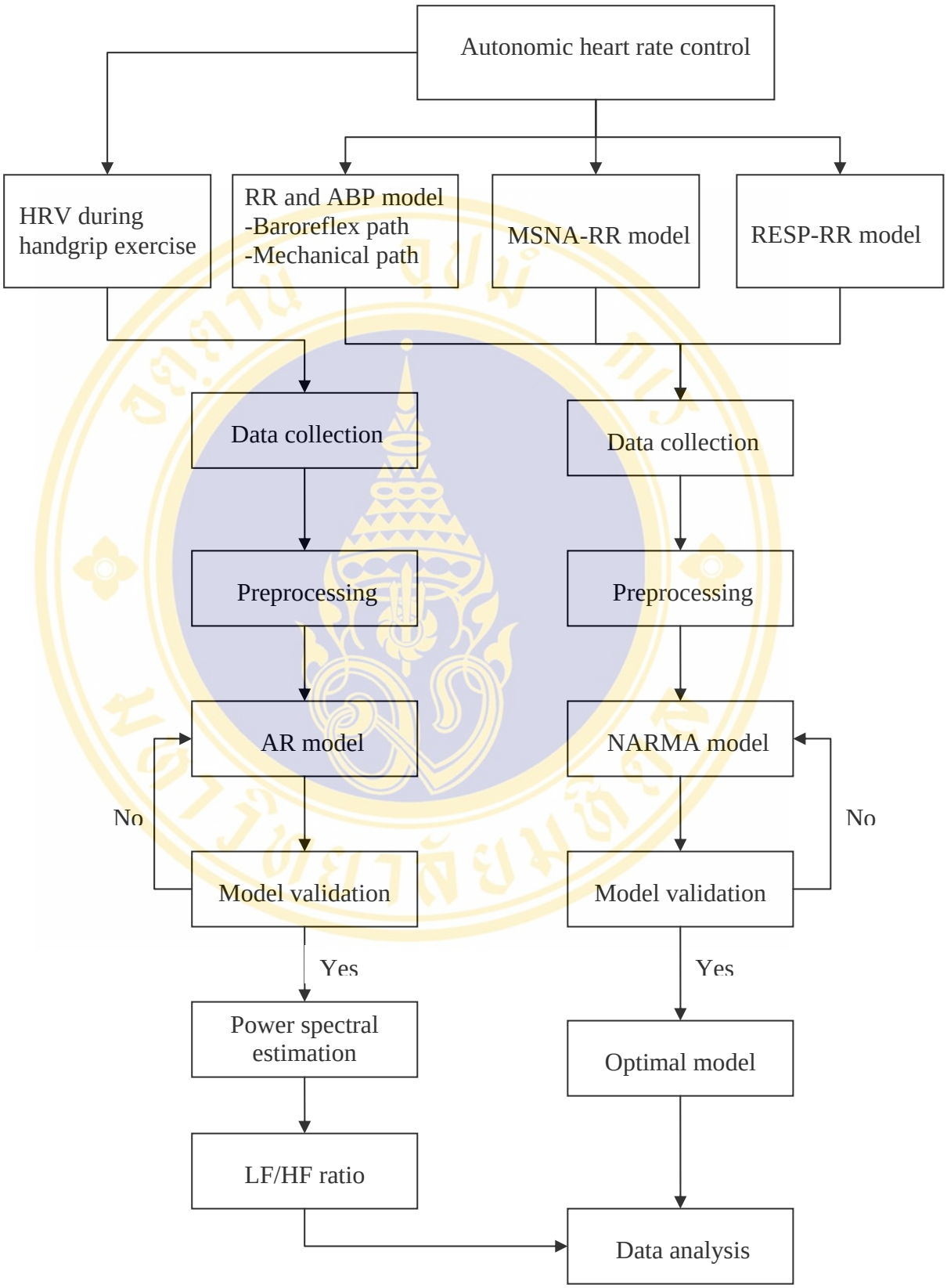

Figure 3.1 Overall of the research.

3.2 Heart rate variability during handgrip exercise

We measured the response of HRV during handgrip exercise for examine autonomic control by using the power spectral analysis. An autoregressive technique was applied to compute the power spectral density of HR.

3.2.1 Data collection and preprocessing

Four healthy subjects provided informed consent prior to the study. Subjects were required to take supine position. Each subject performed brief maximal contractions to determine their maximal voluntary contraction (MVC) by using a handgrip dynamometer. During baseline, the subjects remained at rest quietly in supine position and the baseline recordings of ECG, were performed for 5 minutes. The dynamic handgrip exercises were performed for 15 minutes. Exercises involved the subjects altering consecutively between a five second long sustained handgrip at 50 % of their MVC and a five second period of rest. The ECG was recorded with a sampling frequency of 300 Hz. ECG signals of these subjects were recorded at rest (baseline) condition (5 min) and handgrip exercise (15 min). The ECG signals were sampled and analyzed on off line computer. ECG was passed through the filter in order to eliminate noise. R-R intervals were detected from ECG and smoothed instantaneous HR time series were sampled at 4 Hz [66].

3.2.2 Autoregressive Method and power spectral estimation

The Autoregressive (AR) method is a method that the output value can be calculated by the weighted sum of its previous value. AR model can be denoted as [40]:

$$y(t) = \sum_{i=1}^{p} a_i y(t-i) + e(t). \qquad (3.1)$$

where $y(t)$ is the observed variable of the system; $e(t)$ is the unobserved white noise disturbance; a_i are coefficients and p is the order of the AR model. The coefficients of autoregressive method can be obtained by using Yule-Walker equation. It can be written as:

$$\begin{bmatrix} r(0) & r(1) & \cdots & r(p-1) \\ r(1) & r(0) & \cdots & r(p-2) \\ \vdots & \vdots & \cdots & \vdots \\ r(p-1) & r(p-2) & \cdots & r(0) \end{bmatrix} \begin{bmatrix} a(1) \\ a(2) \\ \vdots \\ a(p) \end{bmatrix} = \begin{bmatrix} -r(1) \\ -r(2) \\ \vdots \\ -r(p) \end{bmatrix} \tag{3.2}$$

where $r(k)$ is a autocorrelation function. It can be calculate by

$$r(k) = \frac{1}{N} \sum_{n=1}^{N-1} y(n) y(n-k) \tag{3.3}$$

The optimal model order (p) can be calculated by choosing the minimum value of the Minimum Descriptive Length Criterion (MDL):

$$\text{MDL}(p) = N \ln s_p^2 + 2(p+1) \tag{3.4}$$

where s_p^2 is the variance of the error sequence. It can be define as [40]:

$$s_p^2 = \frac{TSE}{N} = \frac{1}{N} \sum_{n=p}^{N-1} e_n^2 = r(0) + \sum_{i=1}^{p} a(i) r(i) \tag{3.5}$$

In a final manner, we got the optimum model of AR. Next, the coefficients of AR model were applied to estimate the power spectrum $S(f)$. That is [40]:

$$S(f) = \frac{s_p^2 T}{\left| \sum_{i=0}^{p} a(i) e^{-2\Pi f i T} \right|^2} \tag{3.6}$$

where f is a sampling frequency and T is a sampling interval.

3.2.3 LF/HF ratio

The power spectral analyses of heart rate were applied to demonstrate the cardiac function depending on the autonomic nervous system and physiological control. Power spectral method provides the basic information of the way in distribution of power as a frequency function of HR. The LF band is hypothesized that relates with the sympathetic activation but the HF band is suspected that related with vagal activation [67]. Hence, the LF/HF ratio is an important index for studying the sympathy-vagal balance. LF and HF might also be calculated in normalized units, which established the relative value of each power component in proportion to the total power minus the VLF component [68]. LF and HF normalized power were calculated as

$$LF\ Normalized\ \ Power = \frac{LF\ Power}{Total\ Power - VLF\ Power} \times 100 \tag{3.7}$$

$$HF\ Normalized\ \ Power = \frac{HF\ Power}{Total\ Power - VLF\ Power} \times 100 \tag{3.8}$$

Finally, LF/HF ration was computed to determine the balance between parasympathetic and sympathetic system during handgrip exercise.

3.3 NARMA model of autonomic heart rate control.

We applied the factors (ABP, MSAN, and LBNP) that effect to autonomic heart rate control. Then, the relationships between input and output were analyzed by using NARMA model. In this study, we studied the relationship of autonomic heart rate control by constructing the following model:

- RR and ABP model consists of
    - Baroreflex path
        - SBP (input) – RR (output) model
        - DBP (input) – RR (output) model
    - Mechanical path
        - RR (input) – SBP (output) model
        - RR (input) – DBP (output) model
- MSNA (input) and RR (output) model
- RESP (input) and RR (output) model with LBNP
    - baseline
    - -15 mmHg
    - -30 mmHg
    - recovery period

Theses models were validated to find the optimal model. Finally, the optimal model were analyzed and implemented. The Flowchart of the NARMA model is shown in figure 3.2.

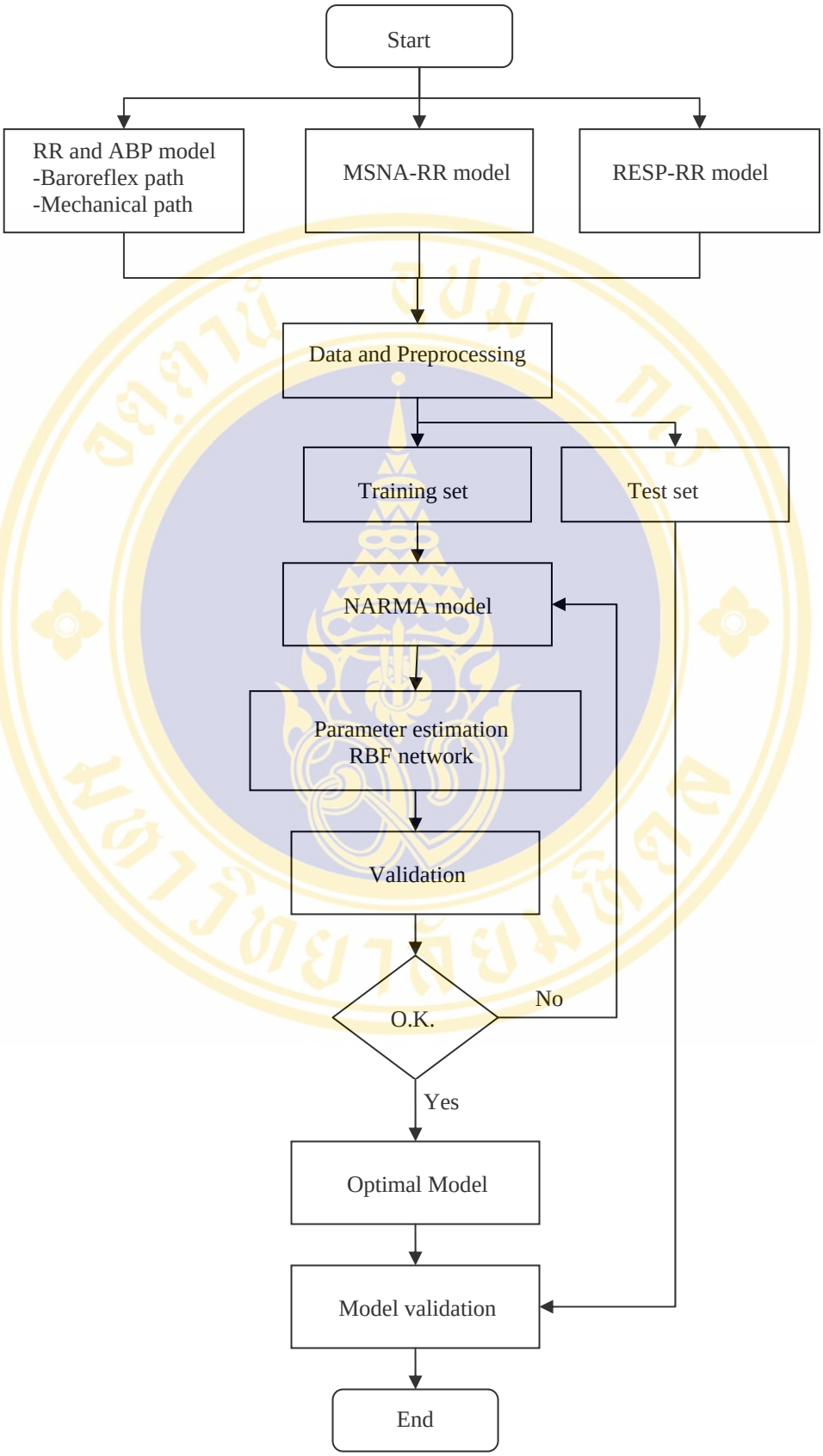

Figure 3.2 The Flowchart of the NARMA model.

3.3.1 Data collection and preprocessing

Subjects were classified into 2 groups: dataset I and dataset II. The dataset I was recorded ECG, ABP, and MSNA signals for 5 minutes. Five healthy subjects provided informed consent prior to this group (three males two females, 27 $\pm$ 2 yrs). The MSNA were measure at the peroneal nerve at the fibular head. A tapered, insulated tungsten electrode with a 200- m-diameter tip and an un-insulated portion approximately 1–2 m in length were inserted percutaneously into the sympathetic bundle of the peroneal nerve. A stainless-steel reference electrode was placed subcutaneously about 2 cm from the recording site. All signals were recorded with a sampling frequency of 300 Hz. The signals were sampled and analyzed on off line computer. All signals were passed through the filter in order to eliminate noise. R-R intervals were detected from ECG. Both systolic blood pressure (SBP) and diastolic blood pressures (DBP) were derived from arterial blood pressure. These signals were resampled at 4 Hz in order to prevent the unnecessary measurement noise and construct equally spaced time series for modeling and data analysis. These signals were implemented and fitted to the NARMA model. These signals were separated into train sets (4 min.) and test sets (1 min.). The signals form this group were applied in RR- ABP model and MSNA-RR model.

In dataset II, six healthy subjects were recorded ECG and respiration for 4 minutes. Subjects were controlled their breath to obtain the broadband respiration. Broadband respiratory activity is elicited by instructing a subject to initiate an inspiratory/expiratory cycle each time he is cued by an audible tone [33]. Moreover, subject were record ECG and respiration signal during various lower body negative pressure (LBNP) such as baseline-15mmHg, -30 mmHg, and recovery period. These signals were recorded with a sampling frequency of 500 Hz. These signals were applied into the preprocessing step. These signals were separated into training sets (3.5 min.) and test sets (30 sec.). The simulated RR interval was evaluated by using NARMA model.

3.3.2 Nonlinear autoregressive moving average (NARMA)

The NARMA model can be described by a linear difference equation as [69]:

$$y(n) = \sum_{i=1}^{p} a(i)y(n-i) + \sum_{j=0}^{q} b(i)u(n-j) + \sum_{i=1}^{p}\sum_{j=1}^{p} a(i,j)y(n-i)y(n-j)$$

$$+ \sum_{i=0}^{q}\sum_{j=0}^{q} b(i,j)u(n-i)u(n-j) + \sum_{i=0}^{p}\sum_{j=1}^{q} c(i,j)y(n-i)u(n-j) + \ldots + e(n)\,. \quad (3.9)$$

where p and q are the model's orders of the autoregressive and moving average terms, respectively. Let $y(n)$ be the system output signal; $u(n)$ be the system input signal; $e(n)$ be an unmodeled noise source. If the input and output satisfy polynomial or power series properties then, the model can be written as [69]:

$$y(n) = \sum_{i=1}^{M} c_i \varphi_i(x_i) + e(n)\,. \quad (3.10)$$

where $\{\varphi_i(x_i)\}_{i=1}^{M}$ is a set of basis function which include past values of $y(n)$, and present and past values of $u(n)$; c_i be the weight of coupling of hidden unit i to the output unit; M is the number of hidden unit and x_i is the weighted sum of input to the hidden unit i. Eq. (3.10) can be expressed as follows:

$$x_i = \sum_{j=1}^{p} w_{ji} y(n-j) + \sum_{j=0}^{q} v_{ji} u(n-j)\,. \quad (3.11)$$

Let $p_i(x)$ be a polynomial function and it can be defined as [69]:

$$\varphi_i(x) = \sum_{m=0}^{M} a_{mi} x^m\,. \quad (3.12)$$

Substituting Eq. (3.12) into Eq. (3.10), obtaining [69]:

$$y(n) = \sum_{m=0}^{M} c_i \left(\sum_{m=0}^{M} a_{mi} x_i^m \right) + e(n)\,. \quad (3.13)$$

Gathering and rearranging terms, Eq.(3.13) is derived as [69]:

$$y(n) = \sum_{i=1}^{M} c_i a_{0i} + \sum_{j=1}^{p} \left(\sum_{i=1}^{M} c_i a_{1i} w_{ij} \right) y(n-j) + \sum_{j=0}^{q} \left(\sum_{i=1}^{M} c_i a_{1i} v_{ij} \right) u(n-j)$$

$$+ \sum_{j=1}^{p}\sum_{k=1}^{p} \left(\sum_{i=1}^{M} c_i a_{2i} w_{ji} w_{ki} \right) y(n-j)y(n-k)$$

$$+ \sum_{j=0}^{q}\sum_{k=0}^{q}\left(\sum_{i=1}^{M} c_i a_{2i} v_{ji} v_{ki}\right) u(n-j)u(n-k)$$

$$+ 2\sum_{j=1}^{p}\sum_{k=0}^{q}\left(\sum_{i=1}^{M} c_i a_{2i} w_{ji} v_{ki}\right) y(n-j)u(n-k)$$

$$+ \ldots + e(n). \qquad (3.14)$$

Note that Eq.(3.9) and Eq.(3.14) are equivalent. The coefficients of NARMA in Eq.(3.9) can be represented by coefficients in Eq.(3.14). The general coefficients of NARMA model is given by [69]:

$$a(i) = \sum_{s=1}^{M} c_s a_{1s} w_{is}$$

$$b(i) = \sum_{s=1}^{M} c_s a_{1s} v_{is}$$

$$a(i,j,k,\ldots,n) = \sum_{s=1}^{M} c_s a_{ns} w_{is} w_{js} w_{ks} \cdots w_{ns}$$

$$b(i,j,k,\ldots,n) = \sum_{s=1}^{M} c_s a_{ns} v_{is} v_{js} v_{ks} \cdots v_{ns}$$

$$c(i,j,k,\ldots,n) = \frac{1}{2}\sum_{s=1}^{M} c_s a_{ns} w_{is} v_{js} \cdots w_{ns} v_{ns}. \qquad (3.15)$$

Hence, NARMA coefficients are computed by using weights $\{w_{io}$ and $v_{io}\}$ and polynomial coefficients $\{a_{ni}\}$. These unknown variables can be obtained by radial basis function networks algorithm.

Based on radial basis function, NARMA coefficients can be derived by using neural networks weight values and polynomial coefficients. The neural networks architecture base on NARMA prediction is shown in figure 3.3. The RR interval and respiration signals were implemented and fitted to the NARMA model.

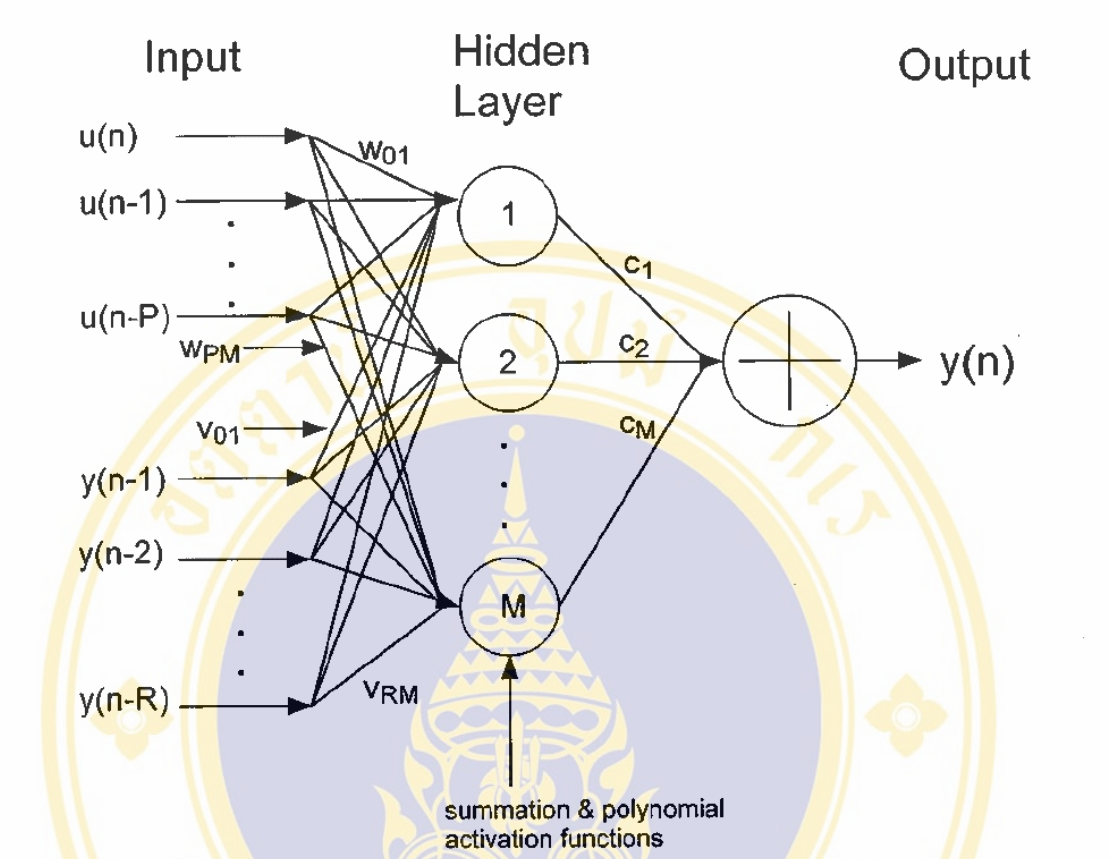

Figure 3.3 Neural model prediction under NARMA model [70].

3.3.3 Radial Basis Function (RBF) Networks

Radial basis functions, artificial neural networks, were invented in the late 1980's. However, this fundamental technique depends on the traditional artificial neural networks, e.g., potential functions, clustering, functional approximation, spline interpolation and mixture models [71]. The output unit generates a sum of hidden layers. The result of the nonlinear RBF neural network input is linear output. Due to its efficiency in nonlinear approximation, it is commonly used for model complex mappings.

The radial basis function technique can be defined as [71]:

$$d_i = F(x_i) = \sum_{i=1}^{M} w_i \varphi_i(\hat{x}) \ . \qquad (3.16)$$

where d is the desired response, w is the linear weight vector, x is the input and i = 1, 2, …, M. The basis function $\varphi_i(\hat{x})$ can be defined as [71]:

$$\varphi_i(\hat{x}) = G(\hat{x}; \hat{x}_i) \tag{3.17}$$

where G is a the matrix of Green's functions. It can be defined as [71]:

$$G(\hat{x}; \hat{x}_i) = \exp(-\frac{1}{2\sigma_i^2}\left\|\hat{x} - \hat{x}_i\right\|^2). \tag{3.18}$$

where $\|\ \|$ is a Euclidean norm.

The **w** is the linear weight vector can be calculated by [71]:

$$\mathbf{w} = (\mathbf{G}^T\mathbf{G})^{-1}\mathbf{G}^T\mathbf{d} \tag{3.19}$$

where

$\mathbf{w} = [\, w_1, w_2, ..., w_M \,]^T$

$\mathbf{d} = [\, d_1, d_2, ..., d_M \,]^T$

$$\mathbf{G} = \begin{pmatrix} G(\hat{x}_1;\hat{x}_1) & G(\hat{x}_1;\hat{x}_2) & \dots & G(\hat{x}_1;\hat{x}_M) \\ G(\hat{x}_2;\hat{x}_1) & G(\hat{x}_2;\hat{x}_2) & \dots & G(\hat{x}_2;\hat{x}_M) \\ \vdots & \vdots & & \vdots \\ G(\hat{x}_M;\hat{x}_1) & G(\hat{x}_M;\hat{x}_2) & \dots & G(\hat{x}_M;\hat{x}_M) \end{pmatrix}.$$

The linear weight vector can be obtained by using Eq. (3.19). Finally, the output or the desired response can be calculated by using weight and the matrix of Green's functions.

If the model does not satisfy, these weights will be updated by using the orthogonal least squares leaning algorithm [72]. This algorithm consists of 3 steps. First, the initial weights (w_{i1}), the orthogonal least square solution (g_{ik}) and an error reduction ratio due to weight (e_{ik}) are compute as:

$$w_i(1) = p_i \tag{3.20}$$

$$g_i(1) = \frac{(w_i(1))^T d}{(w_i(1))^T (w_i(1))} \tag{3.21}$$

$$e_i(1) = \frac{(g_i(1))^2 (w_i(1))^T w_i(1)}{(d)^T (d)} \quad i = 0, 1, ..., p+q \tag{3.22}$$

where $p_i = [x(n) \quad x(n-1) \quad ... \quad x(n-p) \quad y(n-1) \quad y(n-2) \quad ... \quad y(n-q)]$

Find maximum value of $e_i(1)$.

Next, at the k^{th} step, $k \geq 2$ for $i = 0, 1, ..., p+q$

$$\alpha_{ij}(k) = \frac{w_j^T p_i}{w_j^T w_j} \quad j = 0, 1, ..., p+q \tag{3.23}$$

$$w_i(k) = p_i - \sum_{j=1}^{k-1} \alpha_{ij}(k) w_j \tag{3.24}$$

$$g_i(k) = \frac{(w_i(k))^T d}{(w_i(k))^T (w_i(k))} \tag{3.25}$$

$$e_i(k) = \frac{(g_i(k))^2 (w_i(k))^T w_i(k)}{(d)^T (d)} \quad i = 0, 1, ..., p+q \tag{3.26}$$

Find maximum value of $e_i(k)$ and update weight,

$$w_i(k) = p_i - \sum_{j=1}^{k-1} \alpha_{ij}(k) w_j \tag{3.27}$$

Finally, this algorithm is ended at M_s step when

$$1 - \sum_{j=1}^{M_s} e_i < \rho \tag{3.28}$$

where ρ is a chosen tolerance and $0 < \rho < 1$. Normally, the ρ can be calculate as the ratio of the variance residuals and the variance of the desired output. Finally, the weights of model were updated.

According to these step, we obtain the parameters of NARMA model. The model order will be selected by using the Minimum Descriptive Length Criterion (MDL):

$$\text{MDL}(p,q) = N \ln s_{pq}^2 + 2(p+q) \tag{3.29}$$

where s_{pq}^2 is the is the variance of the error. At the end, optimal model will be obtained.

3.3.4 Model validation and Prediction.

The normalized mean squared error (NMSE) and absolute percentage error (MAPE) were calculated to validate the performance of model and they define as [73]:

$$\text{NMSE} = \frac{\sum_{i=1}^{N} (y_i - yp_i)}{\sum_{i=1}^{N} (y_i - \bar{y}_i)} \tag{3.30}$$

$$\text{MAPE} = \frac{100}{N} \times \sum_{i=1}^{N} \left| \frac{y_i - yp_i}{y_i} \right| \tag{3.31}$$

where yp_i is the estimated signal.

The simulated signal will be compare with other system identification method such as nonparametric, linear approach (ARX) and Volterra model to verify the performance of model.

The one way ANOVA with post hoc test (Kruskal-Wallis) was applied in this experiment to compare the differences in the mean of the experimental results.

CHAPTER IV
EXPERIMENTAL RESULTS

In this chapter, the experimental results of autonomic heart rate control based on NARMA model are shown. The experimental results comprise 2 parts: heart rate variability (HRV) during handgrip exercise and NARMA model of autonomic heart rate control.

4.1 Heart rate variability during handgrip exercise

At rest HR was 55.37 ± 4.45 beats/min. HR of 5 min, 10 min and 15 min exercise was 64.13 ± 4.33, 65.51 ± 3.09 and 67.06 ± 2.67 beats/min, respectively. As expected, HR at rest and exercise progressively increased and it also progressively increased with intensity of exercise.

The AR parameters and order were obtained by using Yule-Walker equation and MDL method, respectively. Optimum order of baseline, 5 min exercise, 10 min exercise and 15 min exercise were 13, 13, 10 and 13, respectively. The power spectrum by using parametric method was computed. Average LF and HF components were displayed in the spectra of HR variability as shown in figure 4.1 and 4.2, respectively. Average LF power trended to decrease. There was difference in the mean between during baseline and exercise ($p < 0.05$); however, there was difference in the mean between during baseline and exercise. The Average HF power trended to progressively decrease. There was difference in the mean between during baseline and exercise ($p < 0.05$), there were no differences in the mean during exercise ($p > 0.05$).

During at rest and 5 min exercise, average LF/HF ratio trended to increase as shown in figure 4.3, though there were no differences in the mean in LF/HF ratio ($p > 0.05$).

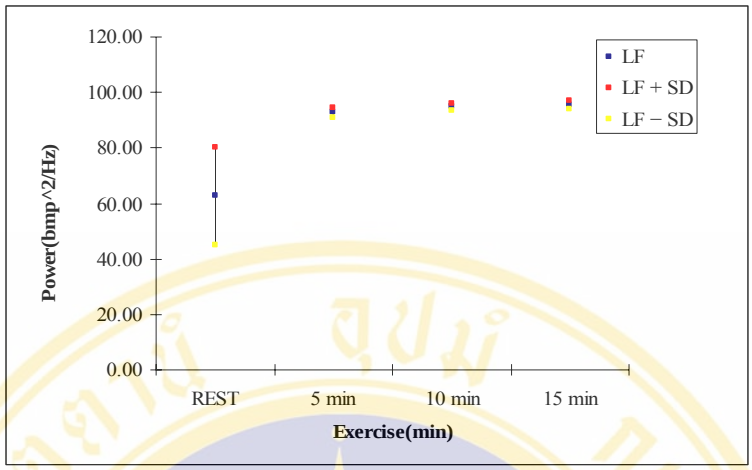

Figure 4.1 The average LF of spectral components.

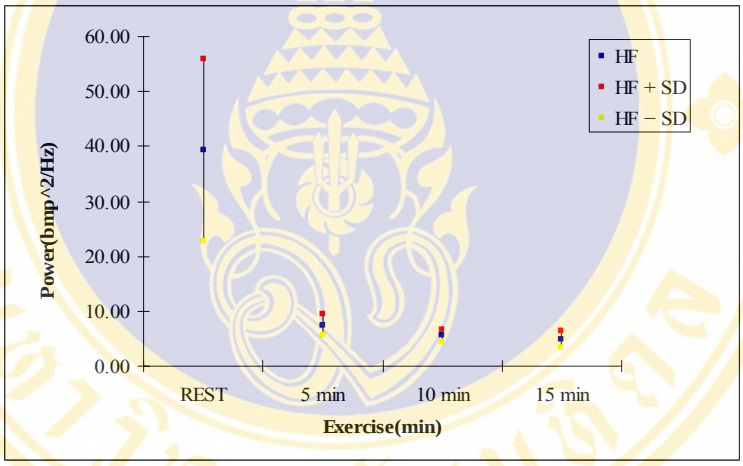

Figure 4.2 The average HF of spectral components.

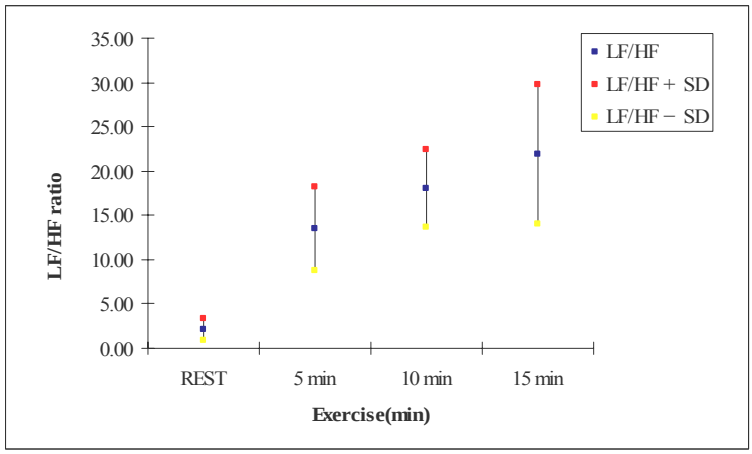

Figure 4.3 The average LF/HF ratio.

4.2 NARMA model of autonomic heart rate control

4.2.1 RR and ABP model

The RR and ABP model can be divided in to the baroreflex path (SBP-RR, and DBP-RR) and mechanical path (RR-SBP and RR-DBP).

4.2.1.1 Baroreflex path model

The baroreflex path model studied the effect of ABP to RR interval. This model can be classified in to the effect of SBP to RR (SBP-RR) and the effect of DBP to RR (DBP) model. We applied ABP as input and RR as output into NARMA model. Results of SBP-RR and DBP-RR model are shown in figure 4.4 and 4.6, respectively.

a)

b)

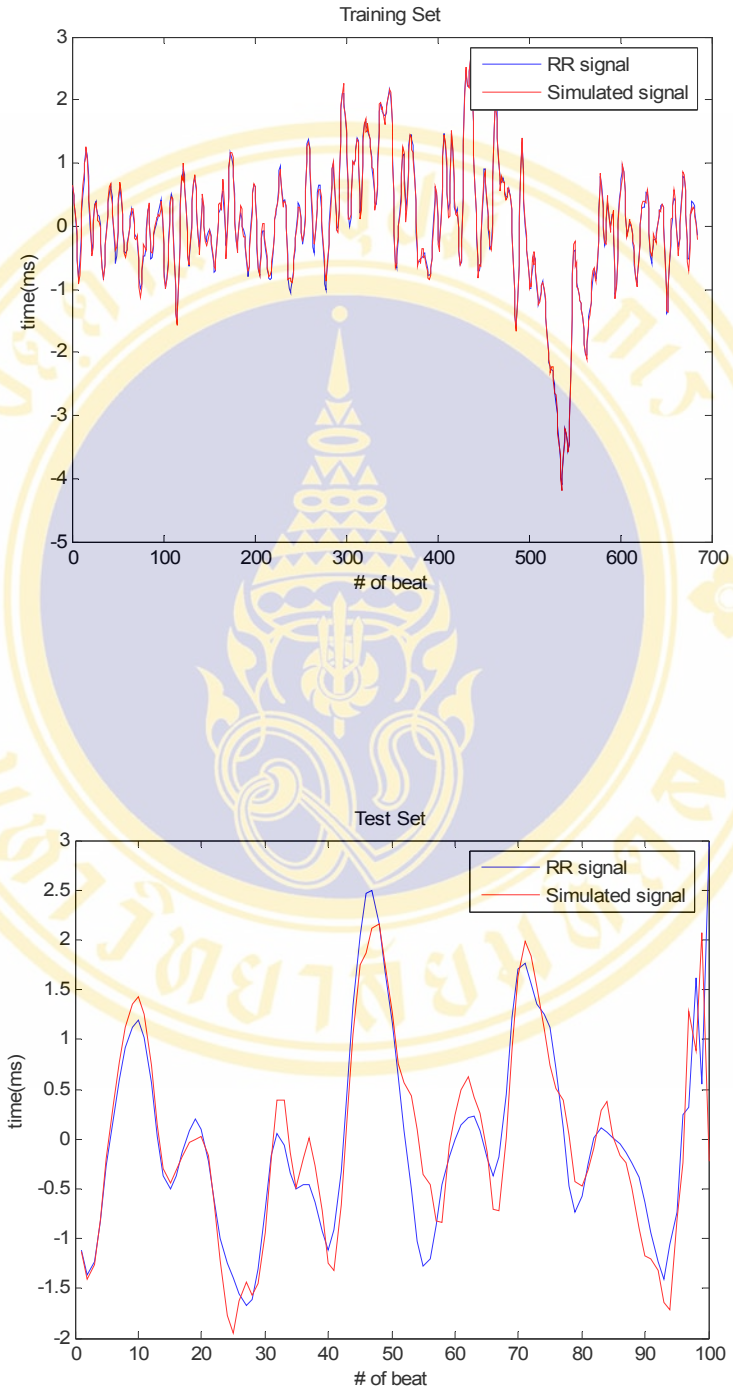

Figure 4.4 Model prediction of SBP-RR model by using NARMA method (input = SBP, output = RR interval).Training set, b) Test set.

a)

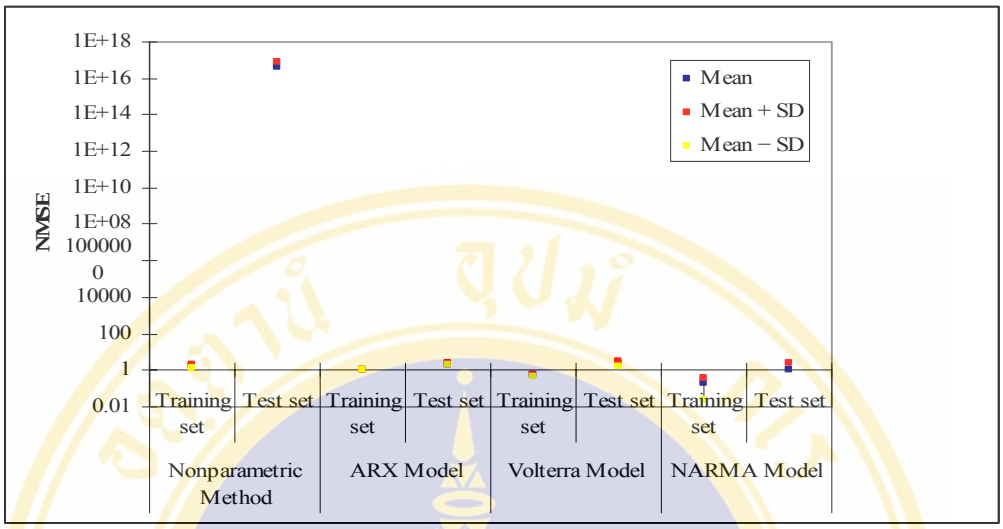

b)

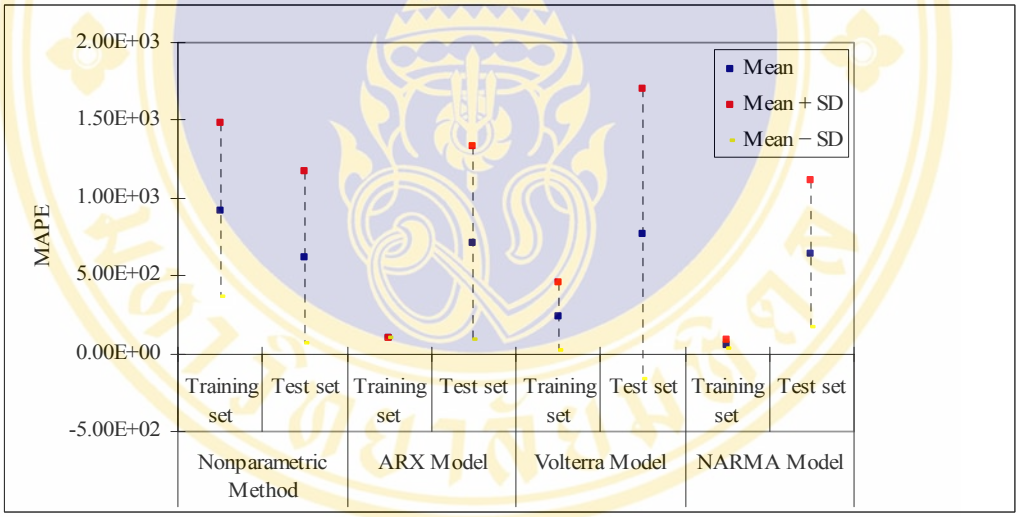

Figure 4.5 Performance of SBP-RR model with nonparametric, ARX, Volterra and NARMA model. a) NMSE, b) MAPE.

As expected, the SBP-RR model by using NARMA model provided minimum NMSE and MAPE. NMSE of NARMA provided a minimum value in training set; however, there were no differences in the mean of NMSE between NARMA and ARX method in test set ($p > 0.05$). MAPE of NARMA were no differences in the mean of with the other methods ($p > 0.05$) except nonparametric and ARX method in training set ($p < 0.05$).

a)

b)

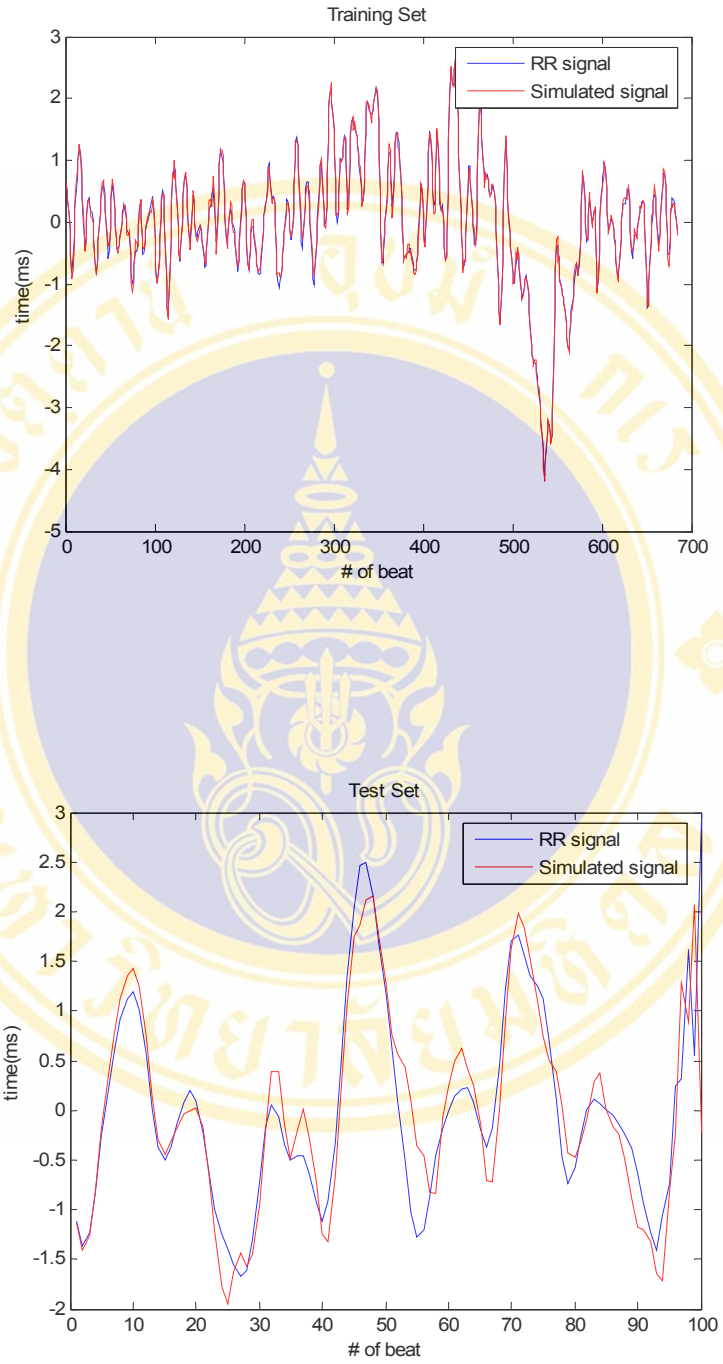

Figure 4.6 Model prediction of DBP-RR model by using NARMA method (input =DBP, output = RR interval). a) Training set, b) Test set.

a)

b)

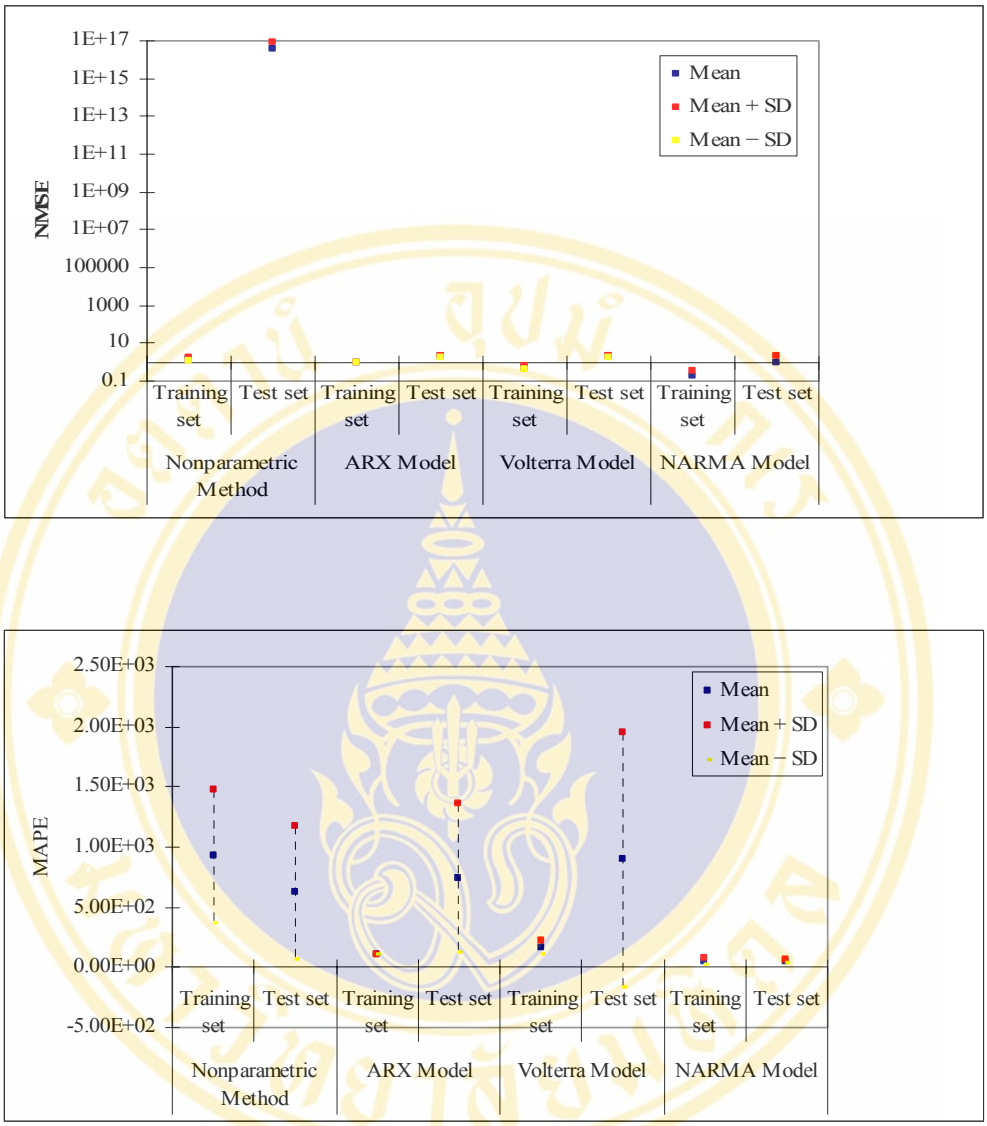

Figure 4.7 Performance of DBP-RR model with nonparametric, ARX, Volterra and NARMA model. a) NMSE, b) MAPE.

As expected, the DBP-RR model by using NARMA model provided minimum NMSE and MAPE. Moreover, the mean of NMSE by using NARMA method give a minimum value than the other methods ($p < 0.05$). Moreover, the MAPE of training set by using NARMA method also gave minimum value when compared with the others methods ($p < 0.05$) in both training and test set, except test set of Volterra method ($p > 0.05$).

4.2.1.2 Mechanical path model

The mechanical path model studied the effect of RR interval to ABP. This model consists of the effect of RR interval to SBP (RR-SBP model) and the effect of RR interval to DBP (RR-DBP model). In mechanical path model, we served RR interval as input and ABP as output. Results of RR-SBP and RR-SBP model are shown in figure 4.8 and 4.10, respectively.

a)

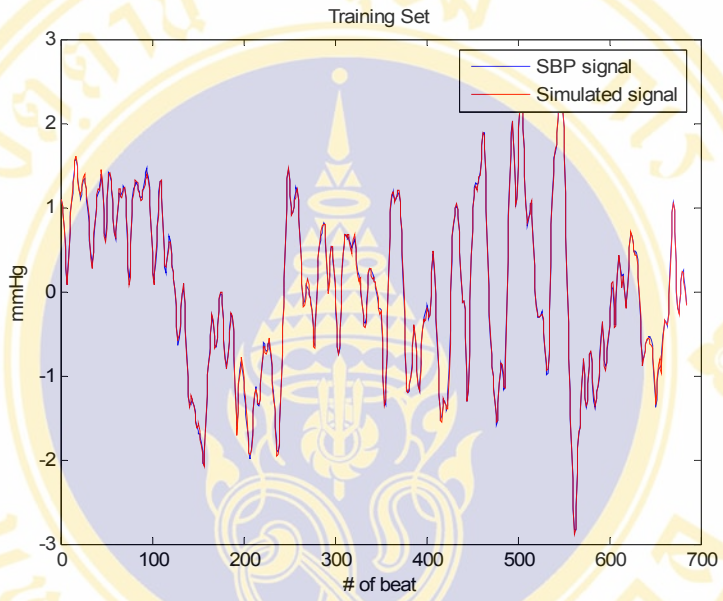

b)

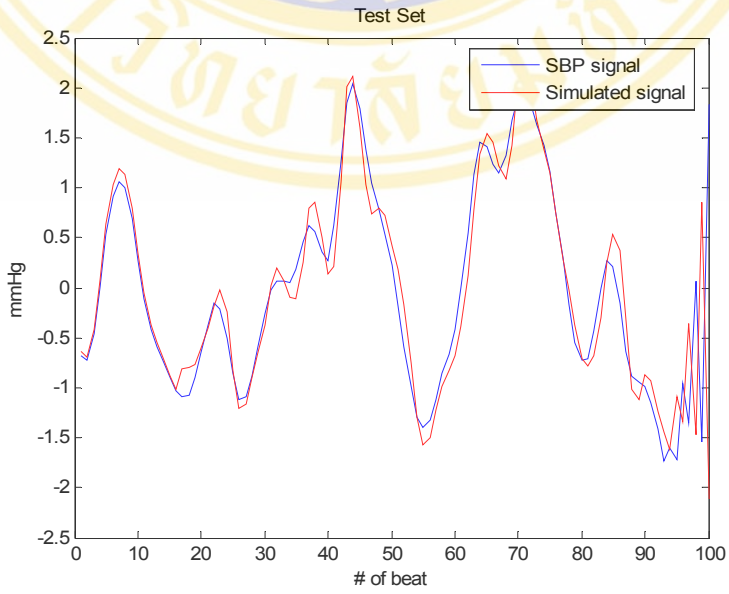

Figure 4.8 Model prediction of RR-SBP model by using NARMA method (input =RR, output =SBP). a) Training set, b) Test set.

a)

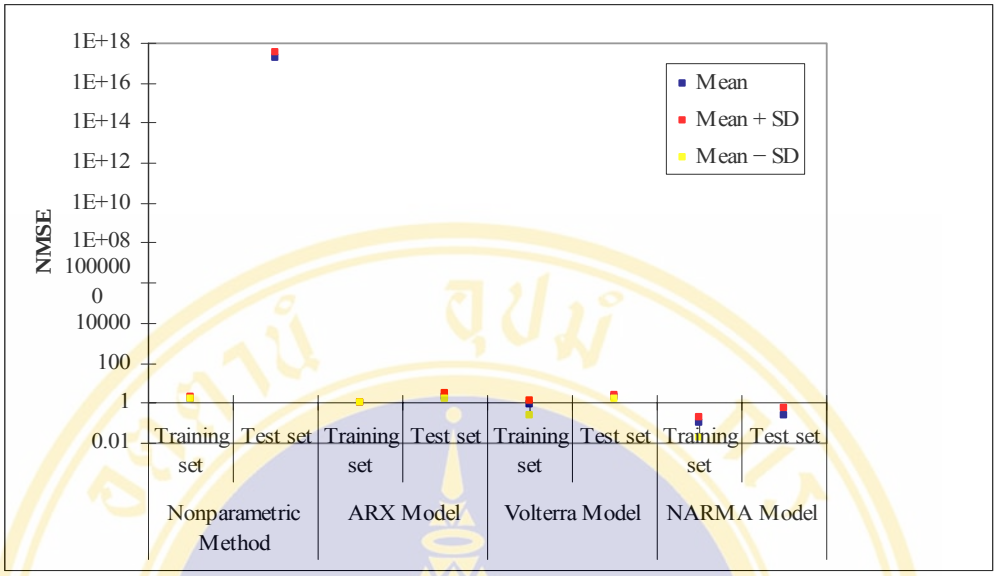

b)

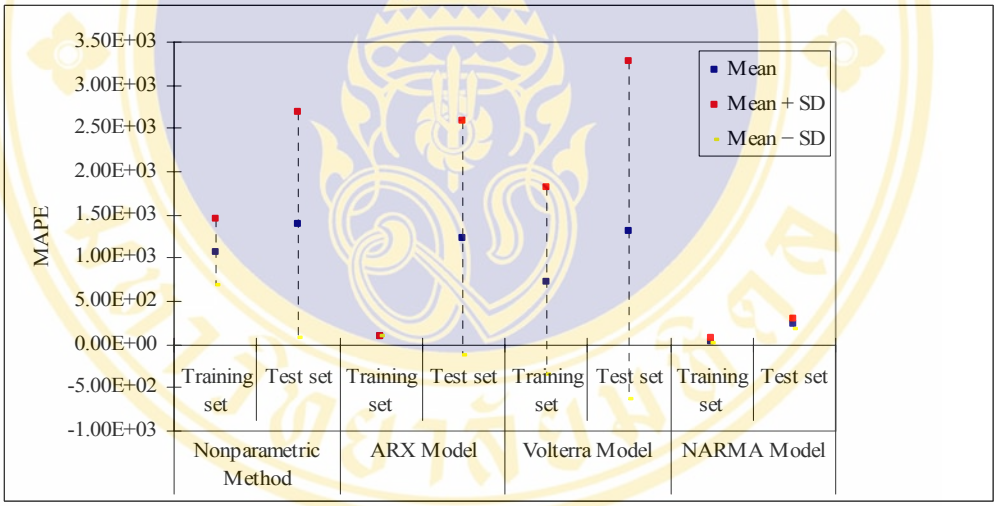

Figure 4.9 Performance of RR-SBP model with nonparametric, ARX, Volterra and NARMA model. a) NMSE, b) MAPE.

The mean NMSE and MAPE of RR–SBP model by using NARMA model gave an idea that they provided minimum values in both training set and test set. The mean of NMSE by using NARMA method give a minimum value than the other methods ($p < 0.05$) in both training set and test set. On the other hand, MAPE of NARMA were no differences in the mean with training set of ARX and Volterra method ($p > 0.05$) in both training and test set.

a)

b)

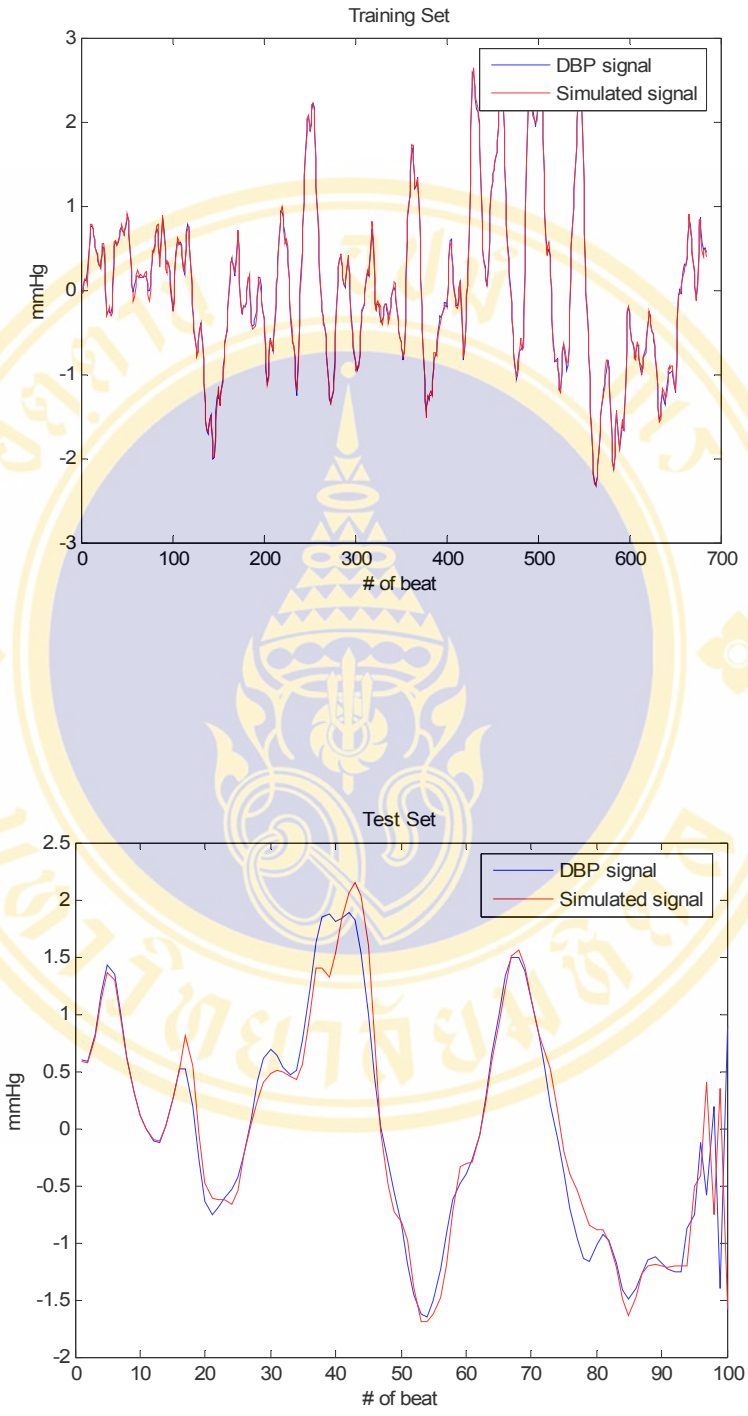

Figure 4.10 Model prediction of RR-DBP model by using NARMA method (input =RR, output =DBP). a) Training set, b) Test set.

a)

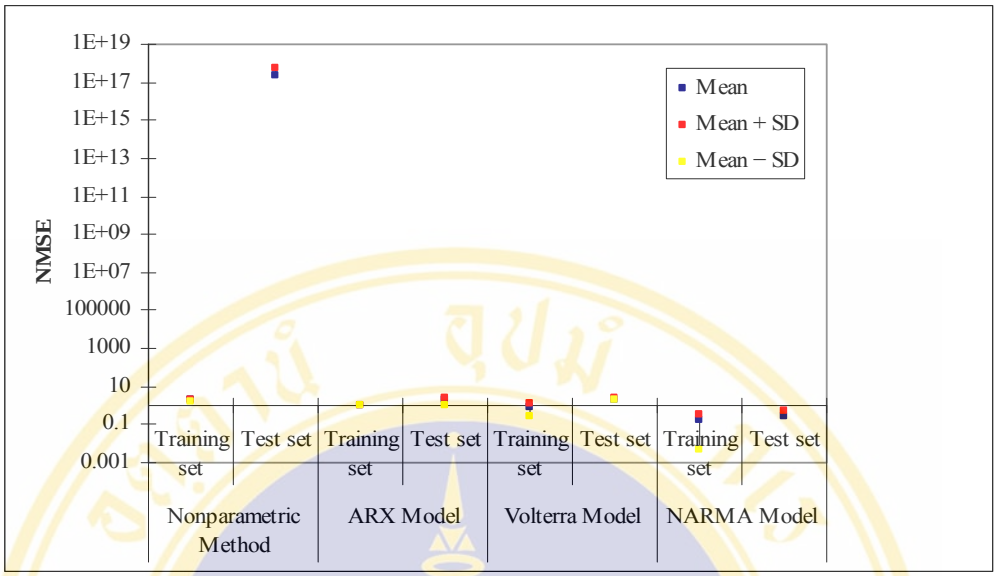

b)

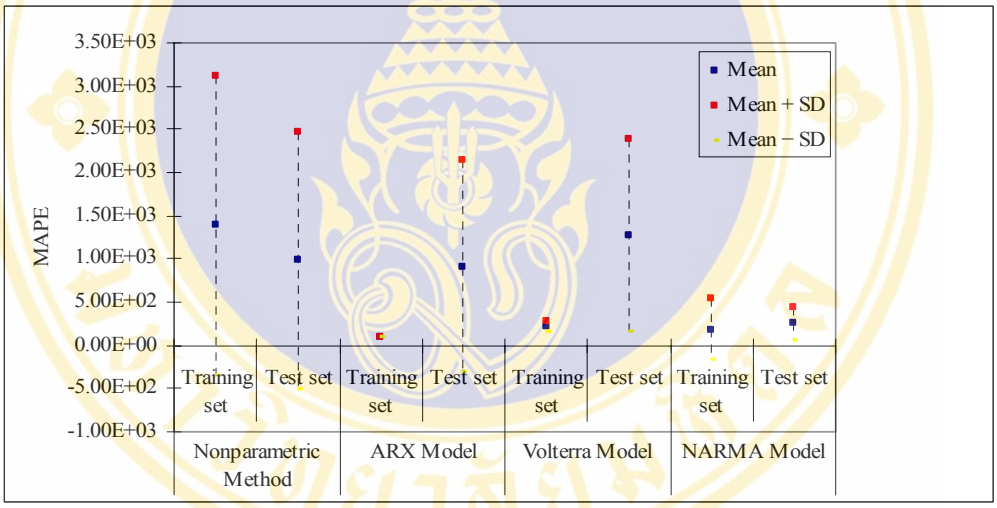

Figure 4.11 Performance of RR-DBP model with nonparametric, ARX, Volterra and NARMA model. a) NMSE, b) MAPE.

Performance of RR-DBP model suggested that the NARMA method gave minimum value of NMSE and MAPE in both training and test sets. When compared these results with statistical method, we found that the mean of NMSE by using NARMA method gave a minimum value than the other methods ($p < 0.05$) in both training and test sets. On the other hand, the there were no differences in the mean of MAPE between NARMA and the other methods ($p < 0.05$) except Volterra method ($p > 0.05$) in test set.

4.2.2 MSNA and RR model

This model studied the effect of MSNA to RR interval by using NARMA model. We defined MSNA as input and RR interval as out put model, the results of model is shown in figure 4.12. Figure 4.13 provided results of MSNA-RR model when compared with nonparametric, ARX and Volterra model.

a)

b)

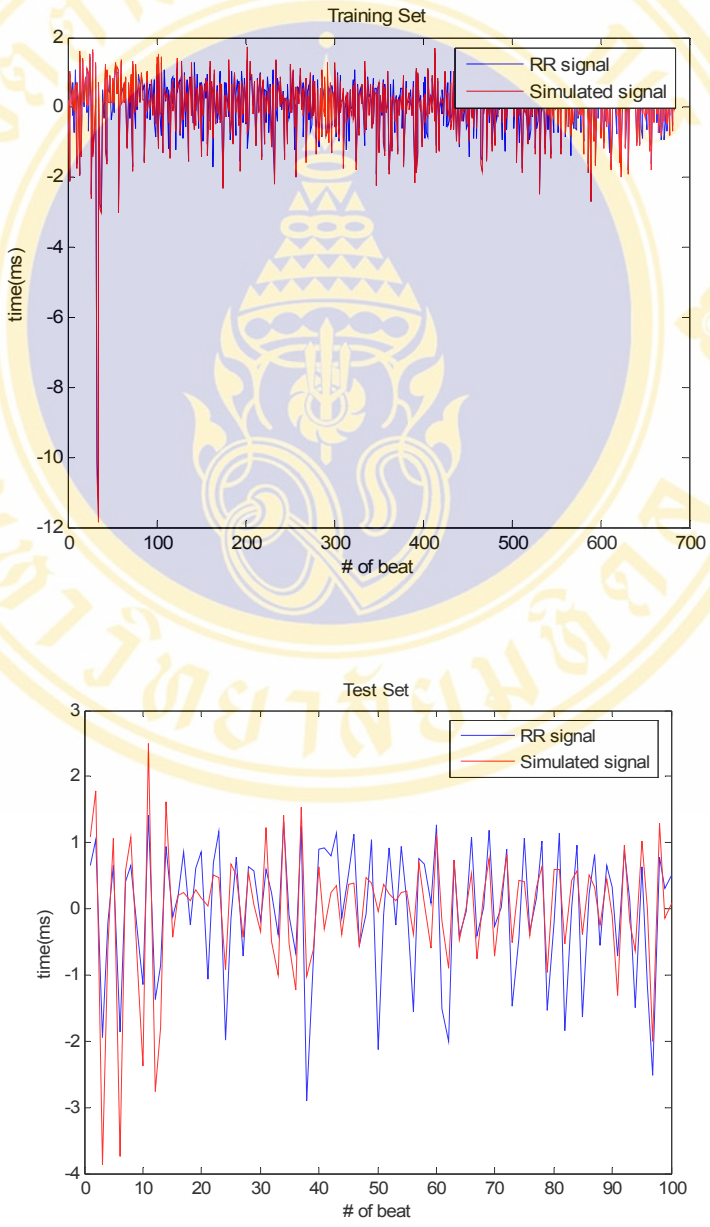

Figure 4.12 Model prediction of MSNA-RR model by using NARMA method (input =MSNA, output =RR). a) Training set, b) Test set.

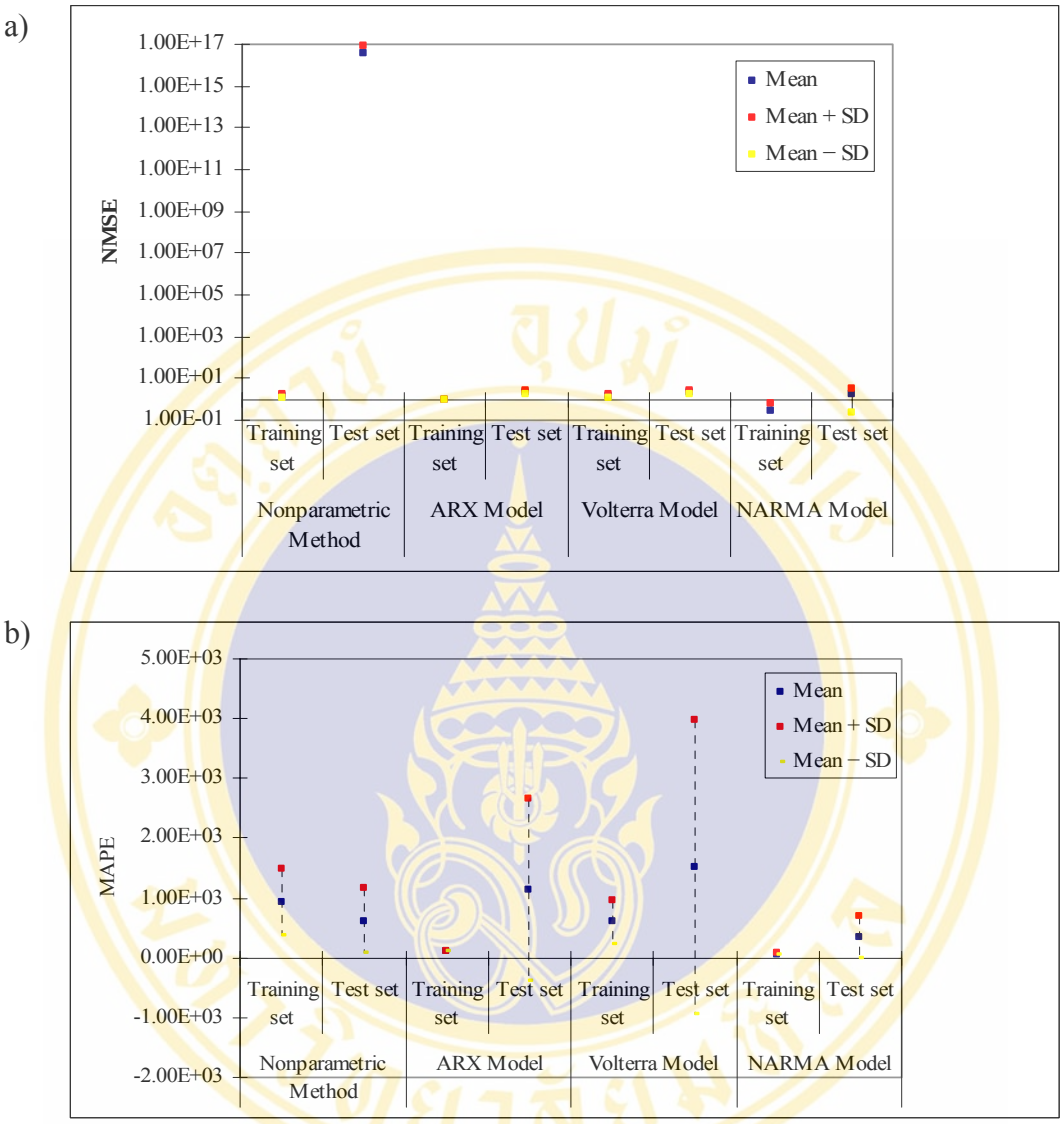

Figure 4.13 Performance of MSNA-RR model with nonparametric, ARX, Volterra and NARMA model. a) NMSE, b) MAPE.

The mean NMSE and MAPE of NARMA method leaded to the best result of validation. NARMA gave a minimum value of NMSE in training set ($p < 0.05$); however, there were no differences in the mean of NMSE between NARMA, ARX and Volterra method in test set ($p > 0.05$). MAPE of NARMA method provided minimum results in training set ($p < 0.05$). Otherwise, there were no differences in the mean of MAPE between NARMA with the other methods in test set ($p > 0.05$).

4.2.3 Respiration and RR model

In respiration and RR model, we studied the effect of respiration to RR interval by using NARMA method. We served respiration as input and RR interval as output of model. Moreover, these signals were interrupted with various LBNP such as baseline, -15 mmHg, -30 mmHg and recovery period. The RESP-RR model predictions at baseline, -15mmHg, 30 mmHg and recovery period are shown in figure 4.14-4.18, respectively.

a)

b)

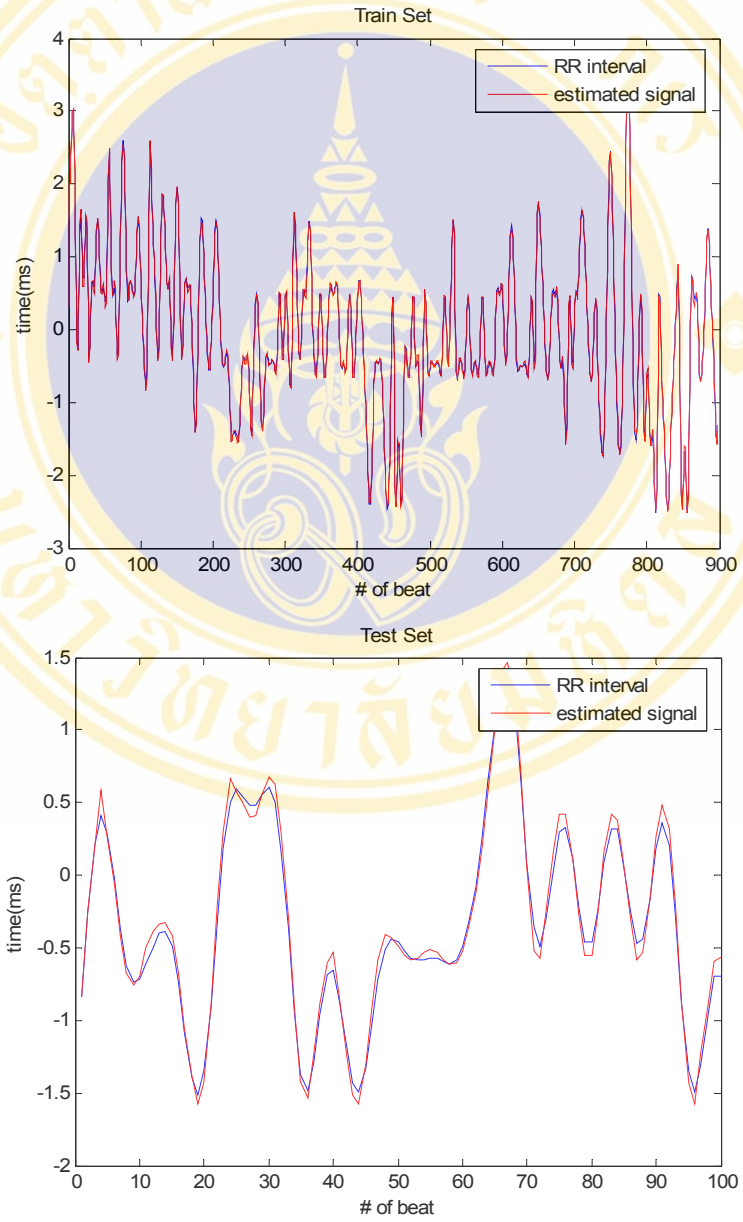

Figure 4.14 Model prediction of RESP-RR model by using NARMA method at base line (input =RESP, output =RR). a) Training set, b) Test set.

a)

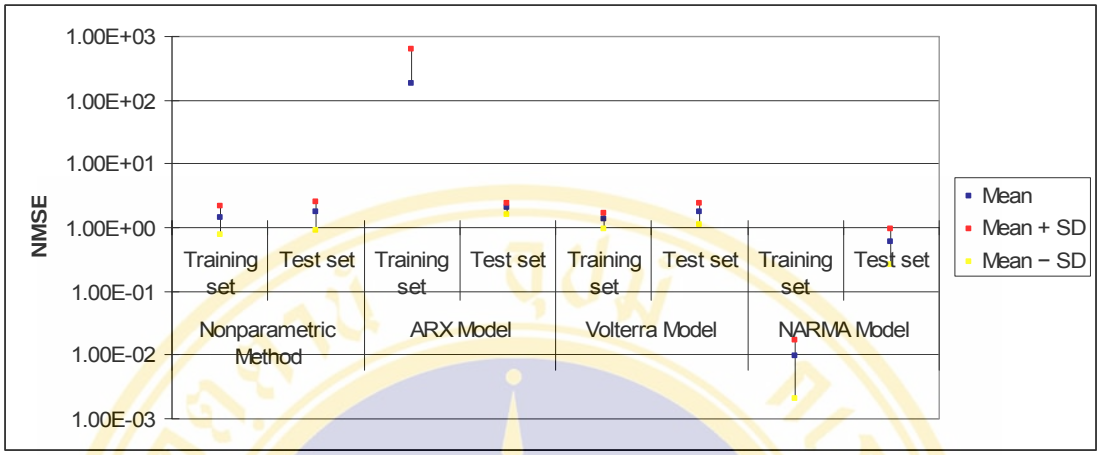

b)

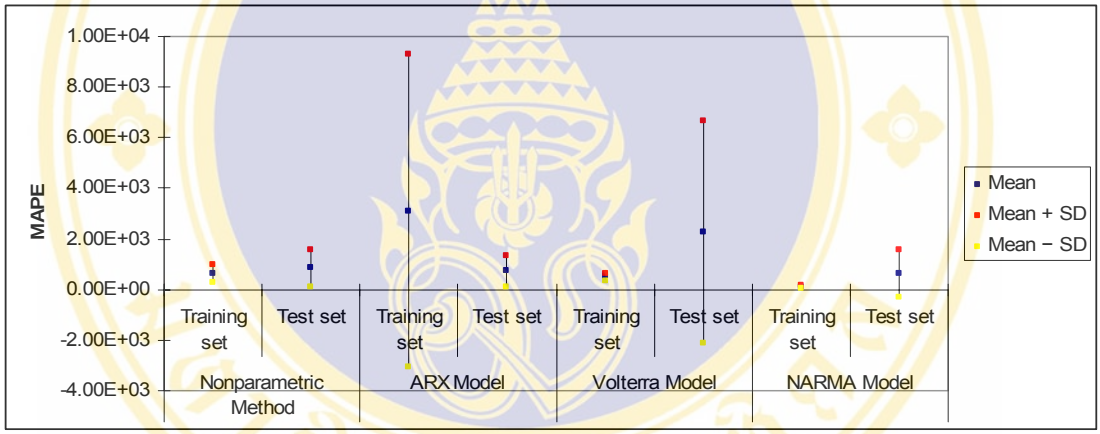

Figure 4.15 Performance of RESP-RR model with nonparametric, ARX, Volterra and NARMA model. a) NMSE, b) MAPE.

The mean NMSE and MAPE of NARMA method leaded to the best result of validation. Moreover, the mean of NMSE provided minimum results in training and test sets ($p < 0.05$) except training set of ARX method ($p > 0.05$). Otherwise, the mean of MAPE in training set by using NARMA method were less than nonparametric and Volterra method ($p < 0.05$) but there were no differences in the mean of MAPE between NARMA with the other methods in test set ($p > 0.05$).

a)

b)

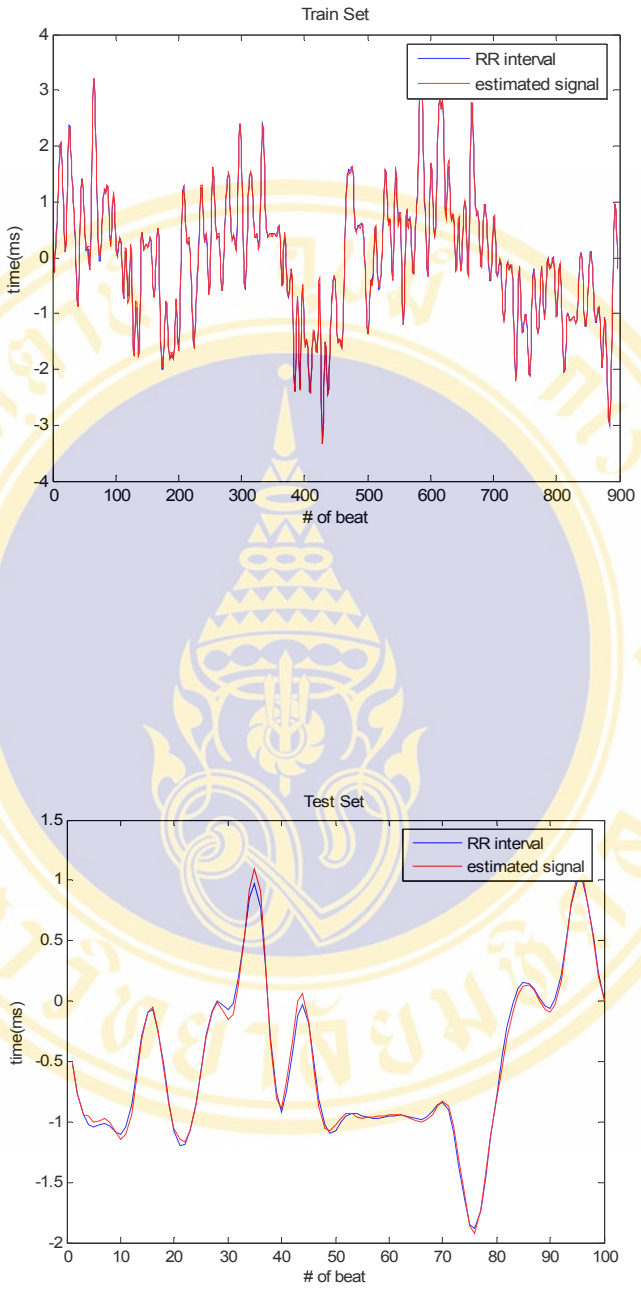

Figure 4.16 Model prediction of RESP-RR model by using NARMA method with -15 mmHg LBNP (input =RESP, output =RR). a) Training set, b) Test set.

a)

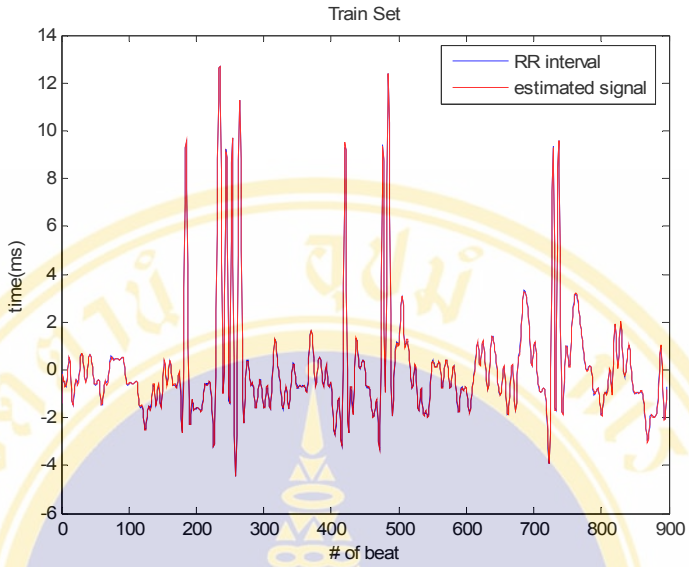

b)

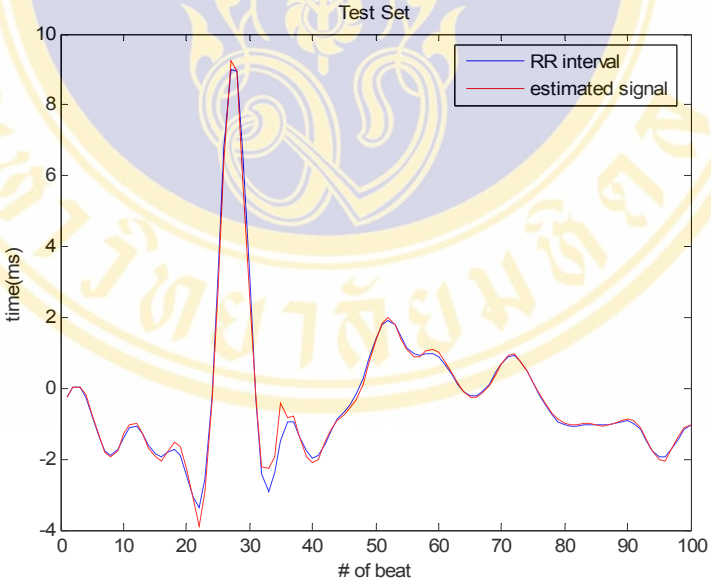

Figure 4.17 Model prediction of RESP-RR model by using NARMA method with -30 mmHg LBNP (input =RESP, output =RR). a) Training set, b) Test set.

a)

b)

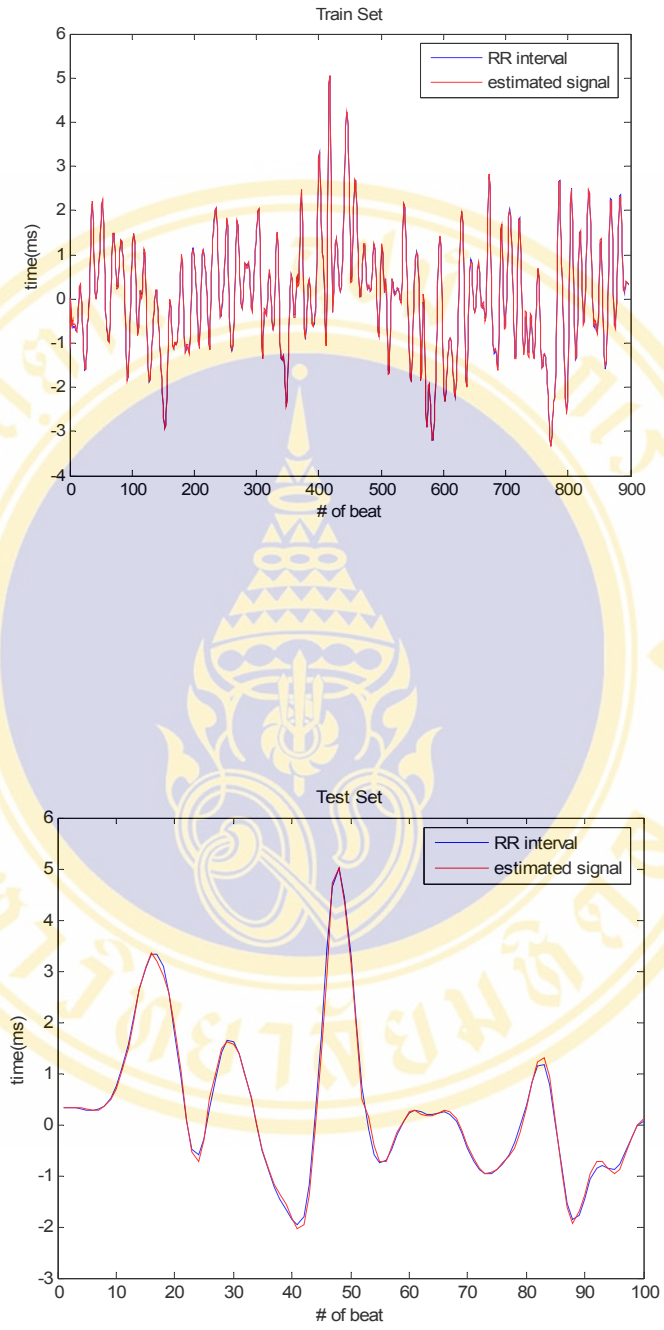

Figure 4.18 Model prediction of RESP-RR model by using NARMA method at recovery period (input =RESP, output =RR). a) Training set, b) Test set.

a)

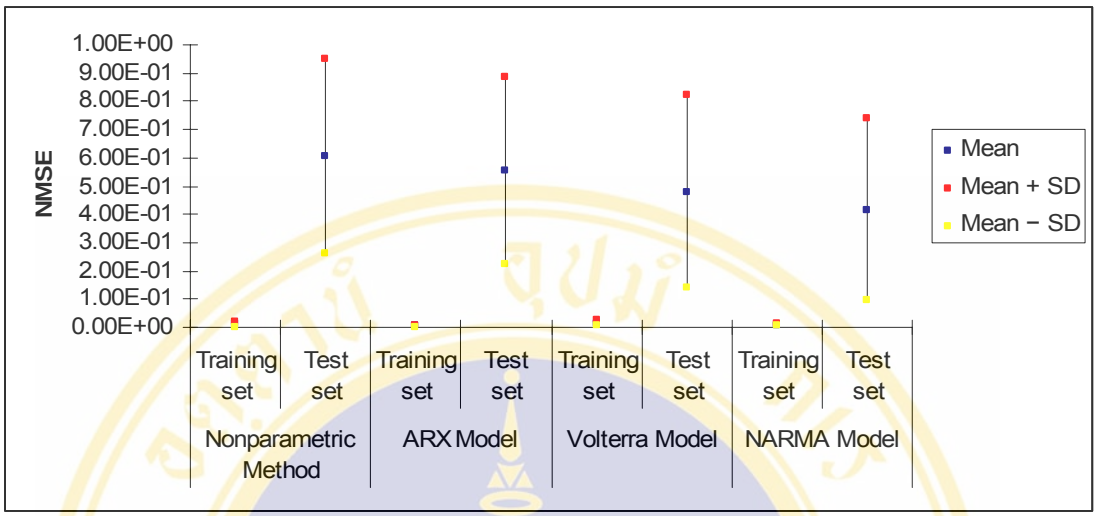

b)

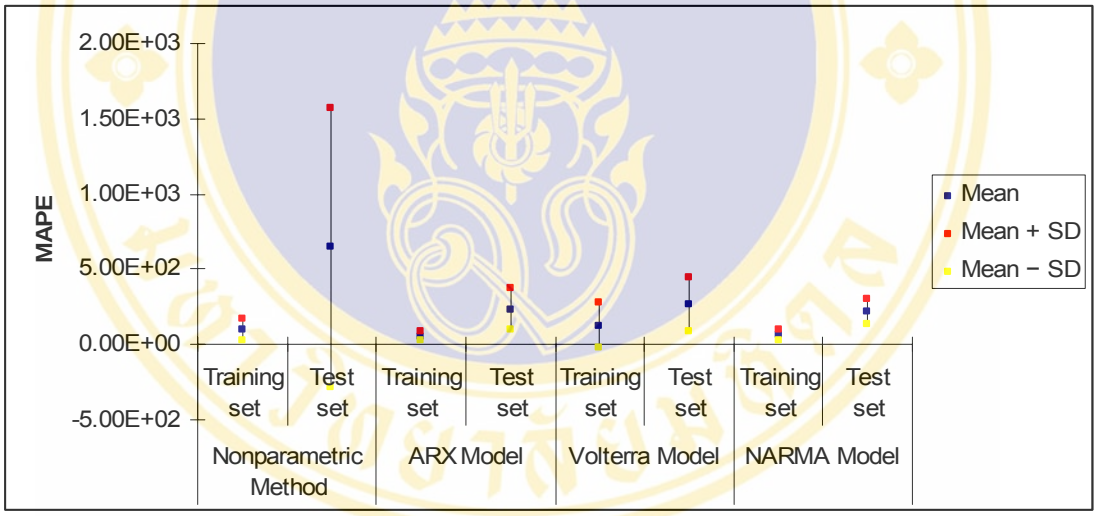

Figure 4.19 Performance of RESP-RR model by using NARMA model with baseline, -15 mmHg, -30 mm Hg and recovery period of LBNP. a) NMSE, b) MAPE.

The effects of LBNP to autonomic heart rate control with broadband respiration were considered in this part. From these results, we found that NMSE and MAPE of recovery period showed a minimum value. At -15 mmHg provided a better prediction than baseline and -30 mmHg. However, there are no differences in the mean of NMSE and MAPE in both training set and test set ($p < 0.05$).

CHAPTER V
DISCUSSION

The experimental results were discussed in this chapter. It can be classified into 3 parts: heart rate variability (HRV) during handgrip exercise, NARMA model of autonomic heart rate control and limitation of this study.

5.1 Heart rate variability during handgrip exercise

This study demonstrated the ability of the spectral analysis by using parametric method to measure the changing in sympatho-vagal balance during handgrip exercise. The normalized spectral components provided an efficient tool of HRV such as assess the progression of sympathetic excitation, a concomitant vagal withdrawal and a shift in sympatho-vagal balance [74]. The present study showed that the normalized LF and HF which reflect sympathetic and vagal activity respectively were decrease during exercise. These results are consistence with the other studies [75-78]. Moreover, intensity exercise increased sympatho-vagal balance. It is consistent with other study, which the sympatho-vagal balance (LF/HF ratio) increased during dynamic handgrip exercise [79]. Linear (spectral) and non-linear (Poincaré plot) parameters of HRV indicated a decrease of both parasympathetic and sympathetic nervous modulation of cardiac function during upwind sailing at different wind velocities despite heart rate increased [80]. The decreased normalized HF powers decreased and the increased LF powers were evidence of withdrawal of vagal activity and enhanced sympathetic outflow during both dynamic exercise and the passive head-up tilt [81]. This is consistent with the notion that change in cardiovascular function with low-intensity exercise are primarily mediated by parasympathetic withdrawal, and as exercise intensity increases, additional cardiovascular reactivity is mediated by increased sympathetic outflow [82].

However, LF and HF power might be influence of different conditions. For example, an increased LF is observed during 90° tilt, standing, mental stress, and moderate exercise in healthy subjects, and during moderate hypotension, physical activity, and occlusion of a coronary artery or common carotid arteries in conscious dogs [27]. Conversely, an increase in HF is induced by controlled respiration, cold stimulation of the face, and rotational stimuli [27].

5.2 NARMA model of autonomic heart rate control.

We studied the effect to autonomic heart rate control with various factors such as ABP, MSAN, and LBNP. Then, these effects were described as the relationship between input and output of NARMA model.

5.2.1 RR and ABP model

The RR and ABP model can be divided in to the baroreflex path (SBP-RR, and DBP-RR) and mechanical path (RR-SBP and RR-DBP).

As results we found that the performance of ABP-RR model (NMSE and MAPE) revealed that the nonlinear (NARMA and Volltera) method predicted the out put of the model better than linear (nonparametric and ARX) method. This result consistence with other researches [83], there are nonlinear feedback control mechanisms. MAPE showed that the DBP predicted RR interval better than SBP in test set ($p<0.05$).

In mechanical path, we also found the NARMA method provided results better than others. Moreover, RR interval provided good prediction of SBP the same as DBP ($p>0.05$). This result do not consistence with the other studies. For example, there are correlation between RR interval and systolic blood pressure. RR interval changes are driven by systolic blood pressure [84]. Beat to beat change of the ECG lag changes in beat to beat systolic blood pressure level [85]. SBP remained significant in multivariate models for predicting the risk of cardiovascular disease in men aged <60 and ≥60 years [86].

5.2.2 MSNA and RR model

As we known that, heart rate is even more markedly influenced by changes in vagal cardiac drive [87,88]. In these results, we found that this model also did not provide good results; there were some error in model prediction. These results might influence the other cardiovascular variables [89].

5.2.3 RESP and RR model

In this study, NARMA model was implemented in extending the understanding the autonomic heart rate control with broadband respiration. As results, we found that the error of NARMA model at baseline was relatively low. The broadband respiration provided a good result to predict heart rate control. This result is consistent with [33,90]. Berger et al found that the autonomic modulation of heart rate was obviously seen over the broadband of frequency (typically from Dc to roughly 0.3 Hz) [33]. Moreover, the fixed frequency breathing at 0.25 Hz, baroreflex mechanism contributed to respiratory fluctuation in RR interval [91].

The results showed that both NMSE and MAPE of nonlinear model is less than linear model in all cases. It can be concluded that there is nonlinear interactions between respiration and RR interval. This result is consistent with the previous study [92]. This nonlinear interaction consisted of the classical feedback and control model of regulatory physiology, the effect of forcing a Van der val oscillator and coupled nonlinear oscillators [92]. This nonlinearity interaction affected to the modulation of heart rate variability by respiration and blood pressure fluctuation [92]. The nonlinearity fluctuation of respiration and blood pressure could be modulating the heart rate variability [29].

Lower body negative pressure (LBNP) is a widely used method for understanding the cardiovascular responses to stimulated orthostatic stress [93]. It enhances the pumping performance of the cardiovascular system. In this study we study LBNP at -15 mmHg, -30mmHg and recovery. As result, we found that NARMA model of LBNP (-15 mmHg and -30 mmHg) gave better result than baseline. These results were consistent with the other studies [94-95]. LBNP reduced the positional reflexes that induced more complex heart rate and blood pressure changes [94-95].

In this study, the NARMA model with -15 mmHg showed better results than -30 mmHg in both MAPE and NMSE prediction. This result might be consistent with [96-97]. LBNP at levels up to -20 mmHg is considered to selectively unload cardiopulmonary receptors, resulting in reflex peripheral vasoconstriction without changes in heart rate [96]. Higher levels of LBNP elicit cardiovascular responses that are mediated by the unloading of both arterial and cardiopulmonary baroreceptors [97].

5.3 Limitation of this study

The NARMA model uses more computation time than the other methods (nonparametric, ARX and Volterra-Weiner model). However, NARMA model provides a superior capability of signal prediction. This result is similar to that found by the other [70,98,99]. Moreover, we also found that MAPE differentiated performance of model better than NMSE.

Autonomic heart rate control related with several simultaneous and interacting parameters. These parameters are not independent and they have reciprocal interactions. Thus, a small change in one parameter may influence the whole structure through the complex mechanical and neural systems. These effects caused error in model validation such as in MSNA-RR model. Age, body mass index (BMI), sex, and race may be effect in measures of MSNA, HR, and blood pressure [2]. Thus the multi input case and physiological effect will be considered in the further study.

CHAPTER VI
CONCLUSION

The mathematical model of autonomic heart rate control provides an importance in physiological mechanisms and clinical practices. From the results, based on power spectral analysis, we found that sympatho-vagal balance (LF/HF ratio) increases during dynamic handgrip exercise. Moreover, we investigate the nonlinear model that assesses the dynamic changes in cardiovascular regulation by using nonlinear autoregressive moving average (NARMA) method. These models were ABP and RR, MSNA-RR and RESP-RR. Consequently, there are nonlinear relation ship between ABP and RR. NARMA model of sympathetic nerve activity and RR interval reveals good prediction. The error of NARMA model at baseline is relatively low; however the error of NARMA model of LBNP (-15 mmHg and -30 mmHg) give better result than baseline.

Finally, NARMA model gave the best prediction in all cases when compare with other methods (nonparametric method, ARX model and Volterra-Weiner model). These finding indicate that NARMA model may be useful to complete the cardiovascular regulation mechanism.

REFERENCES

1 Martini FH, Bartholomew EF. Essential of Anatomy and Physiology. London (UK): Prentice Hall International (UK) Limited; 1997.

2 Chon KH, Mukkamala R, Toska K, Mullen TJ, Armoundas AA, Cohen RJ. Linear and nonlinear system identification of autonomic heart-rate modulation. Engineering in Medicine and Biology Magazine, IEEE. 1997;16(5):96-105.

3 John D, Catherine TM. Heart Rate Variability. Available: http://www.macses.ucsf.edu/Research/Allostatic/notebook/heart.rate.html [Acessed: 15 June, 2006]

4 Byrne EA, Fleg JL, Vaitkevicius PV, Wright J, Porges SW. Role of aerobic capacity and body mass index in the age-associated decline in heart rate variability. J Appl Physiol. 1996 August 1, 1996;81(2):743-50.

5 Davy KP, Miniclier NL, Taylor JA, Stevenson ET, Seals DR. Elevated heart rate variability in physically active postmenopausal women: a cardioprotective effect? Am J Physiol Heart Circ Physiol. 1996 August 1, 1996;271(2):H455-60.

6 De Meersman RE. Heart rate variability and aerobic fitness. Am. Heart J. 1993;125:726–731.

7 Goldsmith RI, Bigger JT, Steinman RC, Fleiss JL. Comparison of 24-hour parasympathetic activity in endurance-trained and untrained young men. J. Am. Coll. Cardiol. 1992;20: 552–558.

8 Lipsitz LA, Mietus J, Moody GB, Goldberger AL. Spectral characteristics of heart rate variability before and duringpostural tilt: relations to aging and risk of syncope Circulation. 1990;81:1803–1810.

9 Shannon DC, Carley DW, Benson H. Aging of modulation of heart rate. Am J Physiol Heart Circ Physiol. 1987 October 1, 1987;253(4):H874-7.

10 Rajendra UA, Kannathal N, Lee Mei Hua, Leong Mei Yi, Study of heart rate variability signals at sitting and lying postures, Bodywork and Movement Therapies, 2004

11 Albert CM, Mittleman MA, Chae CU, Lee IM, Hennekens CH, Manson JE. Triggering of Sudden Death from Cardiac Causes by Vigorous Exertion. N Engl J Med. 2000 November 9, 2000;343(19):1355-61.

12 Mittleman M, Siscovick D. Physical exertion as a trigger of myocardial infarction and sudden cardiac death. Cardiol Clin. 1996;14: 263–270.

13 Kleiger RE, Miller JP, Bigger JJT, Moss AJ. Decreased heart rate variability and its association with increased mortality after acute myocardial infarction. The American Journal of Cardiology. 1987;59(4):256-62.

14 Lanza GA, Guido V, Galeazzi MM, Mustilli M, Natali R, Ierardi C, et al. Prognostic role of heart rate variability in patients with a recent acute myocardial infarction. The American Journal of Cardiology. 1998;82(11):1323-8.

15 Nolan J, Batin PD, Andrews R, Lindsay SJ, Brooksby P, Mullen M, et al. Prospective Study of Heart Rate Variability and Mortality in Chronic Heart Failure : Results of the United Kingdom Heart Failure Evaluation and Assessment of Risk Trial (UK-Heart). Circulation. 1998 October 13, 1998;98(15):1510-6.

16 Heli H, Reijo T, Heimo I, Tutorial on multivariate autoregressive modeling. Clinical Monitoring and Computing, 2006. Available: http://www.mit.tut.fi/staff/Hytti/MAR_tutorial.pdf#search=%22Tutorial%20on%20multivariate%20autoregressive%20modeling%22 [Acessed: 15 June, 2006]

17 Nakata A, Takata S, Yuasa T, Shimakura A, Maruyama M, Nagai H, et al. Spectral analysis of heart rate, arterial pressure, and muscle sympathetic nerve activity in normal humans. Am J Physiol Heart Circ Physiol. 1998 April 1, 1998;274(4):H1211-7.

18 Yoshino K, Matsuoka K. Causal coherence analysis of heart rate variability and systolic blood pressure variability under mental arithmetic task load. Biol Psychol. 2005;69(2):217-27.

19 Delius W., Hagbarth KE., Hongell A, Wallin BG. General characteristics of sympathetic activity in human muscle nerves. Acta Physiol. Scand. 1972; 84: 65–81,

20 Sundlo¨FG,. Wallin BG. The variability of muscle nerve sympathetic activity in resting recumbent man. *J*. Physiol. (Lond.). 1977; 272: 383–397,.

21 Anderson EA, Sinkey CA, Lawton WJ, Mark AL. Elevated sympathetic nerve activity in borderline hypertensive humans. Evidence from direct intraneural recordings. Hypertension. 1989 August 1, 1989;14(2):177-83.

22 Matsukawa, T., E. Gotoh, O. Hasegawa, H. Shionoiri, O. Tochikubo, and M. Ishii. Reduced baroreflex changes in muscle sympathetic nerve activity during blood pressure elevation in essential hypertension. J. Hypertens. 1991;9: 537–542.

23 Hoffman RP, Sinkey CA, Anderson EA. Muscle sympathetic nerve activity is higher in intensively versus conventionally treated IDDM subjects. Diabetes Care. 1995 March 1, 1995;18(3):287-91.

24 Middlekauff HR, Hamilton MA, Stevenson LW, Mark AL. Independent control of skin and muscle sympathetic nerve activity in patients with heart failure. Circulation. 1994 October 1, 1994;90(4):1794-8.

25 Grossman P, Wilhelm FH, Spoerle M. Respiratory sinus arrhythmia, cardiac vagal control, and daily activity. Am J Physiol Heart Circ Physiol. 2004 August 1, 2004;287(2):H728-34.

26 Malliani A. Association of heart rate variability components with physiological regulatory mechanisms. In: *Heart Rate Variability*, edited by Malik M, and Camm AJ.. Armonk, NY: Futura, 1995;173-188.

27 Electrophysiology. Heart Rate Variability: Standards of Measurement, Physiological Interpretation, and Clinical Use. Circulation. 1996 March 1, 1996;93(5):1043-65.

28 Bock J, Gough DA. Toward prediction of physiological state signals in sleep apnea. Biomedical Engineering, IEEE Transactions on. 1998;45(11):1332-41.

29 Jo JA, Khoo MCK, Blasi A, Baydur A, Juarez R. Detection of autonomic abnormality in obstructive sleep apnea using a nonlinear model of heart-rate variability. 2002; 2002. p. 1554-5 vol.2.

30 Blasi A, Jo JA, Valladares E, Juarez R, Baydur A, Khoo MCK. Autonomic Cardiovascular Control Following Transient Arousal From Sleep: A Time-Varying Closed-Loop Model. Biomedical Engineering, IEEE Transactions on. 2006;53(1):74-82.

31 Laederach H, Mussgay, Winter, Klinkenberg, Ruddel. Early autonomic dysfunction in patients with diabetes mellitus assessed by spectral analysis of heart rate and blood pressure variability. Clinical Physiology. 1999;19(2):97-106.

32 Saul JP, Berger RD, Albrecht P, Stein SP, Chen MH, Cohen RJ. Transfer function analysis of the circulation: unique insights into cardiovascular regulation. Am J Physiol Heart Circ Physiol. 1991 October 1, 1991;261(4):H1231-45.

33 Berger RD, Saul JP, Cohen RJ. Assessment of autonomic response by broad-band respiration: IEEE Trans Biomed Eng. 1989:36:1061-1065.

34 Robert CL, William CL, Physiology of the heart and circulation. Year book medical publisher, INC. 1989.

35 Ljung L., System Identification, Theory for the User. Upper Saddle River, NJ: Prentice Hall, 1999

36 Berger RD, Saul JP, Cohen RJ. Transfer function analysis of autonomic regulation. I. Canine atrial rate response. Am J Physiol Heart Circ Physiol. 1989 January 1, 1989;256(1):H142-52.

37 Saul JP, Berger RD, Chen MH, Cohen RJ. Transfer function analysis of autonomic regulation. II. Respiratory sinus arrhythmia. Am J Physiol Heart Circ Physiol. 1989 January 1, 1989;256(1):H153-61.

38 Ikeda Y, Kawada T, Sugimachi M, Kawaguchi O, Shishido T, Sato T, et al. Neural arc of baroreflex optimizes dynamic pressure regulation in achieving both stability and quickness. Am J Physiol Heart Circ Physiol. 1996 September 1, 1996;271(3):H882-90.

39 Saul JP, Berger RD, Albrecht P, Stein SP, Chen MH, Cohen RJ. Transfer function analysis of the circulation: unique insights into cardiovascular regulation. Am J Physiol Heart Circ Physiol. 1991 October 1, 1991;261(4):H1231-45.

40 Richard S. Introduction to applied statistical signal analysis. Aksen Associated Incoorperated Publishers, 1991.

41 Djuric PM, Kay SM, Vijay KM, Douglas BW. Spectrum Estimation and Modeling, *Digital Signal Processing Handbook* CRC Press LLC. 1999.

42 Perrott MH, Cohen RJ. An efficient approach to ARMA modeling of biological systems with multiple inputs and delays. Biomedical Engineering, IEEE Transactions on. 1996;43(1):1.

43 Xiao X, Mullen TJ, Mukkamala R. System identification: a multi-signal approach for probing neural cardiovascular regulation. Physiol. Meas. 2005; 26:R41–R71.

44 Panos ZM, Vasilis ZM. Analysis of physiological system: The white noise approach.Plenum Press, 1977.

45 Berger RD, Saul JP, Cohen RJ. Transfer function analysis of autonomic regulation. I. Canine atrial rate response. Am J Physiol Heart Circ Physiol. 1989 January 1, 1989;256(1):H142-52.

46 Saul JP, Berger RD, Chen MH, Cohen RJ. Transfer function analysis of autonomic regulation. II. Respiratory sinus arrhythmia. Am J Physiol Heart Circ Physiol. 1989 January 1, 1989;256(1):H153-61.

47 Ikeda Y, Kawada T, Sugimachi M, Kawaguchi O, Shishido T, Sato T, et al. Neural arc of baroreflex optimizes dynamic pressure regulation in achieving both stability and quickness. Am J Physiol Heart Circ Physiol. 1996 September 1, 1996;271(3):H882-90.

48 Saul JP, Berger RD, Albrecht P, Stein SP, Chen MH, Cohen RJ. Transfer function analysis of the circulation: unique insights into cardiovascular regulation. Am J Physiol Heart Circ Physiol. 1991 October 1, 1991;261(4):H1231-45.

49 Berger RD, Saul JP, Albrecht P, Stein SP, Cohen RJ. Respiratory effects on arterial pressure: a novel signal analysis approach. Proc. IEEE EMBS.1988;10: 533-534.

50 Saul JP, Berger RD, Cohen RJ. A simple analytical model mimics complex physiological behavior. 1989; 1989. p. 335-8.

51 Barbieri R, Triedman J.K, Di Virgilio V, Cerutti S, Saul J.P. Arterial pressure control during non-hypo/hypertensive changes in central venous volume: assessment with multivariate autoregressive modeling. Computers in Cardiology 1996 8-11 Sept. 1996:85–88.

52 Aljuri AN, Marini RP, Cohen RJ. A Conscious Sheep Model for the Examination of Arterial and Cardiopulmonary Baroreceptors in the Dynamic Closed-loop Control of Total Peripheral Resistance, Computers in Cardiology. 2000;27:41-44.

53 Nikolai A, Bursac N, Marini R, Cohen R.J. System Identification of Dynamic Closed-Loop Control of Total Peripheral Resistance by Arterial and Cardiopulmonary Baroreceptors. Acta Astronautica. , 2001;49(3-10):167-170.

54 Mullen TJ, Appel ML, Mukkamala R, Mathias JM, Cohen RJ. System identification of closed-loop cardiovascular control: effects of posture and autonomic blockade. Am J Physiol Heart Circ Physiol. 1997;272: H448-H461.

55 Mukkamala R, Mathias JM, Mullen TJ, Cohen RJ, Freeman R. System identification of closed-loop cardiovascular control mechanisms: diabetic autonomic neuropathy. Am J Physiol Regul Integr Comp Physiol. 1999 March 1, 1999;276(3):R905-12.

56 Lang E, Caminal P, Horvath G, Jane R, Vallverdu M, Slezsak I, Bayes de Luna A., Spectral analysis of heart period variance (HPV)--a tool to stratify risk following myocardial infarction. J Med Eng Technol. 1998;22(6):248-56.

57 Chatlapalli S, Nazeran H, Melarkod V, Krishnam R, Estrada E, Pamula Y, et al. Accurate derivation of heart rate variability signal for detection of sleep disordered breathing in children. 2004; 2004. p. 538-41 Vol.1.

58 Cerutti S, Bianchi A, Bontempi B, Comi G, Gianoglio P, Liberati D, et al. Quantitative analysis of heart rate variability signal in diabetic subjects. 1988; 1988. p. 145-6 vol.1.

59 Cerutti S, Bianchi A, Bontempi B, Comi G, Gianoglio P, Natali MG. Power spectrum analysis of heart rate variability signal in the diagnosis of diabetic neuropathy. 1989; 1989. p. 12-3 vol.1.

60 Chon KH, Mullen TJ, Cohen RJ. A dual-input nonlinear system analysis of autonomic modulation of heart rate. Biomedical Engineering, IEEE Transactions on. 1996;43(5):530-44.

61 Alexander J, Kawada T, Sugimachi M, Miyano H, Sato T. The significance of dynamic nonlinerities in the autonomic regulation of heart rate, IEEE Trans Biomed Eng. 1998; 20(1): 310-313

62 Jo J, Khoo MCK, Blasi A, Baydur A, Juarez R. Detection of autonomic abnormality in obstructive sleep apnea using a nonlinear model of heart rate variability. Proc. 2nd Joint EMBS-BMES Conference, 2002:1554-1555.

63 Korenberg MJ, A robust orthogonal algorithm for system identification and time series analysis, Biol Cybern. 1989;60: 267-276.

64 Marmarelis VZ. Identification of nonlinear biological system using Laguerre expansion of kernels. Ann Biomed Eng. 1993;21:573-589.

65 French AS, Sekizawa SI, Hoger U, Torkkeli PH. Predicting the responses of mechanoreceptor neurons to physiological inputs by nonlinear system identification. Ann Biomed Eng. 2001 Mar;29(3):187-94.

66 Kleiger RE, Miller P, Bigger JT, Moss AJ, Decreased heart rate variability and its association with increased mortality after acute myocardial infarction, Am J Cardiol, 1987; 59, pp. 256–262,.

67 U. Rajendra Acharya, N. Kannathal, Lee Mei Hua, and Leong Mei Yi, “Study of heart rate variability signals at sitting and lying postures,” *Bodywork and Movement Therapies,* 2004

68 Task Force of the European Society of Cardiology and the North American Society of Pacing and Electrophysiology. “Heart Rate Variability:

Standards of Measurement, Physiological Interpretation and Clinical Use", *Circulation*, 93, 5, pp. 1043-1065, 1996

69 Alippi C; Piuri V, Neural methodology for prediction and identification of nonlinear dynamic systems**.** 1996 International Workshop on Neural Networks for Identification, Control, Robotics, and Signal/Image Processing (NICROSP '96). 1996; 305–313**.**

70 Chon KH., Hoyer D, Armoundas AA, Holstein-Rathlou N-H, Mash DJ. Robust Nonlinear autoregressive moving average model parameter estimation using stochastic recurrent artificial neural networks, Annals of Biomedical Engineering. 1999; 27:538–547.

71 Haykin S. Neural networks: A Comprehensive Foundation. Macmillan College, 1994.

72 Chen S, Cowan CFN, Grant PM. Orthogonal least squares leaning algorithm for radial basis function networks. IEEE Transactions on Neural networks. 1991: 2(2) 302- 9

73 Kate AS. Neural network: An introduction. **Available:** http://www.idea-group.com/downloads/excerpts/1930708319BookEx.pdf#search=%22Neural%20network%3A%20An%20introduction%20Kate%20A%20smith%22 **[Acessed: 15 June, 2006]**

74 Montano N, Ruscone TG, Porta A, Lombardi F, Pagani M, Malliani A. Power spectrum analysis of heart rate variability to assess the changes in sympathovagal balance during graded orthostatic tilt. Circulation. 1994 October 1, 1994;90(4):1826-31.

75 Perini R, Orizio C, Milesi S, et al: Body position affects the power spectrum of heart rate variability during dynamic exercise. Eur J Appl Physiol Occup Physiol. 1993; 66:207-213

76 Dixon EM, Kamath MV, McCartney N, et al: Neural regulation of heart rate variability in endurance athletes and sedentary controls. Cardiovasc Res. 1992;26: 713-719.

77 Hagerman I, Berglund M, Lorin M, Nowak J, Sylven C. Chaos-related deterministic regulation of heart rate variability in time- and frequency

domains: effects of autonomic blockade and exercise. Cardiovascular Research. 1996;31(3):410-8.

78 Pichon AP, De Bisschop CD, Rouland M, et al: Spectral analysis of heart rate variability during exercise is trained subjects. Med Sci Sports Exerc, 2004;36:1702- 1708.

79 Heidi A, Wood RH, Welsch MA Vagal modulation of the heart and central hemodynamics during handgrip exercise. Am J Physiol Heart Circ Physiol. 2000;279:. H1648–H1652.

80 Princi T, Accardo A, Nevierov L, Peterec D. Linear and Non-linear Parameters of Heart Rate Variability in a High Performance World Class Sailor. International Journal of Bioelectromagnetism, 2003;5;145 – 146.

81 Butler CG, Yamamoto Y, Xing HC, Northey DR, Hughson RL. Heart rate variability and fractal dimension duringorthostatic challenges. J Appl Physiol, 1993;75: 2602–2612, 1993.

82 Tulppo MP, Makikallio TH, Seppanen T, Laukkanen RT, Huikuri HV. Vagal modulation of heart rate during exercise: effects of age and physical fitness. Am J Physiol Heart Circ Physiol. 1998 February 1, 1998;274(2):H424-9.

83 Wang, H.,K. Ju and K.H. Chon: Closed-loop Nonlinear System Identification via the Vector Optimal Parameter Search Algorithm: Application to Heart Rate Baroreflex Control, 2005.

84 Korhonen I. Assessment of arterial and cardiopulmonary baroreflex gains from simultaneous recordings of spontaneous cardiovascular and respiratory variability. J Hypertens. 2001 Feb;19(2):351-2.

85 Bowers E, Murray A. Interaction between cardiac beat-to-beat interval changes and systolic blood pressure changes. Clinical Autonomic Research. 2004;14(2):92-8.

86 Sesso HD, Stampfer MJ, Rosner B, Hennekens CH, Gaziano JM, Manson JE, Glynn RJ. Systolic and diastolic blood pressure, pulse pressure, and mean arterial pressure as predictors of cardiovascular disease risk in Men. Hypertension. 2000: 36(5): 801-7.

87 Levy MN, Martin PJ. Autonomic control of cardiac conduction and automaticity. In: Shepherd JT, Vatner SF (editors): Nervous control of the heart. Amsterdam: Harwood Academic Publishers; 1996:201–226.

88 5 Mancia G, Mark AL. Arterial baroreflexes in humans. In: Abboud FM, Shepherd JT (editors*):* Handbook of physiology, the cardiovascular system, III. *Bethesda*, Maryland: American Society of Physiology; 1983:755–793.

89 Montano N. Spectral analysis of arterial pressure variability, heart rate, and muscular sympathetic nerve activity in man. Cardiologia. 1999 Dec;44 Suppl 1(Pt 2):775-9

90 Yang CCH, Kuo TBJ. Assessment of cardiac sympathetic regulation by respiratory-related arterial pressure variability in the rat. J Physiol (Lond). 1999 March 15, 1999;515(3):887-96.

91 Keyl C, Dambacher M, Schneider A, Schneider A, Passino C, Wegenhorst U, Bernardi L. Cardiocirculatory coupling during sinusoidal baroreceptor stimulation and fixed-frequency breathing. Clin Sci. 2000; 99: 113–124

92 Saul JP, Kaplan DT, Kitney RJ. Nonlinear interactions between respiration and heart rate: classical physiology or entrained nonlinear oscillators. 1988; 1988. p. 299-302.

93 Brown CM, Hecht MJ, Neundorfer B, Hilz MJ. Effects of lower body negative pressure on cardiac and vascular responses to carotid baroreflex stimulation. Physiol Res. 2003;52(5):637-45.

94 Borst C, Weiling W, Van Brederode JFM, Hond A, De Rijk LG, Dunning AJ. Mechanisms of initial heart rate response to postural change. Am J Physiol 1982;243: H676–H681.

95 Dikshit MB. Lower-body suction and cardiovascular reflexes: physiological and applied considerations. Indian J Physiol Pharmacol 1990;34:3–12.

96 Zoller RP, Mark AL, Abboud FM, Schmid PG, Heistad DD. The role of low pressure baroreceptors in reflex vasoconstrictor responses in man. J Clin Invest 1972;51: 2967-2972

97 Furlan R, Jacob G, Palazzolo L, Rimoldi A, Diedrich A, Harris PA, et al. Sequential Modulation of Cardiac Autonomic Control Induced by

Cardiopulmonary and Arterial Baroreflex Mechanisms. Circulation. 2001 December 11, 2001;104(24):2932-7.

98 Chon KH, Cohen RJ, Holstein-Rathlou NH. Compact and accurate linear and nonlinear autoregressive moving average model parameter estimation using laguerre functions. Ann Biomed Eng. 1997 Jul-Aug;25(4):731-8.

99 Chon KH, Cohen RJ. Linear and nonlinear ARMA model parameter estimation using an artificial neural network. IEEE Trans Biomed Eng. 1997 Mar;44(3):168-74.

APPENDIX

APPENDIX A
All Test Data

Table I The LF and HF of spectral components and LF/HF ratio.

	LF				HF				LF/HF Ratio			
Subject	Rest	5 min	10 min	15 min	Rest	5 min	10 min	15 min	Rest	5 min	10 min	15 min
1	79.96	91.48	96.92	98.28	24.04	9.10	4.21	2.73	3.33	10.05	23.02	36.07
2	48.19	95.80	96.04	95.80	53.03	4.26	4.04	4.33	0.91	22.50	23.75	22.12
3	35.80	91.24	93.34	95.68	64.90	8.88	6.85	4.42	0.55	10.28	13.62	21.63
4	78.74	93.65	94.05	93.11	23.56	6.64	6.14	7.13	3.34	14.11	15.32	13.06
5	70.15	91.87	93.84	94.57	31.00	8.58	6.54	5.85	2.26	10.70	14.35	16.17
Average	62.57	92.81	94.84	95.49	39.31	7.49	5.56	4.89	2.08	13.53	18.01	21.81

Table II NMSE of SBP-RR model prediction.

	Nonparametric Method		ARX Model		Volterra Model		NARMA Model	
Subject	Training set	Test set	Training set	Test set	Training set	Test set	Training set	Test set
1	9.71E-01	3.46E+15	9.97E-01	2.36E+00	4.96E-01	1.46E+00	5.32E-01	1.75E+00
2	1.78E+00	2.49E+16	1.00E+00	1.71E+00	4.88E-01	2.40E+00	2.31E-01	3.07E+00
3	1.70E+00	1.43E+16	9.99E-01	2.00E+00	4.45E-01	2.14E+00	9.38E-02	9.38E-02
4	1.45E+00	1.10E+17	1.00E+00	2.15E+00	5.12E-01	2.42E+00	5.39E-02	2.50E-01
5	1.71E+00	3.34E+16	1.00E+00	2.16E+00	6.59E-01	3.00E+00	1.61E-01	2.50E-01
Average	1.52E+00	3.73E+16	1.00E+00	2.08E+00	5.20E-01	2.28E+00	2.14E-01	1.08E+00

Table III MAPE of SBP-RR model prediction.

	Nonparametric Method		ARX Model		Volterra Model		NARMA Model	
Subject	Training set	Test set	Training set	Test set	Training set	Test set	Training set	Test set
1	1.01E+03	2.66E+02	1.04E+02	2.84E+02	6.20E+02	2.55E+02	8.00E+01	2.65E+02
2	3.57E+02	2.02E+02	9.98E+01	2.40E+02	1.21E+02	1.43E+02	9.98E+01	1.36E+03
3	1.83E+03	7.97E+02	1.01E+02	1.34E+03	1.69E+02	7.47E+02	3.91E+01	6.51E+02
4	6.68E+02	3.19E+02	1.00E+02	2.56E+02	1.18E+02	3.17E+02	2.97E+01	7.79E+02
5	7.38E+02	1.51E+03	1.00E+02	1.44E+03	1.46E+02	2.39E+03	4.32E+01	1.57E+02
Average	9.21E+02	6.18E+02	1.01E+02	7.11E+02	2.35E+02	7.70E+02	5.84E+01	6.42E+02

Table IV NMSE of DBP-RR model prediction

	Nonparametric Method		ARX Model		Volterra Model		NARMA Model	
Subject	Training set	Test set	Training set	Test set	Training set	Test set	Training set	Test set
1	9.71E-01	3.46E+15	9.99E-01	2.04E+00	6.13E-01	1.95E+00	4.07E-01	5.00E-01
2	1.78E+00	2.49E+16	1.00E+00	1.59E+00	4.92E-01	2.30E+00	3.05E-01	2.80E+00
3	1.70E+00	1.43E+16	9.99E-01	2.14E+00	4.52E-01	2.00E+00	7.73E-02	5.94E-01
4	1.45E+00	1.10E+17	1.00E+00	2.08E+00	4.96E-01	2.04E+00	1.11E-02	0.00E+00
5	1.71E+00	3.34E+16	1.00E+00	1.93E+00	6.54E-01	1.68E+00	3.38E-02	5.00E-01
Average	1.52E+00	3.73E+16	1.00E+00	1.96E+00	5.41E-01	2.00E+00	1.67E-01	8.79E-01

Table V MAPE of DBP-RR model prediction

	Nonparametric Method		ARX Model		Volterra Model		NARMA Model	
Subject	Training set	Test set	Training set	Test set	Training set	Test set	Training set	Test set
1	1.01E+03	2.66E+02	1.01E+02	2.72E+02	2.67E+02	3.93E+02	3.85E+01	5.60E+01
2	3.57E+02	2.02E+02	9.99E+01	2.08E+02	1.13E+02	1.50E+02	4.31E+01	6.91E+01
3	1.83E+03	7.97E+02	1.00E+02	1.38E+03	1.71E+02	7.92E+02	3.93E+01	4.29E+01
4	6.68E+02	3.19E+02	1.00E+02	4.08E+02	1.17E+02	3.81E+02	1.04E+02	2.92E+01
5	7.38E+02	1.51E+03	1.00E+02	1.45E+03	1.51E+02	2.75E+03	2.78E+01	4.75E+01
Average	9.21E+02	6.18E+02	1.00E+02	7.43E+02	1.64E+02	8.93E+02	5.06E+01	4.89E+01

Table VI NMSE of RR-SBP model prediction.

	Nonparametric Method		ARX Model		Volterra Model		NARMA Model	
Subject	Training set	Test set	Training set	Test set	Training set	Test set	Training set	Test set
1	1.76E+00	7.28E+16	9.98E-01	1.66E+00	7.16E-01	1.83E+00	1.43E-02	0.00E+00
2	1.76E+00	7.28E+16	1.00E+00	2.15E+00	8.01E-01	2.04E+00	1.28E-01	0.00E+00
3	1.79E+00	2.37E+17	9.99E-01	2.79E+00	3.60E-01	1.70E+00	6.55E-02	5.71E-01
4	1.96E+00	1.90E+16	1.00E+00	1.31E+00	1.69E+00	1.77E+00	6.55E-02	5.71E-01
5	1.67E+00	4.41E+17	1.00E+00	2.96E+00	3.84E-01	3.03E+00	2.20E-01	1.67E-01
Average	1.79E+00	1.68E+17	1.00E+00	2.17E+00	7.91E-01	2.07E+00	9.85E-02	2.62E-01

Table VII MAPE of RR-SBP model prediction

	Nonparametric Method		ARX Model		Volterra Model		NARMA Model	
Subject	Training set	Test set	Training set	Test set	Training set	Test set	Training set	Test set
1	1.47E+03	2.80E+03	1.02E+02	3.64E+03	6.18E+02	4.81E+03	3.19E+01	1.75E+02
2	1.47E+03	2.80E+03	9.99E+01	7.57E+02	1.43E+02	5.29E+02	4.46E+01	3.41E+02
3	8.38E+02	4.87E+02	1.00E+02	5.84E+02	1.28E+02	4.11E+02	2.81E+01	2.34E+02
4	9.86E+02	2.12E+02	1.00E+02	3.54E+02	2.63E+03	3.38E+02	2.81E+01	2.34E+02
5	5.78E+02	6.12E+02	1.01E+02	8.00E+02	1.09E+02	4.93E+02	7.94E+01	1.81E+02
Average	1.07E+03	1.38E+03	1.01E+02	1.23E+03	7.25E+02	1.32E+03	4.24E+01	2.33E+02

Table VIII NMSE of RR-DBP model prediction.

	Nonparametric Method		ARX Model		Volterra Model		NARMA Model	
Subject	Training set	Test set	Training set	Test set	Training set	Test set	Training set	Test set
1	2.09E+00	2.41E+16	1.00E+00	1.74E+00	6.64E-01	2.29E+00	4.69E-01	7.55E-02
2	1.71E+00	1.05E+16	9.99E-01	2.28E+00	6.16E-01	2.05E+00	8.90E-02	1.16E-01
3	1.77E+00	2.06E+17	9.99E-01	2.58E+00	4.20E-01	2.06E+00	1.32E-01	1.52E-01
4	2.19E+00	1.52E+16	9.97E-01	8.25E-01	1.61E+00	1.89E+00	9.38E-02	4.29E-02
5	1.77E+00	8.80E+17	9.99E-01	1.55E+00	5.50E-01	2.44E+00	7.73E-02	8.33E-01
Average	1.91E+00	2.27E+17	9.99E-01	1.79E+00	7.73E-01	2.15E+00	1.72E-01	2.44E-01

Table IX MAPE of RR-DBP model prediction.

	Nonparametric Method		ARX Model		Volterra Model		NARMA Model	
Subject	Training set	Test set	Training set	Test set	Training set	Test set	Training set	Test set
1	8.22E+02	4.34E+02	1.01E+02	4.82E+02	2.21E+02	5.60E+02	3.45E+01	1.09E+02
2	4.47E+03	3.64E+03	1.06E+02	3.09E+03	2.71E+02	2.49E+03	8.29E+02	3.48E+02
3	5.37E+02	3.04E+02	1.00E+02	4.23E+02	1.00E+02	2.42E+02	2.45E+01	5.29E+02
4	4.12E+02	1.44E+02	1.02E+02	2.73E+02	2.71E+02	2.49E+03	1.72E+01	2.08E+02
5	6.73E+02	3.70E+02	1.00E+02	2.92E+02	2.21E+02	5.60E+02	1.64E+01	6.04E+01
Average	1.38E+03	9.79E+02	1.02E+02	9.12E+02	2.17E+02	1.27E+03	1.84E+02	2.51E+02

Table X NMSE of MSNA-RR model prediction.

	Nonparametric Method		ARX Model		Volterra Model		NARMA Model	
Subject	Training set	Test set	Training set	Test set	Training set	Test set	Training set	Test set
1	9.71E-01	3.46E+15	1.00E+00	2.28E+00	1.28E+00	1.84E+00	1.18E-01	4.00E+00
2	1.78E+00	2.49E+16	1.00E+00	1.95E+00	1.53E+00	2.60E+00	4.31E-03	2.67E+00
3	1.70E+00	1.43E+16	1.00E+00	2.33E+00	1.52E+00	2.37E+00	5.29E-01	1.43E-01
4	1.45E+00	1.10E+17	1.00E+00	2.42E+00	8.93E-01	2.75E+00	9.21E-02	2.00E+00
5	1.71E+00	3.34E+16	1.00E+00	1.79E+00	1.49E+00	1.87E+00	6.83E-01	4.20E-01
Average	1.52E+00	3.73E+16	1.00E+00	2.16E+00	1.35E+00	2.29E+00	2.85E-01	1.85E+00

Table XI MAPE of MSNA-RR model prediction.

	Nonparametric Method		ARX Model		Volterra Model		NARMA Model	
Subject	Training set	Test set	Training set	Test set	Training set	Test set	Training set	Test set
1	1.01E+03	2.66E+02	1.00E+02	2.61E+02	1.15E+03	3.51E+02	7.32E+01	1.40E+02
2	3.57E+02	2.02E+02	1.00E+02	2.78E+02	2.25E+02	2.57E+02	5.97E+01	7.89E+01
3	1.83E+03	7.97E+02	1.00E+02	8.02E+02	7.55E+02	7.76E+02	5.67E+01	5.14E+02
4	6.68E+02	3.19E+02	1.00E+02	4.42E+02	4.28E+02	2.91E+02	5.37E+01	1.08E+02
5	7.38E+02	1.51E+03	1.00E+02	3.82E+03	4.18E+02	5.92E+03	4.45E+01	8.67E+02
Average	9.21E+02	6.18E+02	1.00E+02	1.12E+03	5.94E+02	1.52E+03	5.75E+01	3.41E+02

Table VIII The NMSE of RESP-RR model at base line

	Nonparametric Method		ARX Model		Volterra Model		NARMA Model	
Subject	Training set	Test set	Training set	Test set	Training set	Test set	Training set	Test set
1	1.61E-01	3.82E-02	1.75E+00	1.38E+00	1.79E+00	2.08E+00	1.20E-02	9.91E-01
2	1.77E+00	1.81E+00	1.14E+00	1.91E+00	1.69E+00	1.83E+00	2.32E-02	3.56E-01
3	1.84E+00	2.30E+00	1.08E+03	2.50E+00	8.60E-01	4.80E-01	3.87E-03	6.29E-01
4	2.05E+00	2.16E+00	1.83E+00	2.39E+00	1.07E+00	2.07E+00	1.12E-02	1.06E+00
5	1.36E+00	2.04E+00	1.45E+00	1.82E+00	1.16E+00	2.18E+00	1.83E-03	2.82E-01
6	1.63E+00	2.05E+00	1.47E+00	2.06E+00	1.42E+00	1.96E+00	6.37E-03	3.32E-01
Average	1.47E+00	1.73E+00	1.81E+02	2.01E+00	1.33E+00	1.77E+00	9.75E-03	6.07E-01

Table IX The MAPE of RESP-RR model at base line.

Subject	Nonparametric Method		ARX Model		Volterra Model		NARMA Model	
	Training set	Test set	Training set	Test set	Training set	Test set	Training set	Test set
1	3.49E+02	5.82E+02	4.44E+02	9.61E+02	4.88E+02	6.65E+02	1.61E+02	4.60E+02
2	7.56E+02	4.04E+02	3.52E+02	3.53E+02	6.51E+02	6.03E+02	1.42E+02	2.25E+02
3	4.83E+02	3.04E+02	1.57E+04	2.47E+02	2.16E+02	1.35E+02	2.42E+01	2.25E+02
4	1.27E+03	2.27E+03	1.20E+03	1.91E+03	5.83E+02	1.13E+04	4.81E+01	2.53E+03
5	4.23E+02	8.68E+02	3.44E+02	3.42E+02	4.47E+02	4.23E+02	1.76E+02	2.26E+02
6	4.41E+02	5.99E+02	5.90E+02	5.34E+02	5.07E+02	5.03E+02	3.74E+01	1.99E+02
Average	6.20E+02	8.38E+02	3.10E+03	7.24E+02	4.82E+02	2.27E+03	9.82E+01	6.45E+02

Table X The NMSE of RESP-RR model at base line, -15 mmHg , -30 mmHg and recovery period.

Subject	Baseline		-15 mmHg		-30 mmHg		Recovery	
	Training set	Test set	Training set	Test set	Training set	Test set	Training set	Test set
1	1.20E-02	9.91E-01	8.51E-03	4.58E-01	3.12E-03	2.06E-01	1.07E-02	6.53E-01
2	2.32E-02	3.56E-01	2.28E-03	1.14E+00	1.35E-02	3.56E-01	1.17E-02	9.52E-01
3	3.87E-03	6.29E-01	2.60E-03	1.57E-01	7.43E-03	1.92E-01	5.21E-03	9.09E-02
4	1.12E-02	1.06E+00	9.10E-03	6.58E-01	9.67E-03	1.11E+00	1.28E-02	2.07E-01
5	1.83E-03	2.82E-01	4.51E-03	4.67E-01	3.30E-02	4.85E-01	5.41E-03	2.95E-01
6	6.37E-03	3.32E-01	8.42E-03	4.32E-01	2.05E-02	5.23E-01	9.77E-03	2.99E-01
Average	9.75E-03	6.07E-01	5.90E-03	5.52E-01	1.45E-02	4.79E-01	9.25E-03	4.16E-01

Table XI The MAPE of RESP-RR model at base line, -15 mmHg, -30 mmHg and recovery period.

Subject	Baseline		-15 mmHg		-30 mmHg		Recovery	
	Training set	Test set	Training set	Test set	Training set	Test set	Training set	Test set
1	1.61E+02	4.60E+02	6.65E+01	1.51E+02	4.02E+01	2.38E+02	5.68E+01	2.69E+02
2	1.42E+02	2.25E+02	1.04E+02	4.73E+02	5.82E+01	9.32E+01	1.31E+02	2.17E+02
3	2.42E+01	2.25E+02	2.24E+01	7.70E+01	3.48E+01	1.67E+02	7.61E+01	1.02E+02
4	4.81E+01	2.53E+03	4.95E+01	2.58E+02	5.83E+01	5.71E+02	4.35E+01	1.37E+02
5	1.76E+02	2.26E+02	5.43E+01	2.51E+02	1.47E+02	1.42E+02	3.39E+01	3.26E+02
6	3.74E+01	1.99E+02	3.38E+01	1.83E+02	4.26E+02	3.96E+02	4.05E+01	2.32E+02
Average	9.82E+01	6.45E+02	5.51E+01	2.32E+02	1.27E+02	2.68E+02	6.37E+01	2.14E+02

APPENDIX B
Source code of mathematical modeling

Nonparametric method source code

```
%============================================================
% This m.file calculate output of system by using nonparametric method.
% Last modified 11/07/06
%============================================================
clear all; close all;
load RR6_b;
load RESP6_b;
N = 800;
n = 100;
nn = N-n;
RR = resample(RR,N,length(RR));
RESP = resample(RESP,N,length(RESP));
% detrend and scale data
RR = detrend(RR);
RESP = detrend(RESP);
RR = (RR-mean(RR))/std(RR);
RESP = (RESP -mean(RESP))/std(RESP);
% seperate data into training and test sets
xi = RESP(1:nn);    %training set (input)
yi = RR(1:nn);      %training set (output)
xp = RESP(nn+1:N);  %test set   (input)
yp = RR(nn+1:N);    %test set   (output)
% resize of data
A = size(xi);
B = size(yi);
if A(1) ~= 1
       xi = xi';
       xp = xp';
end
if B(1)~= 1
       yi = yi';
       yp = yp';
end
% calculate output of system
[output_non, ypre_non] = pred_non(yi,yp);
% downsample for validating data
output_non = resample(output_non,nn,length(output_non));
y_pre = resample(ypre_non,n,length(ypre_non));
%scaling
output_non = (output_non-mean(output_non))/std(output_non);
```

```
y_pre = (y_pre-mean(y_pre))/std(y_pre);
yi = (yi-mean(yi))/std(yi);
yp = (yp-mean(yp))/std(yp);
% calculate error
e1 = yi - output_non;
mse1 = (sum(e1.*e1))/nn;
mape1 = 100*sum(abs(e1./yi))/(nn);
nmse1 = (sum(e1.*e1))/ sum((yi-mean(yi)).^2);
e2 = yp - y_pre';
mse2 = (sum(e2.*e2))/n;
nmse2 = (sum(e2.*e2))/ sum((yp-mean(yp)).^2);
mape2 = 100*sum(abs(e2./yp))/(n);
nmse = [mape1 mape2 nmse1 nmse2 mse1 mse2];
% plot model prediction
figure(1); title('training set'); plot(1:nn,yi,1:nn,output_non); title('Training Set');
ylabel('time(ms)');xlabel('# of beat');
legend('RR interval', 'estimated signal');
figure(2); title('test set'); plot(1:n,yp,1:n,y_pre'); title('Test Set'); ylabel('time(ms)');
xlabel('# of beat');
legend('RR interval', 'estimated signal');

%=========================================================
%estimate predicted signal by using nonparametric method
function [output, y_pre] = pred_non(input,testset);
Nn = length(input);
h = hanning(Nn);
input2 = input'.*h; % filter by hanning window
T = 1;
PL = 0.36 ;%process loss factor
% calculate transfer function
dft_n = T*fft(input2);
h = (abs(dft_n(1:(fix(Nn/2)))).^2)/(Nn*T*PL);
f = (0:fix(Nn/2)-1)/(Nn*T);
% calculate inpluse response and simulated output
im1 = ifft((h));
y3 = conv(h,input);
output = real(y3);

% validate nonparametric method
y3 = conv(im1,testset);
y_pre = real(y3);
%=========================================================
```

ARX method source code

```
%============================================================
% This m.file calculate output of system by using ARX method.
% Last modified 11/07/06
%============================================================
% clear all; close all
load RR6_b;
load RESP6_b;
N = 800;
n = 100;
nn = N-n;
RR = resample(RR,N,length(RR));
RESP = resample(RESP,N,length(RESP));
% detrend and scale data
RR = detrend(RR);
RESP = detrend(RESP);
RR = (RR-mean(RR))/std(RR);
RESP = (RESP -mean(RESP))/std(RESP);
% seperate data into training and test sets
xi = RESP(1:nn);    %training set (input)
yi = RR(1:nn);      %training set (output)
xp = RESP(nn+1:N);  %test set   (input)
yp = RR(nn+1:N);    %test set   (output)
% resize of data
A = size(xi);
B = size(yi);
if A(1) ~= 1
       xi = xi';
       xp = xp';
end
if B(1)~= 1
       yi = yi';
       yp = yp';
end
% calculate output of system
[output_para, ypre_para] = est_ARX(xi,yi,xp,yp);
% scaling
output_para = (output_para-mean(output_para))/std(output_para);
ypre_para = (ypre_para-mean(ypre_para))/std(ypre_para);
yi = (yi-mean(yi))/std(yi);
yp = (yp-mean(yp))/std(yp);
% calculate error
e1 = yi - output_para;
mse1 = (sum(e1.*e1))/nn;
mape1 = 100*sum(abs(e1./yi))/(nn);
nmse1 = (sum(e1.*e1))/ sum((yi-mean(yi)).^2)
```

```
e2 = yp - ypre_para;
mse2 = (sum(e2.*e2))/n;
mape2 = 100*sum(abs(e2./yp))/(n);
nmse2 = (sum(e2.*e2))/ sum((yp-mean(yp)).^2)
nmse = abs([mape1 mape2 nmse1 nmse2 mse1 mse2]);
% plot model prediction
figure(1)
plot(1:nn,yi',1:nn,output_para,'-.'); xlabel('time(ms)'); ylabel('# of beat');
legend('actual RR','simulated RR')
figure(2)
plot(1:n,yp,1:n,ypre_para,'-.'); xlabel('time(ms)'); ylabel('# of beat');
legend('actual RR','simulated RR')
%=========================================================
%estimate predicted signal by using ARX method
function [output, ypre] = est_ARX(xi,yi,xp,yp);
% order
p = 2;
q = 1;
% training set
   % AR parameter Estimation
     M = 7;
    MM = p+q+M;
    at = autocor(yi,MM);       % use Unbiased estimator
    at = at';
   c2s = [fliplr(at(2:MM+1)) at];
  %c2s = cu2es(y,y,MM);       % use Biased estimator
   for T = 1:MM
     for i = 1:p
       Am(T,i) = c2s(-T+i+MM+1);
     end;
       A1(T) = c2s(-T+MM+1);
   end;
   Am = Am(q+1:MM,:);      % T start from q+1 to MM or T =1:MM
   A1 = A1(q+1:MM);        % T start from q+1 to MM or T =1:MM
  arr = -1*inv(Am'*Am)*Am'*A1';
   a1 = [1;arr];          % ar parameter
  rst = filter(a1,1,yi);   % Find the residual
 %  MA parameter Estimation
   L = fix(nn/5);
  XX = autocor(xi,L);
  X1 = XX(2:L+1);
  Xm = toeplitz(XX(1:L));
  aa = -1*inv(Xm)*X1;
  YY = autocor(aa',q);
  Y1 = YY(2:q+1);
  Ym = toeplitz(YY(1:q));
  bb = -1*inv(Ym)*Y1;
```

```
   bb = [1 bb'];
   rst = filter(a1,bb,yi);
   loss = sum(rst.*rst)/nn;
   mdl =  nn*log10(loss) + log10(nn)*(p+q);
   % simulate RR
    h = freqz(bb,a1,nn);
    im1 = ifft((h));
    y3 = conv(im1,yi);
    output2 = real(y3);
% test set
yr = yp';
xr = xp';
 h2 = freqz(bb,a1,n);
 im2 = ifft((h2));
 y3 = conv(im2,yr);
 ypre2 = real(y3);
% downsample for validating data
output = resample(output2,nn,length(output2));
ypre = resample(ypre2,n,length(ypre2) )';
%=========================================================
```

Volterra-Weiner method source code

```
%============================================================
% This m.file calculate output of system by using Volterra-Weiner method.
% Last modified 11/07/06
%============================================================
clear all; close all;
load RR6_b;
load RESP6_b;
N = 800;
n = 100;
nn = N-n;
RR = resample(RR,N,length(RR));
RESP = resample(RESP,N,length(RESP));

% detrend and scale data
RR = detrend(RR);
RESP = detrend(RESP);
RR = (RR-mean(RR))/std(RR);
RESP = (RESP -mean(RESP)/std(RESP));
% seperate data into training and test sets
xi = RESP(1:nn);    %training set (input)
yi = RR(1:nn);      %training set (output)
xp = RESP(nn+1:N);  %test set   (input)
ypp = RR(nn+1:N);    %test set   (output)
% resize of data
A = size(xi);
B = size(yi);
if A(2) ~= 1
       xi = xi';
       xp = xp';
end
if B(2)~= 1
       yi = yi';
       ypp =ypp';
end
beta = [ 0.8 0.8];
[h, q] = nltick(xi,yi,n,1); % generate Nonparametric second-order Volterra System
yp = nlgen(xi,h,q); % Computes the output of a second-order Volterra system.
invfft = ifft(h); % calculate impluse response
linp = conv(invfft,xi);% convolution of impluse response and output
ylp = resample(linp,length(yp),length(linp));
ynp = yp - real(ylp); % compute nonlinear part
betafit = nlinfit(xi,yi,@volterra_fun,beta); % estimate coefficient of linear and
% nonlinear
output_vol = betafit(1)*yp + betafit(2)*ynp; % predict HR
```

```
% test set
yp2 = nlgen(xp,h,q);
linp2 = conv(invfft,xp);% convolution of impluse response and output
ylp2 = resample(linp2,length(yp2),length(linp2));
ynp2 = yp2 - real(ylp2); % compute nonlinear part
ypre_vol = betafit(1)*yp2 + betafit(2)*ynp2; % predict HR
close all;
% scaling
output_vol = (output_vol-mean(output_vol))/std(output_vol);
ypre_vol = (ypre_vol-mean(ypre_vol))/std(ypre_vol);
yi = (yi-mean(yi))/std(yi);
ypp = (ypp-mean(ypp))/std(ypp);
ypp = smooth(ypp,'loess');
% calculate error
e1 = yi - output_vol;
mse1 = (sum(e1.*e1))/nn;
mape1 = 100*sum(abs(e1./yi))/(nn);
nmse1 = (sum(e1.*e1))/ sum((yi-mean(yi)).^2)
e2 = ypp - ypre_vol;
mse2 = (sum(e2.*e2))/n;
nmse2 = (sum(e2.*e2))/ sum((ypp-mean(ypp)).^2)
mape2 = 100*sum(abs(e2./yp))/(n);
nmse = abs([mape1 mape2 nmse1 nmse2 mse1 mse2]);
nmse = abs(nmse);
% plot model prediction
figure(1);
plot(1:nn,yi,1:nn,output_vol)
    title('Training Set'); ylabel('time(ms)'); xlabel('# of beat');
    legend('RR interval', 'estimated signal');
figure(2);
plot(1:n,ypp,1:n,ypre_vol)
title('Test Set'); ylabel('time(ms)'); xlabel('# of beat');
legend('RR interval', 'estimated signal');
```

NARMA method source code

```
%=========================================================
% This m.file calculate output of system by using NARMA method.
% Last modified 11/07/06
%=========================================================
clear all; close all;
load RR6_b;
load RESP6_b;
N = 800;
n = 100;
nn = N-n;
RR = resample(RR,N,length(RR));
RESP = resample(RESP,N,length(RESP));
% detrend and scale data
RR = detrend(RR);
RESP = detrend(RESP);
RR = (RR-mean(RR))/std(RR);
RESP = (RESP -mean(RESP)/std(RESP));
% seperate data into training and test sets
xi = RESP(1:nn);    %training set (input)
yi = RR(1:nn);      %training set (output)
xp = RESP(nn+1:N);  %test set   (input)
ypp = RR(nn+1:N);    %test set   (output)
% resize of data
A = size(xi);
B = size(yi);
if A(2) ~= 1
       xi = xi';
       xp = xp';
end
if B(2)~= 1
       yi = yi';
       ypp =ypp';
end
% model order
    p = 3; q = 1; r = p+q;
    j = 1;
    for i=1:p
       output(i)=yi(i);
    end
    for i = p+1:nn
           input(j,:) = [ yi(i-1:-1:i-p) xi(i-1)]; j = j+1;
    end
           input = input';
           target = yi(p+1:nn);
           net = newrb(input,target,1e-7,1,300,200);
```

```
            output = sim(net,input);
% test set
    for i=1:p
       testset(i)=yp(i);
    end
    for i = p+1:n
            test = [ yp(i-1:-1:i-p) xp(i-1)]';
            testset(i) = sim(net,test);
    end
% scaling
   yp = (yp-mean(yp))/std(yp);
   target = (target-mean(target))/std(target);
   output = (output-mean(output))/std(output);
   testset = (testset-mean(testset))/std(testset);
% calculate error
    e = target - output;
    mse1 = (e*e')/(nn-p);
    mape1 = 100*sum(abs(e./target))/(nn-p);
    nmse1 = sum(e - mean(e))/ sum((yi-mean(yi)).^2)
          e1 = testset - yp;
          mse2 = (e1*e1')/(n);
          mape2 = 100*sum(abs(e1./testset))/(n-p);
          nmse2 = sum(e1 - mean(e1))/ sum((yp-mean(yp)).^2)
    nmse = abs([mape1 mape2 nmse1 nmse2 mse1 mse2]);
% plot model prediction
figure(1)
plot(1:nn-p,target,1:nn-p,output,'r');
title('Training Set'); ylabel('time(ms)'); xlabel('# of beat');
legend('RR interval ', 'estimated signal');
figure(2)
plot(1:n,yp',1:n,testset,'r');
title('Test Set'); ylabel('time(ms)'); xlabel('# of beat');
legend('RR interval', 'estimated signal');
```

BIOGRAPHY

NAME	Miss Piyawan Massa-ard
DATE OF BIRTH	1 July 1979
PLACE OF BIRTH	Kalasin, Thailand
INSTITUTIONS ATTENED	Mahidol University (1998-2001) Bachelor of Science (Mathematics) Mahidol University (2002-2006) Master of Engineering (Biomedical Engineering)
HOME ADDRESS	85 Tambon Phonthong Muang Kalasin Thailand 46000 E-mail : piyawan93@hotmail.com